



# Contents

**Director's Message**   *i*

**Executive Summary**   *v*

## **Indian Nuclear Power Programme**

- Development of Inspection Systems   **2**
- Recovery of Nuclear Minerals   **3**
- Environment Monitoring   **5**
- Nuclear Hydrogen   **5**
- Advanced Reactors & Associated Materials   **6**
- Spent Fuel Reprocessing & Radioactive Waste Management   **9**

## **Advanced Technologies, Radiation Technologies and Applications**

- Research Reactors   **14**
- Accelerator, Laser and Plasma   **15**
- Sensors, Detectors and Specialized Instruments   **16**
- Radiopharmaceuticals   **19**
- Water Purification, Water Resources Management & Solid Waste Management   **19**
- Agriculture and Food Technologies   **21**

- Technologies for Health Safety **23**
- Energy Storage Materials **25**
- Hydrogen Technologies **26**
- Specialized Technologies **28**

#### **Basic and Directed Research**

- Astrophysical Sciences **32**
- Solid State Physics **33**
- Technical Physics **34**
- Nuclear Physics **36**
- Synchrotron Beamline **37**
- Atomic & Molecular Physics **37**
- Chemical Sciences **37**
- Analytical Services **46**
- Environmental and Separation Science **46**
- Materials Science **48**
- Computation and Modelling **50**
- Cancer Studies **53**
- Bio-Science **56**
- Healthcare and Drug Discovery **61**
- Machine Learning and AI **66**

#### **Human Resources, Scientific Information and Technology Management **70****

#### **SciTech Outreach **82****

#### **Safe and Secured Workplace **88****

#### **Infrastructure Development **92****





# निदेशक का संदेश



हमारे संस्थान की आत्मा एक ऐसी विरासत है जो सात दशकों से अधिक की वैज्ञानिक उपलब्धि और तकनीकी नवाचार में समृद्ध है। इस संस्थान की स्थापना के आरंभिक दिनों से ही, हम डॉ. होमी जे. भाभा जैसे दूरदर्शी व्यक्तित्व के आदर्शों से मार्गदर्शन प्राप्त करते रहे हैं, जिन्होंने नाभिकीय विज्ञान एवं प्रौद्योगिकी में उत्कृष्टता हेतु एक समर्पित केंद्र की आवश्यकता को तभी महसूस कर लिया था जब वैश्विक स्तर पर इसकी संकल्पना अपने आरंभिक चरण में ही थी। समाज के उत्थान हेतु नाभिकीय प्रौद्योगिकी का उपयोग करने की उनकी प्रतिबद्धता ने हमारे संस्थागत लोकाचार को आकार दिया है, जिससे हम वैज्ञानिक ज्ञान और प्रगति के एक आधार-स्तंभ के रूप में उभरने में सक्षम हुए हैं।

भाभा परमाणु अनुसंधान केंद्र (बीएआरसी) के बहु-आयामी अनुसंधान कार्यक्रम नाभिकीय विज्ञान की प्रत्येक शाखा यथा - मौलिक अनुसंधान से लेकर परमाणु रिएक्टरों, ईंधन चक्रों, उच्च ऊर्जा त्वरकों, स्वास्थ्य सेवा, कृषि, जल प्रबंधन, स्वास्थ्य संरक्षा, ज्ञान प्रबंधन और कई अन्य क्षेत्रों के अनुप्रयुक्त प्रौद्योगिकी विकास तक में, पल्लवित हो रहा है। इन क्षेत्रों में निरंतर उत्कृष्टता तथा नवीन एवं उभरते विषयों के माध्यम से, हमने उल्लेखनीय प्रगति प्राप्त की है जिसने देश की आत्मनिर्भरता में महत्वपूर्ण योगदान दिया है।

उच्च उपलब्धता कारकों के साथ हमारे अनुसंधान रिएक्टरों का प्रचालन, उन्नत ईंधन निर्माण क्षमताओं का विकास, एवं पुनः प्रसंस्करण तथा अपशिष्ट प्रबंधन में हमारी विशेषज्ञता नाभिकीय ईंधन चक्र में दक्षता हासिल करने की हमारी प्रतिबद्धता का प्रतिफल है। इसके साथ ही, रेडियोआइसोटोप उत्पादन एवं नवीन रेडियोभेषजिक सहित स्वास्थ्य सेवा में हमारे नवाचार व्यापक सामाजिक कल्याण हेतु नाभिकीय प्रौद्योगिकी को अपनाने के प्रति हमारे समर्पण को प्रदर्शित करते हैं।

उच्च उपज देने वाली, रोग प्रतिरोधी फसलों की किस्मों के विकास एवं प्रसार सहित विकिरण प्रौद्योगिकी के अनुप्रयोग के माध्यम से कृषि क्षेत्र में हमारी सफलताएं खाद्य सुरक्षा को सुदृढ़ करने के हमारे मिशन को दर्शाती हैं। इसी तरह, सैकड़ों गांवों में प्रतिनियोजित हमारी जल शोधन प्रौद्योगिकियाँ बुनियादी सामाजिक चुनौतियों का समाधान करने के प्रति हमारी प्रतिबद्धता को रेखांकित करती हैं।

स्वदेशी प्रौद्योगिकी विकास को साकार करना ही हमारे केंद्र का दूरगामी मिशन रहा है। हमारे नवाचार अत्याधुनिक परमाणु हाइड्रोजन उत्पादन प्रणालियों से लेकर रिएक्टर घटकों हेतु उन्नत निरीक्षण उपकरणों तक कई क्षेत्रों में फैले हुए हैं। प्रतिवर्ष उद्घवन कार्यक्रमों में सम्मिलित होकर उद्योग भागीदारों को तीस से अधिक प्रौद्योगिकियों का हस्तांतरण, प्रयोगशाला की खोजों को व्यावहारिक अनुप्रयोगों में परिवर्तित करने की हमारी प्रतिबद्धता को दर्शाता है।

अपने मुख्य नाभिकीय अधिदेश से परे, हमने विश्व स्तरीय अनुसंधान सुविधाएं स्थापित की हैं जो वैज्ञानिक समुदाय को व्यापक सेवा प्रदान करती हैं। हमारी न्यूट्रॉन कणपुंज अनुसंधान सुविधाएं, सिंक्रोट्रॉन कणपुंजरेखा एवं विशिष्ट प्रयोगशालाएं ज्ञान प्रसार के माध्यम से वैज्ञानिक प्रगति के लिए एक सहयोगी पारिस्थितिकी तंत्र को बढ़ावा देते हुए देश भर के विश्वविद्यालयों और संस्थानों के शोधकर्ताओं को सहयोग प्रदान करती हैं।

भापअके आकर्षक संगोष्ठियों, प्रदर्शनियों एवं जन-संपर्क कार्यक्रमों के द्वारा देश भर में विज्ञान के प्रति जिज्ञासा का संचार करता है जिसके दौरान हम अपने प्रौद्योगिकियों की प्रदर्शनी के माध्यम से शिक्षाविदों, उद्योग और आम जनता के साथ सीधा संवाद करते हैं। अपने जन-संप्रेषण में, भापअके भारत सरकार के राजभाषा प्रतिबद्धताओं का पालन करता है।

इनमें से कोई भी उपलब्धि हमारे समर्पित कार्यबल के बिना संभव नहीं है। हमारे वैज्ञानिक प्रभागों एवं सहायक सेवाओं-प्रशासनिक, अभियांत्रिकी, चिकित्सा, संरक्षा और सुरक्षा - के बीच निर्बाध समन्वय हमारी तकनीकी उपलब्धियों की नींव डालता है।

हम अपने संस्थापकों के आत्मनिर्भरता एवं उत्कृष्टता के दृष्टिकोण के लिए प्रतिबद्ध हैं। हम, न केवल वैज्ञानिक एवं तकनीकी उपलब्धियों पर, बल्कि देश के विकास को अग्रसर रखने तथा नागरिकों के जीवन-स्तर में सुधार करने, आत्मनिर्भर भारत के निर्माण में योगदान करने पर भी ध्यान केंद्रित करते हैं।

बीएआरसी-विस्टा 2024 भापअके और नाभिकीय ऊर्जा के विशिष्ट क्षेत्रों में हो रही गतिविधियों के बारे में जिज्ञासा रखने वाले व्यक्ति के लिए एक अमूल्य संदर्भ सिद्ध होगा। मैं, इस व्यापक दस्तावेज़ को ससमय एवं व्यवस्थित प्रयासों से संकलित करने के लिए वैज्ञानिक सूचना संसाधन प्रभाग की सराहना करता हूँ।

विवेक भसीन



This page intentionally left blank



# Director's Message



At the heart of our institution lies a legacy that spans more than seven decades of scientific achievement and technological innovation. Since our founding, we have been guided by the visionary ideals established by Dr. Homi J. Bhabha, who recognized the need for a dedicated center of excellence in nuclear science and technology when such pursuits were still in their infancy globally. His commitment to harnessing nuclear technology for societal betterment has shaped our institutional ethos, enabling us to emerge as a beacon of scientific knowledge and advancement.

The multi-pronged research programs of Bhabha Atomic Research Centre (BARC) span the full spectrum of nuclear sciences — from fundamental research to applied technology development in atomic reactors, fuel cycles, high-energy accelerators, healthcare, agriculture, water management, health safety, knowledge management, and numerous other domains. Through sustained excellence in these fields and new and emerging disciplines, we have achieved remarkable strides that have contributed significantly to national self-reliance.

The operation of our research reactors with high availability factors, the development of advanced fuel fabrication capabilities, and our expertise in reprocessing and waste management exemplify our commitment to mastering the nuclear fuel cycle. Simultaneously, our innovations in healthcare, including radioisotope production and novel radiopharmaceuticals, demonstrate our dedication to applying nuclear technology for broader societal welfare.

Our agricultural breakthroughs through the application of radiation technology, including the development and dissemination of high-yielding, disease-resistant crop varieties, reflect our mission to enhance food security. Similarly, our water purification technologies deployed across hundreds of villages underscore our commitment to addressing fundamental societal challenges.

The pursuit of indigenous technology development remains central to our life-long mission. Our innovations span numerous fields, from state-of-the-art nuclear hydrogen production systems to advanced inspection tools for reactor components. The transfer of numerous technologies to industry partners in tandem with incubation programs annually illustrates our commitment to translating laboratory discoveries into practical applications.

Beyond our core nuclear mandate, we have established world-class research facilities that serve the broader scientific community. Our neutron beam research facilities, synchrotron beamlines, and specialized laboratories support researchers from universities and institutions nationwide, fostering a collaborative ecosystem for scientific advancement through knowledge sharing.

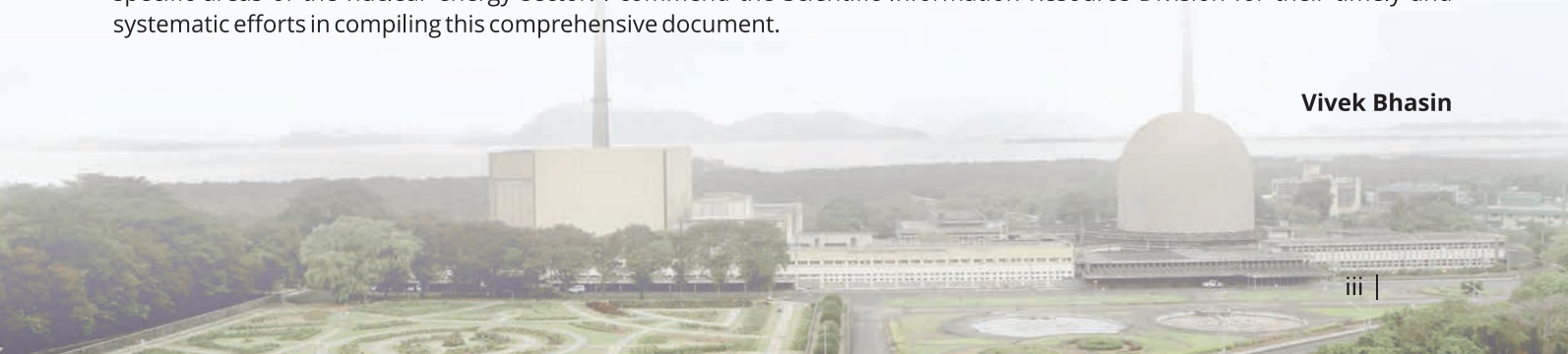
BARC sparks curiosity nationwide with engaging seminars, exhibitions, and outreach programs that showcase our technologies and connect with academia, industry, and the public. In its public communication, BARC adheres to the Official Language commitments of the Govt. of India.

None of these achievements would be possible without our dedicated workforce. The seamless coordination between our scientific divisions and support services—administrative, engineering, medical, safety, and security — creates the foundation for our technical accomplishments.

We remain committed to our founder's vision of self-reliance and excellence, focusing not just on scientific and technical achievements but on advancing national development and improving quality of life, contributing to the vision of Aatmanirbhar Bharat.

BARC VISTA 2024 will be a valuable reference for anyone seeking information about ongoing activities within BARC and specific areas of the nuclear energy sector. I commend the Scientific Information Resource Division for their timely and systematic efforts in compiling this comprehensive document.

**Vivek Bhasin**





This page intentionally left blank

# कार्यकारी सारांश

## भारतीय नाभिकीय ऊर्जा कार्यक्रम

रिएक्टर कोर की गहराई से लेकर चिकित्सा अनुप्रयोगों की सीमाओं तक, भाभा परमाणु अनुसंधान केंद्र (भापअ केंद्र) नाभिकीय विज्ञान एवं प्रौद्योगिकी के विभिन्न क्षेत्रों में संभावनाओं को तलाश रहा है।

**रिएक्टर निरीक्षण** में, भापअ केंद्र IS प्रणाली ने राजस्थान परमाणु बिजली परियोजना-7 और काकड़ापार परमाणु बिजली परियोजना-4 में महत्वपूर्ण सेवा-पूर्व निरीक्षण कार्य सफलतापूर्वक पूरा कर लिया है, जबकि नवोन्नत ECT-आधारित उपकरण अब 540MWe दायित भारी पानी रिएक्टर दाब नलिका के लिए मौजूदा निरीक्षण तकनीकों के पूरक हैं। काकड़ापार परमाणु बिजली परियोजना-4 में, BARCIS ने 18 शीतलक चैनलों और 25 बेल्लित युग्मपकों का आयतनी निरीक्षण किया। नाभिकीय ईंधन सम्मिश्र में ईंधन छड़ क्रमवीक्षण हेतु स्वतचालित प्रणाली के गुणवत्ता का निर्धारण करते हैं, जिसमें एक नए क्ष-किरण प्रतिबिंब प्रणाली सॉफ्टवेयर ने अधिक समय लेने वाले मैनुअल निरीक्षण को समाप्त कर दिया।

**रिएक्टर विकास** ने शानदार प्रगति दिखाई, जिसमें भापअ केंद्र ने शीतलक चैनल और भरण नलिका प्रतिस्थापन के बाद राजस्थान परमाणु बिजली स्टेशन-3 स्टार्टअप के लिए महत्वपूर्ण सहायता प्रदान की, और काकड़ापार परमाणु बिजली परियोजना-3 के पूर्ण क्षमता के साथ प्रचालन और काकड़ापार परमाणु बिजली परियोजना-4 की क्रांतिकता के लिए अभिकल्प सत्यापन और संरक्षा विश्लेषण में महत्वपूर्ण भूमिका निभाई। IPWRs और SMRs के लिए चुंबकीय जैक प्रतिक्रियाशीलता नियंत्रण तंत्र का पूरा होना भविष्य की रिएक्टर प्रौद्योगिकियों को प्रोन्नत करता है। हाइड्रोजन उत्पादन के लिए अभिकल्पित एक छोटा गैस-शीतित रिएक्टर ने पूरे बर्न-अप के दौरान ऋणात्मक प्रतिक्रियाशीलता गुणांक बनाए रखा। इसी समय, प्रायोगिक भारतीय द्रवित लवण रिएक्टर ने परीक्षण के अपने पहले चरण को सफलतापूर्वक पूरा कर लिया है।

**भापअ केंद्र** ने द्रुत रिएक्टर प्रौद्योगिकी के लिए, आदिप्ररूप द्रुत प्रजनक रिएक्टर के लिए ईंधन भरण मशीन को अभिकल्पित और विकसित किया है, नियमित रूप से मॉक्स ईंधन और विशेष उच्च तापमान वाले न्यूट्रॉनिक संसूचक और संरक्षा प्रणाली का निर्माण किया है। एक डिजिटल रेडियोग्राफी प्रणाली और स्वचालित वेल्डिंग एंड प्लग मेट्रोलॉजी प्रणाली अब द्रुत प्रजनक परीक्षण रिएक्टर ईंधन पिन निर्माण को गति दे रहा है।

**पदार्थ विज्ञान नवाचारों** में जर्कलॉय-4 पर क्रोमियम लेपन के साथ दुर्घटना-सह्य ईंधन आवरण का विकास शामिल है, जो उच्च तापमान पर उल्लेखनीय ऑक्सीकरण प्रतिरोध दर्शाता है। द्रविभूत लवण प्रजनक रिएक्टर लूप के लिए स्वदेशी NiMoCrTi-C मिश्रधातु प्लेटों का सफलतापूर्वक उत्पादन किया गया है, जबकि नैनोस्ट्रक्चर्ड बोरॉन कार्बाइड बेहतर यांत्रिक एवं उष्मीय गुणधर्मों को प्रदर्शित करता है। मद्रास परमाणु बिजली स्टेशन, राजस्थान परमाणु बिजली स्टेशन और कैगा जेनरेटिंग स्टेशनसे दाब नलिकाओं की व्यापक विकिरणों उपरांत जांच से महत्वपूर्ण जानकारी प्राप्त हुई है, जिसमें अप्सरा-U की बेरिलिया रिफ्लेक्टर असेंबली और कामिनीरिएक्टर की ईंधन उप-असेंबली की पहली जांच शामिल है।

**कार्बनिक रूप से** बंधे ट्रिशियम और C-14 को मापने के लिए पर्यावरण निगरानी प्रणालियों को बेहतर संवेदनशीलता के साथ अर्ध-स्वचालित नमूना ऑक्सीकरण प्रौद्योगिकी के साथ उन्नत किया गया है। टीएलडीद्वारा व्यक्तिगत निगरानी में लगभग 23,000 विकिरण श्रमिकों की सुरक्षा को जारी रखा है।

**अपशिष्ट प्रबंधन** ने महत्वपूर्ण उपलब्धियां हासिल की हैं, जिसमें 70 के आयतन न्यूनीकरण घटक के और 4000 विसंद्रुषक घटक के साथ मध्यम स्तर के रेडियोधर्मी तरल अपशिष्ट का उपचार शामिल है। ट्रॉम्बे, तारापुर और कल्पाक्रम में पश्च भाग ईंधन चक्र सुविधाओं ने शानदार तरीके से काम किया, रेडियोधर्मी विसर्जन को प्रतिबंधित करते हुए मूल्यवान संसाधनों को निकाला। प्रिफ्री-2 तारापुर और ट्रॉम्बे में प्लूटोनियम प्लांट ने नवीनीकरण के बाद पुनः सफलतापूर्वक प्रचालन शुरू कर दिया है। द्रवीकृत बेड रिएक्टर में यूरेनिल नाइट्रेट के प्रत्यक्ष विनाइट्रीकरण ने नाभिकीय ईंधन चक्र में ऑक्साइड रूपांतरण को सरल बनाने में एक नई उपलब्धि को दर्शाया है।

भूक्तशेष ईंधन पुनर्संसाधन गतिविधियों के चिकित्सा अनुप्रयोग भापअ केंद्र के द्वारा मानवीय कल्याण को उजागर करते हैं, जिसमें नेत्र कैंसर के उपचार के लिए Ru-106 प्लॉक का निरंतर उत्पादन और न्यूरोएंडोक्राइन ट्यूमर थेरेपी के लिए क्लिनिकल-ग्रेड इट्रियम-90 का विकास शामिल है। ध्रुव के लिए उपयुक्त एक नई ईंधन भरण मशीन ऑरिफिस असेंबली विखंडन मोली ट्रे रॉड्स की ऑन-पावर प्रहस्तन में सुधार करती है, जबकि कैगा जेनरेटर स्टेशन-3 में प्रदर्शित एक अंडरवाटर रिमोट कटिंग प्रणाली में कोबाल्ट-60 रेडियोआइसोटोप उत्पादन को बढ़ाने की क्षमता है।

भापअ केंद्र की उच्च दक्षता वाली बंद आसवन स्तंभ प्रौद्योगिकी भारी पानी के उन्नयन के माध्यम से न्यूक्लियर पावर कॉर्पोरेशन ऑफ इंडिया लिमिटेड की फ्लीट मोड दाबित भारी पानी रिएक्टरपरियोजनाओं का सहयोग किया है। तुम्मलापल्ली यूरेनियम अयस्क के शुद्धिकरण के लिए विकसित एक नवीन प्रक्रिया, प्रचालन चरणों को कम करते हुए प्रतिप्राप्ति को बढ़ाकर अर्थव्यवस्था में सुधार कर रही है।

ये बहु-विषयक नवाचार, संरक्षा, दक्षता और सामाजिक कल्याण को प्राथमिकता देते हुए नाभिकीय प्रौद्योगिकी को उन्नत करने के प्रति भापअ केंद्र के व्यापक दृष्टिकोण को प्रदर्शित करते हैं।

## प्रगत प्रौद्योगिकियाँ, विकिरण प्रौद्योगिकियाँ और अनुप्रयोग

अनुसंधान रिएक्टर अप्सरा-यू 88% उपलब्धता के साथ प्रचालित रहा, जिससे कोर अभिक्रियाशीलता बढ़ी और न्यूट्रॉन प्रतिबिंबन में सुधार हुआ। ध्रुव 70 % उपलब्धता पर प्रचालित रहा, सैकड़ों नमूनों को किरणित किया तथा संरक्षा एवं शीतलन प्रणालियों में सुधार किया। भारी पानी उन्नयन संयंत्र ने 11 टन डाउनग्रेडेड भारी पानी को संसाधित किया, जबकि महत्वपूर्ण सुविधा ने विविध प्रयोगों में सहयोग किया। साइरसने रक्षा प्रकाशकों का उत्पादन और नये आइसोटोप सुविधाओं को चालू करने, वि-कमीशनिंग की ओर कदम बढ़ाया। पुराने अप्सरा को विज्ञान संग्रहालय के रूप में परिवर्तित किया जा रहा है। राष्ट्रीय सुविधा ध्रुव में न्यूट्रॉन कणपुंज अनुसंधान हेतु 75 से अधिक अनुसंधान समूहों ने न्यूट्रॉन प्रकीर्णन प्रयोग किए।

त्वरक, लेज़र और प्लाज्मा नवाचारों में, 10 MeV इलेक्ट्रॉन RF Linac ने बायो-हाइड्रोजेल उत्पादन और नाभिकीय अपशिष्ट पदार्थों के विकिरण परीक्षण जैसे नए उपयोग प्राप्त किए गए। एक नए निम्न-शीतित CO लेज़र ने विषाक्त गैसों के बिना स्थिर, उच्च-शक्ति उत्सर्जन प्राप्त किया। गैस शोधन और उत्प्रेरक प्रक्रियाओं सहित अनुप्रयोगों के लिए एक छह-इलेक्ट्रोड ग्लाइडिंग आर्क डिस्चार्ज टॉर्च विकसित किया गया। चुंबकीय पल्स वेल्डिंग परमाणु ईंधन अनुप्रयोगों में धातुओं को जोड़ने के लिए प्रभावी सिद्ध हुई, जिससे मजबूत, रिसाव-रोधी बंधन सुनिश्चित हुए।

संवेदक, संसूचक और विशेष उपकरणों में प्रगति में रिएक्टर शीतलक निगरानी के लिए स्वदेशी ताप वैद्युत युग्म संवेदक और विश्वसनीयता के लिए अतिरिक्त CPU के साथ उन्नत PLC प्रणाली शामिल हैं। एक नए फाइबर ऑप्टिक डुअल रिंग नेटवर्क ने वास्तविक समय के डेटा संचार में सुधार किया। बैगेज स्कैनर और छोटे He-3 न्यूट्रॉन संसूचकों के लिए क्ष-किरण संसूचक बनाया गया। उच्च तापमान वाले बोरोन-लेपित आयन कक्ष और एक स्वचालित दाबित भारी पानी रिएक्टर ईंधन छड़क्रमवीक्षण प्रणाली नाभिकीय संरक्षा में सुधार किया। स्वदेशी PuCAM लगातार हवा में मौजूद प्लूटोनियम की निगरानी करता है। प्लास्टिक सिंटिलेटर के लिए पॉलीस्टाइरिन पेलेट और कंपन माप के लिए एक लेज़र-आधारित वाइब्रोसेंस उपकरण विकसित किया गया। भापअ केंद्र द्वारा विकसित क्ष-किरण प्रकीर्णन को इसरो के एक्सपोसैट मिशन में एकीकृत किया गया।

रेडियोभेषजिक में, ल्यूटीशियम-177, आयोडीन-131 और मोलिब्डेनम-99 के बड़े पैमाने पर उत्पादन ने नैदानिक उपयोग को बढ़ावा दिया। यकृत कैंसर के लिए भाभास्फ़ीयर और गठिया के लिए Er-लेबल वाले सूक्ष्मकणों जैसे नए संरूपण ने आशाजनक परिणाम दिखाए। नए रेडियोलेबल यौगिकों ने कैंसर का पता लगाने के साथ उपचार को बेहतर बनाया, जिसमें स्तन कैंसर को लक्षित करने वाली रेडियोइम्यूनोथेरेपी भी शामिल है।

जल शोधन, भूजल प्रबंधन और ठोस अपशिष्ट प्रबंधन के क्षेत्र में, इलेक्ट्रॉन कणपुंज उपचार ने कपड़ा उद्योग के अपशिष्ट जल प्रदूषकों को काफी हद तक कम किया। विकिरण-सहायता प्राप्त अधिशोषक और सेल्यूलोज-आधारित सामग्री ने रंगों और पारे को कुशलतापूर्वक अलग किया। सुपरहाइड्रोफोबिक जूट के कपड़ों ने 95% से अधिक माइक्रोप्लास्टिक कम किया है। भापअ केंद्र को प्रौद्योगिकी से युक्त जल शोधन इकाइयाँ भारत भर में व्यापक रूप से परिनियोजित की गईं, जिनमें प्रमुख रेलवे स्टेशन और सीमा चौकियाँ शामिल हैं। परमाणु विलवणीकरण प्रदर्शन संयंत्र ने बिजली स्टेशनों को लाखों लीटर शुद्ध जल की आपूर्ति की।



विकिरण प्रौद्योगिकी ने नई, उच्च उपज देने वाली किस्मों को जारी करने में मदद की, जिससे कुल किस्मों की संख्या 70 हो गई और भापअ केंद्र के भंडारण प्रोटोकॉल ने दीर्घकालिक भंडारण के बाद 1,000 टन प्याज के सफल विपणन को सक्षम बनाया। विक्रम ट्रॉम्बे छत्तीसगढ़ चावल के प्रमाणित बीज किसानों को वितरित किए गए, जिससे बेहतर फसल की उम्मीद जगी।

स्वच्छ ऊर्जा की खोज में, कॉपर-क्लोरीन चक्र के लिए एक बेंच-स्केल एकीकृत सुविधा को 165 घंटे से अधिक समय तक लगातार प्रचालित किया गया, जिससे हाइड्रोजन उत्पादन में वृद्धि हुई —यह शुद्ध-शून्य भविष्य की ओर एक महत्वपूर्ण कदम है। उच्च शुद्धता वाली कैल्शियम धातु निष्कर्षित की गई और संयंत्र जोखिमों को मापने के लिए एक संभाव्य संरक्षा मूल्यांकन सॉफ्टवेयर टूल विकसित किया गया। नाल्को के सहयोग से, भापअ केंद्र ने एल्यूमिना की पहली स्वदेशी प्रमाणित संदर्भ सामग्री का उत्पादन किया, जिससे औद्योगिक गुणवत्ता मानकों को मज़बूती मिली।

इन प्रगतियों ने स्वास्थ्य, पर्यावरणीय स्थिरता और प्रौद्योगिकी की आत्मनिर्भरता में योगदान दिया।

## बुनियादी और निर्देशित अनुसंधान

भापअ केंद्र में बुनियादी और निर्देशित अनुसंधान प्रयास एक सहक्रियात्मक मॉडल का निर्माण करते हैं, जहाँ मूलभूत विज्ञान प्रौद्योगिकी नवाचार को आगे बढ़ाया जाता है, और लक्षित अनुसंधान को एक मज़बूत वैज्ञानिक आधार से लाभान्वित होता है। यह एकीकृत दृष्टिकोण भारत की नाभिकीय एवं वैज्ञानिक क्षमताओं में निरंतर प्रगति सुनिश्चित करता है।

अक्टूबर 2024 में, भापअ केंद्र ने लद्दाख के हानले में एशिया की सबसे बड़ी और दुनिया की सबसे ऊंची MACE (मेस) इमेजिंग चेरेंकोव वेधशाला का उद्घाटन किया। यह अत्याधुनिक वेधशाला खगोल भौतिकी में अनुसंधान को महत्वपूर्ण रूप से आगे बढ़ाएगी, विशेष रूप से उच्च-ऊर्जा गामा किरणों का पता लगाने में, और वैश्विक वैज्ञानिक अनुसंधान में भारत की स्थिति को मज़बूत करते हुए भारतीय वैज्ञानिकों की भावी पीढ़ियों को प्रेरित करेगी।

ठोस अवस्था भौतिकी में, भापअ केंद्र ने उल्लेखनीय प्रगति की, जिसमें फोनन व्यवहार और MLMD सिमुलेशन के माध्यम से वैनेडियम के विषम उष्मीय विस्तार की व्याख्या करना शामिल है। प्रमुख विकासों में स्थिर पतली-फिल्म बैटरी के लिए LiPON ठोस इलेक्ट्रोलाइट्स का निर्माण और  $TiS_3$  और इन्सुलेटिंग N-डोप  $LuH_3$  चरणों में दबाव-प्रेरित अर्धचालकसेधातु संक्रमण की खोज भी शामिल है। तकनीकी भौतिकी में, भापअ केंद्र ने एक 50 cc HPGेससूचक विकसित किया, जिसने 662 keV पर 0.39% का ऊर्जा रिज़ॉल्यूशन हासिल किया, जिससे यह उच्च-सटीक गामा स्पेक्ट्रमदर्शी के लिए उपयुक्त हो गया। इस क्षेत्र में अतिरिक्त सफलताओं में विरासत अध्ययनों के लिए न्यूट्रॉन टोमोग्राफी, उच्च-परावर्तकता वाले क्ष-किरण सुपरमिरर का निर्माण, नाभिकीय ईंधन विश्लेषण के लिए इन-हाउस मास स्पेक्ट्रोमीटर और वैज्ञानिक उपकरणों के लिए कॉम्पैक्ट इलेक्ट्रॉनिक्स और उच्च-स्थिरता वाले उच्च-वोल्टेज मॉड्यूल का विकास शामिल है।

नाभिकीय भौतिकी में भी उल्लेखनीय प्रगति हुई है, भापअ केंद्र-टीआईएफआरशोधकर्ताओं ने प्री-एक्टिनाइड नाभिक में एक नए द्रव्यमान-असममित विखंडन द्वीप की खोज कर रहा है, जो वर्तमान मॉडलों को चुनौती देता है। अध्ययनों ने धीमी अर्ध-विखंडन में शेल प्रभावों की भूमिका की पुष्टि की, और भारी-आयन विखंडन में नए प्रोटॉन उत्सर्जन पैटर्न देखे गए। न्यूट्रिनो, गामा और सिंक्रोट्रॉन-आधारित अध्ययनों में प्रगति ने नाभिकीय विज्ञान में समझ को आगे बढ़ाया। क्वांटम भौतिकी में, भापअ केंद्र ने स्वदेशी लेज़र-वाष्पीकरण सेटअप का उपयोग करके छोटे लैथेनाइड धातु और ऑक्साइड समूहों को सफलतापूर्वक स्थिर संरचनाएँ निर्दिष्ट किया। क्वांटम संसूचन में, रुबिडियम परमाणुओं में बढ़ी हुई दो-फोटॉन सुसंगत समष्टि पाश को लांबिक चुंबकीय क्षेत्रों के साथ द्विवर्णी गोलाकार ध्रुवीकृत प्रकाश का उपयोग करके प्रदर्शित किया गया, जिसने क्वांटम संसूचन अनुप्रयोगों की प्रगति में योगदान दिया।

रासायनिक विज्ञान के क्षेत्र में, भापअ केंद्र ने नैनोप्रौद्योगिकी और दवा वितरण के बारीक पहलुओं में नई प्रगति पाई है। क्यूकरबिट्यूरिल-फंक्शनलाइज्ड गोल्ड नैनोपार्टिकल्स ( $CB7AuNPs$ ), जो एंटीबायोटिक गतिविधि को बढ़ाते हैं, और  $SCx6AuNPs$ , जो लक्षित दवा वितरण और जैव प्रतिबिंबन के लिए आशाजनक हैं, विकसित किए गए। भापअ केंद्र ने संवेदन और उत्प्रेरक में भी महत्वपूर्ण प्रगति की है, सेरोटोनिन और  $NO_2$  का पता लगाने के लिए संसूचक विकसित किए हैं, साथ ही हाइड्रोजन उत्पादन और  $Ag-MOF/g-C_3N_4$  पदार्थों का उपयोग करके फोटोकैटलिटिक सुधार हेतु वैनेडियम कंपोजिट विकसित किए हैं। माइक्रो-रमन स्पेक्ट्रमदर्शी का उपयोग से किए गए अध्ययनों

से पता चला है कि सोडियम आयोडाइड-मैलोनिक अम्ल एरोसोल में आयोडाइड की कमी बढ़ती आर्द्रता के साथ तीव्र होती है, जो वायुमंडलीय आयोडीन रसायन विज्ञान में सापेक्ष आर्द्रता की महत्वपूर्ण भूमिका को उजागर करती है।

**भापअ केंद्र ने NALCO (नाल्को) के सहयोग से-B1301 जारी किया, जो ISO मानकीकृत एक प्रमाणित एल्यूमिना संदर्भ सामग्री है।** इस विकास को पड़ोसपरियोजनाओं के लिए विश्लेषणात्मक सेवाओं में भापअ केंद्र के समर्थन द्वारा पूरक बनाया गया। भापअ केंद्र ने अनुसंधान उद्देश्यों हेतु तांबे के सबस्ट्रेट से चुनिंदा रूप से Lu आइसोटोप को निष्कर्षित करने के लिए प्रोटोकॉल का भी बीड़ा उठाया। भापअ केंद्र में पर्यावरण और स्थिरता अनुसंधान के परिणामस्वरूप मूल में तीव्र यूरेनियम पॉलिमरिक अधिशोषक के आकलन के लिए, पानी से यूरेनियम निष्कर्षण हेतु ZIF-67 मिश्रित मोती और जर्कोनियम मिश्रधातुओं से नायोबियम पृथक्करण के लिए विलायक निष्कर्षण विधियों का विकास हुआ। इसके अतिरिक्त, रेडियोन्यूक्लाइड उपचार के लिए संशोधित ग्रेफीन ऑक्साइड और कार्बन नैनोट्यूब की खोज की गई और कार्बनिक प्रदूषक क्षरण के लिए सोने के नैनोकणों का उपयोग करने वाली एक उत्प्रेरक प्रणाली विकसित की गई।

**परिकलनात्मक द्रव गतिकी (सीएफडी) और आप्विक गतिकी (एमडी) मॉडल का उपयोग करते हुए,** भापअ केंद्र ने विभिन्न घटनाओं का अध्ययन किया जैसे कि स्पंदनशील प्रवाह में बुद्बुदकी गतिविधि, डूबे हुए नोज़ल पर बूंद का निर्माण, कण प्रवाह की गतिकी और नैनोट्यूब झिल्ली का उपयोग करके समुद्री जल विलवणीकरण। अन्य सिमुलेशन में एक्टिनाइड धातुओं की तापीय चालकता और झिल्ली के माध्यम से आयन परिवहन की जांच शामिल थी।

**स्वास्थ्य सेवा और कैंसर अनुसंधान में,** डायहाइड्रॉक्सीस्टिलबेन को टैलाज़ोपैरिब के साथ मिलाकर, शोधकर्ताओं ने डीएनए क्षति को प्रेरित करने और डिम्बग्रंथि के कैंसर कोशिकाओं को मारने में सक्षम बनाया। अन्य प्रगति में प्रोस्टेट कैंसर कोशिका क्षय को बढ़ाने के लिए PSMA-लक्षित डॉक्सोरेबिसिन का विकास और कैंसर कोशिकाओं में CHK1 और TOP1 के ATR विनियमन की पहचान शामिल है। TFEB नॉकडाउन को PARP अवरोधकों के लिए अग्राशय दोनों के कैंसर की संवेदनशीलता में वृद्धि करता हुआ पाया गया, जबकि माइटोकरक्यूमिन ने स्तन और अग्राशय के कैंसर कोशिकाओं को लक्षित करने में प्रभावशीलता का प्रदर्शन किया है।

**कृषि में जैव-विज्ञान अनुसंधान** ने भी बहुमूल्य जानकारी प्रदान की है, जिसमें मूंगफली के उत्परिवर्ती की पहचान की गई है, जिसमें 70% अधिक बीज भार है, जो एक विशिष्ट जीन के डाउनरेगुलेशन से जुड़ा है। बाजरे में 53 अमोनियम ट्रांसपोर्टर जीन की खोज की गई है और पाया गया है कि MusaDREB1 जैसे प्रोटीन केले के प्रतिबल सह्यता को बढ़ाते हैं। अन्य अध्ययनों से पता चला है कि बायोचार चावल में आर्सेनिक के स्तर को कम कर सकता है, और ट्राइकोडर्मा विरेन सोयाबीन में पोटेसियम की कमी को दूर कर सकता है।

**भापअ केंद्र के स्वास्थ्य सेवा और दवा खोज अनुसंधान** ने फेफड़े के सर्फेक्टेंट पर थोरियम के प्रभाव का पता लगाया है और रेडियो प्रतिरोध के तंत्र की जांच की है, जिससे रेडियोप्रोटेक्टिव अभिकर्मक विकसित हुए हैं। कैंसर अनुसंधान के क्षेत्र में, भापअ केंद्र ने प्रोटीन बाइंडर, CPL-एक्टिव डाई और गामा डोज़ीमीटर सहित नए प्रतिदीप्त, जैव-निम्नीकरण यौगिकों और कैंसररोधी कर्मक पर ध्यान केंद्रित किया है, जो निदान, चिकित्सीय अनुप्रयोगों और पर्यावरण उपचार में प्रगति को दर्शाता है।

## मानव संसाधन, वैज्ञानिक सूचना और प्रौद्योगिकी प्रबंधन

**डॉ. होमी जे. भाभा** ने पड़ोस में प्रशिक्षण विद्यालय प्रणाली के स्थापना की परिकल्पना की, और पहला प्रशिक्षण विद्यालय वर्ष 1957 में तत्कालीन बॉम्बे (अब मुंबई) में स्थापित किया गया था, जिसने आंतरिक प्रयासों के माध्यम से पेशेवरों के प्रशिक्षण के लिए एक उत्कृष्ट केंद्र के रूप में प्रतिष्ठा पाई। इन वर्षों में, लगभग 11,000 प्रशिक्षुओं ने प्रशिक्षण विद्यालयों के प्रांगण से उमंग एवं उत्साह के साथ स्नातक किया।

**भापअ के प्रशिक्षण विद्यालय** ओसीईएस/डीजीएफएस-2023 कार्यक्रम के 67वें बैच के कुल 177 स्नातक प्रशिक्षु वैज्ञानिक अधिकारियों (73 अभियांत्रिकी + 58 विज्ञान, जिसमें 12 विकिरणकीय सुरक्षा और पर्यावरण विज्ञान (आर. एस. ई. एस.) शामिल हैं) को एक वर्ष का प्रशिक्षण सफलतापूर्वक पूरा करने के बाद भापअ के विभिन्न प्रभागों में शामिल किया गया। इन प्रशिक्षुओं में 10 प्रशिक्षु रक्षा अधिकारी थे, जो इस बैच के साथ उत्तीर्ण हुए और उन्हें स्नातकोत्तर प्रौद्योगिकी (एम. टेक) के लिए परियोजना आरंभ करने हेतु विभिन्न प्रभागों/इकाइयों में नियुक्त किया गया। एनटीपीसी के दो अधिकारियों ने ओसीईएस/डीजीएफएस-2023 बैच में भी अपना प्रशिक्षण कार्य पूर्ण किया।

**भापअ केंद्र ने ट्रॉम्बे संगोष्ठी का आयोजन किया,** जिसमें विविध वैज्ञानिक क्षेत्रों से पांच प्रख्यात वक्ताओं ने भाग लिया, उन्होंने हमारे ब्रह्मांड के भविष्य से लेकर भारतीय वैक्सीन के विकास तक के विषयों पर अपने विचार साझा किए। वक्ताओं में राष्ट्रीय विज्ञान अध्ययन एवं

अनुसंधान संस्थान, भुवनेश्वर के मानद शिक्षावृत्तिभोगी प्रो. अशोक सेन, भारतीय आयुर्विज्ञान संस्थान, नई दिल्ली के कार्डियोथोरेसिक सेंटर के प्रमुख प्रो. बलराम भार्गव, इंडिया टुडे ग्रुप के समूह संपादन निदेशक श्री राज चेंगप्पा, विश्व स्वास्थ्य संगठन की पूर्व मुख्य वैज्ञानिक डॉ. सौम्या स्वामीनाथन और भारत सरकार के अंतरिक्ष आयोग के सदस्य श्री ए.एस. किरण कुमार शामिल थे।

भापअ केंद्र ने चिंतन बैठक का भी आयोजन किया, जो भापअ केंद्र समुदाय के लिए एक सहयोग मंच था, जिसमें प्रोटॉन त्वरक और अमृतकाल लक्ष्यों के साथ संरक्षण पर चर्चा के साथ अनुसंधान एवं विकास गतिविधियों पर ध्यान केंद्रित किया गया।

भापअ केंद्र ने तीन पुस्तकें- “IMPACT 2019-2024” जिसमें वैज्ञानिक गतिविधियों का दस्तावेजीकरण किया गया है, “जैविक प्रणालियों में आयनकारी विकिरण के लाभकारी प्रभाव” और भापअ केंद्र के वामनवृक्ष संग्रह के बारे में “द मिनिचर मार्बल्स”

भापअ केंद्र अपने ज्ञान एवं सूचना संसाधनों को व्यापक रूप से सुदृढ़ बनाया है। यहां वैज्ञानिक पुस्तकों की प्रदर्शनियों का आयोजन किया जाता है और सूचना बुलेटिनों तथा नाभिकीय वेब डाइजैस्ट के साथ-साथ केंद्र के वैज्ञानिक एवं प्रौद्योगिकी परिणामों को प्रदर्शित करने वाले रोचक विषयों पर केंद्रित समाचार पत्र एवं स्मारिकाएं समय-समय पर जारी किए जाते हैं।

शैक्षणिक संसाधनों में सदस्यता के माध्यम से 1,400 से अधिक पत्रिकाओं तक पहुंच शामिल है, जिसमें भापअ केंद्र शोधकर्ताओं द्वारा वर्ष 2024 में लगभग 1500 प्रकाशन किया जा रहा है। इसने अपने वैज्ञानिक समुदाय तक जर्नल संसाधनों की पहुंच का विस्तार करने के लिए एक पञ्च एक सदस्यता की संरचना को (ODOS) सक्रिय रूप से लागू किया है।

राजभाषा (हिंदी) कार्यान्वयन में, भापअ केंद्र ने 198 अधिकारियों के लिए तैमासिक कार्यशालाएं और भाषा पाठ्यक्रम आयोजित किए, हिंदी प्रयोग में उत्कृष्ट प्रदर्शन करने वाले 81 अधिकारियों को नकद प्रोत्साहन पुरस्कार प्रदान किए गए। प्रतियोगिताओं और सांस्कृतिक गतिविधियों के साथ विश्व हिंदी दिवस और हिंदी माह का आयोजन किया गया। न्यूकडेका और तकनीकी लेख सारांश सहित नई हिंदी कृतियाँ प्रकाशित की गईं और जनवरी 2025 में भापअ केंद्र की आधिकारिक हिंदी वेबसाइट का शुभारंभ किया गया। संसदीय राजभाषा समिति द्वारा दिनांक 19 जनवरी, 2024 को भापअ केंद्र का राजभाषा कार्यान्वयन संबंधी निरीक्षण किया।

प्रौद्योगिकी प्रबंधन के लिए, भापअ केंद्र ने 43 प्रौद्योगिकियों के लाइसेंस के लिए 53 फर्मों के साथ 60 समझौते किए, 9 नई प्रौद्योगिकियों को सार्वजनिक क्षेत्रों के लिए जारी किया, 11 प्रौद्योगिकियों के उद्घवन के साथ अटल उद्घवन केंद्र की स्थापना की, और शैक्षणिक संस्थानों के साथ 8 नए समझौतों के माध्यम से ग्रामीण एवं शहरी प्रौद्योगिकी कार्यान्वयन के लिए आकृतिकार्यक्रम का विस्तार किया।

## विज्ञान एवं प्रौद्योगिकी जन-संपर्क

भापअ केंद्र नागरिकों के साथ संवाद स्थापित करने तथा विज्ञान एवं प्रौद्योगिकी को बढ़ावा देने के लिए व्यापक जन-संपर्क कार्यक्रमों का आयोजन करता है। यह केंद्र भारत के, विभिन्न संस्थानों के छात्रों को ट्रॉम्बे परिसर स्थित बहु-विषयक शोध गतिविधियों को देखने और वैज्ञानिक करियर के प्रति प्रेरित करने के लिए भ्रमण की सुविधा प्रदान करता है। इस अवधि के दौरान भाग लेने वाले संस्थानों में मुंबई, महाराष्ट्र और पड़ोसी राज्यों जैसे SVNIT सूरत, कार्मेल कॉलेज, गोवा तथा विल्सन कॉलेज और पोद्दार इंटरनेशनल स्कूल सहित मुंबई स्थित कई संस्थान शामिल हैं।

अगस्त 2024 में, भापअ केंद्र ने नाभिकीय प्रौद्योगिकी से संबंधित जानकारी साझा करने के लिए रायपुर, छत्तीसगढ़ में एक जन-संपर्क कार्यक्रम आयोजित किया, जिसमें पांच कॉलेजों के लगभग 1,200 विद्यार्थियों और शिक्षकों ने भाग लिया।

विद्यालय जनसंपर्क के नए कार्यक्रम “परमाणु ज्योति” के अभियान-IV के भाग के रूप में, भापअ केंद्र के वैज्ञानिक अधिकारियों ने चार उत्तर भारतीय राज्यों के 48 जवाहर नवोदय विद्यालयों और परमाणु ऊर्जा केंद्रीय विद्यालयों का दौरा किया, तथा 18,000 से अधिक छात्रों तक पहुँच बनाई।

राष्ट्रीय विज्ञान दिवस 2024, जिसका विषय था “समाज के लिए परमाणु: जल, भोजन एवं स्वास्थ्य की सुरक्षा,” इस अवसर पर प्रोफेसर के. विजयराघवन (होमी भाभा चेयर प्रोफेसर और भारत सरकार के पूर्व प्रधान वैज्ञानिक सलाहकार) मुख्य अतिथि के रूप में उपस्थित हुए, जबकि



राष्ट्रीय प्रौद्योगिकी दिवस 2024 के अवसर पर जनरल अनिल चौहान उपस्थित हुए। ये कार्यक्रम राष्ट्रीय विकास में भापअ केंद्र के योगदान को प्रदर्शित करते हैं और छात्रों को प्रसिद्ध वैज्ञानिकों के साथ संवाद करने के लिए एक मंच प्रदान करते हैं।

## सुरक्षित एवं संरक्षित कार्यस्थल

भापअ केंद्र सुरक्षा परिषद (बीएससी) ने व्यापक सुविधा समीक्षाओं के माध्यम से कार्यस्थल सुरक्षा के लिए मज़बूत प्रतिबद्धता प्रदर्शित की है। वर्ष 2024 में, बीएससी और इसकी समितियों ने 8 परिषद बैठकें और 178 समिति सत्र आयोजित किए, जिसके परिणामस्वरूप 92 सुविधा को संस्वीकृति, 65 रेडियोधर्मी अपशिष्ट प्रबंधन प्राधिकरण और 109 विकिरण स्रोत को अनुमोदन प्रदान किया गया। इसने 124 विनियामक निरीक्षण किए, 30 रेडियोधर्मी शिपमेंट को मंजूरी दी और 46 आपातकालीन तैयारी अभ्यासों की देखरेख की।

प्रचालन कार्य के अतिरिक्त, बीएससी ने विनियामक प्रक्रियाओं पर एक नई सुरक्षा मार्गदर्शिका प्रकाशित की, घटना रिपोर्टिंग और निरीक्षण प्रक्रियाओं पर दस्तावेज़ तैयार किए, और कई स्थानों पर प्रशिक्षण पाठ्यक्रम आयोजित किए। इन प्रयासों का समापन विकिरण सुविधा विनियामक उपायों पर दिसंबर 2024 की थीम बैठक में हुआ, जिसमें अपने प्रचालन के दौरान असाधारण सुरक्षा मानकों को बनाए रखने के लिए भापअ केंद्र की प्रतिबद्धता पर प्रकाश डाला गया।

## आधारभूत ढांचे का विकास

भापअ केंद्र ने अपनी सुविधाओं और स्थिरता को बढ़ाने के लिए कई आधारभूत ढांचा परियोजनाएं कार्यान्वित की हैं।

अणुशक्ति नगर में एचआरडीडी प्रशिक्षण विद्यालय परिसर में एक अत्याधुनिक डिजिटल स्टूडियो की स्थापना की गई, जिसमें नाभिकीय विज्ञान एवं अभियांत्रिकी में प्रसारण-गुणवत्ता वाली ई-लर्निंग सामग्री के लिए सटीक ध्वनिक अभिकल्पन और उन्नत ऑडियो-विजुअल उपकरण शामिल हैं। स्टूडियो वीडियो रिकॉर्डिंग, संपादन, वेब स्ट्रीमिंग, दूरस्थ शिक्षण और साक्षात्कार सहित विभिन्न कार्यों को सहयोग प्रदान करता है। इसके अतिरिक्त, प्रशिक्षण विद्यालय परिसर में छह व्याख्यान कक्षों को अत्याधुनिक एवी प्रणाली के साथ आधुनिक बनाया गया।

भापअ केंद्र अस्पताल के लिए शून्य-निर्वहन आवश्यकताओं को पूरा करने और संभावित जल की कमी को दूर करने के लिए 250 kLD वाहित मल शोधन संयंत्र स्थापित किया गया। यह संयंत्र महाराष्ट्र प्रदूषण नियंत्रण बोर्ड के मानकों को पूरा करने वाले खाद-उपयोग योग्य ठोस अपशिष्ट और उपचारित तरल का उत्पादन करने के लिए भापअ केंद्र की अनुक्रमिक बैच रिएक्टर तकनीक का उपयोग करता है।

भाभा वनस्पति उद्यान को पौधों की प्रजातियों और जैव विविधता संरक्षण के लिए एक जीवंत भंडार के रूप में पुनः विकसित किया गया है, जिसमें एक ध्यान क्षेत्र भी है। यहां सौर ऊर्जा चालित सिंचाई के लिए 70 वर्ष पुराने दो कुएं और छाया के लिए जालीदार पौधे लगाए गए हैं।

ओडिशा में ओएससीओएम में, जल आवश्यकताओं को पूरा करते हुए स्वदेशी प्रौद्योगिकियों का परीक्षण करने के लिए 5.0 एमएलडी विलवणीकरण परियोजना के लिए समुद्री जल अंतर्ग्रहण प्रणाली विकसित की गई।

प्रशिक्षण विद्यालय छात्रावास परिसर में 50 किलोग्राम दैनिक क्षमता वाला एक पोर्टेबल निसर्गुना बायोगैस संयंत्र चालू किया गया, जिसमें सर्पिल पाइप निर्माण के साथ एक कॉम्पैक्ट अभिकल्प है जो पारंपरिक गड्डों की आवश्यकता को पूरा करता है और समृद्ध जैविक खाद का उत्पादन करता है।

लद्दाख में 14,000 फीट की ऊंचाई पर स्थित एमएसीई सुविधा का दौरा करने वाले अधिकारियों के लिए एक उच्च ऊंचाई वाले अतिथिगृह का निर्माण किया गया, जिसमें ठंड से बचाव के लिए सौर-निष्क्रिय अभिकल्पन तत्वों को शामिल किया गया।

संग्रहित वर्षा जल से बिजली उत्पन्न करने के लिए प्लूटोनियम प्लांट झील पर 15 किलोवाट की सूक्ष्म जल विद्युत इकाई स्थापित की गई।

विदेशी फूलों और उष्णकटिबंधीय ऑर्किड की खेती के लिए भापअ केंद्र, ट्रॉम्बे में तीन पूर्ण स्वचालित पॉलीहाउस विकसित किए गए, जो पौधों के प्रसार, संरक्षण और नई प्रजातियों के अनुकूलन में सहायक होंगे।

# Executive Summary

## INDIAN NUCLEAR POWER PROGRAMME

From the depths of reactor cores to the frontiers of medical applications, the Bhabha Atomic Research Centre (BARC) continues to push boundaries across multiple domains of nuclear science and technology.

**In reactor inspection**, BARCIS systems have successfully completed critical pre-service inspections at RAPP-7 and KAPP-4, while innovative ECT-based tools now complement existing inspection technologies for 540MWe PHWR pressure tubes. At KAPP-4, BARCIS conducted a volumetric inspection of 18 coolant channels and 25 rolled joints. Automated systems for fuel pellet scanning ensure manufacturing quality at the Nuclear Fuel Complex, with a new X-ray imaging system software eliminating time-consuming manual inspections.

**Reactor development** showed impressive progress, with BARC providing crucial support for RAPS-3 startup after coolant channel and feeder pipe replacement and playing key roles in design validation and safety analysis for KAPP-3 full power operation and KAPP-4 criticality. Completing magnetic jack reactivity control mechanisms for IPWRs and SMRs advances future reactor technologies. A small gas-cooled reactor designed for hydrogen production maintains negative reactivity coefficients throughout burn-up. At the same time, the experimental Indian Molten Salt Reactor has completed its first phase of testing.

**BARC has designed and developed the fuelling machine** for the Prototype Fast Breeder Reactor for fast reactor technology, fabricated MOX fuel regularly and created specialized high-temperature neutronic detectors and safety systems. A digital radiography system and automated welding end plugs metrology system now augment Fast Breeder Test Reactor fuel pin fabrication.

**Materials science** innovations include the development of accident-tolerant fuel cladding with a chromium coating on Zircaloy-4, showing remarkable oxidation resistance at high temperatures. Indigenous NiMoCrTi-C alloy plates have been successfully produced for molten salt breeder reactor loops, while nanostructured boron carbide demonstrates superior mechanical and thermal properties. Comprehensive post-irradiation examination of pressure tubes from MAPS, RAPS, and KGS provides valuable insights, with the first-ever examination of APSARA-U's Beryllia Reflector Assembly and KAMINI reactor's fuel sub-assembly.

**Semi-automatic sample oxidation technology** has enhanced environmental monitoring systems for measuring Organically Bound Tritium and C-14 with improved sensitivity. TLD personnel monitoring continues to protect approximately 23,000 radiation workers.

**Waste management** has contributed significant achievements, including treating intermediate-level radioactive liquid waste with volume reduction factors of 70 and decontamination factors of 4000. Back-end fuel cycle facilities at Trombay, Tarapur, and Kalpakkam operated excellently, extracting valuable resources while restricting radioactive discharge. PREFRE-2 Tarapur and Plutonium Plant at Trombay have successfully resumed operations after refurbishment. The direct denitration of uranyl nitrate in a fluidized bed reactor marks a new achievement in simplifying oxide conversion in the nuclear fuel cycle.

**Medical applications of spent fuel reprocessing** activities highlight BARC's humanitarian impact, with continued production of Ru-106 plaques for eye cancer treatment and development of clinical-grade Yttrium-90 for neuroendocrine tumor therapy. A new fuelling machine orifice assembly qualified for DHRUVA improves on-power handling of fission moly tray rods. At the same time, an underwater remote-cutting system demonstrated at KGS-3 can potentially increase Cobalt-60 radioisotope production.

**BARC's high-efficiency packed distillation column technology** for heavy water upgrades has supported NPCIL's fleet mode PHWR projects. An innovative process for the purification of

Tummalapalle uranium ore improves the economy by enhancing recovery while reducing operating steps.

These multidisciplinary innovations demonstrate BARC's comprehensive approach to advancing nuclear technology while prioritizing safety, efficiency, and societal welfare.

## **ADVANCED TECHNOLOGIES, RADIATION TECHNOLOGIES AND APPLICATIONS**

**Research Reactor** Apsara-U operated with 88% availability, enhancing core reactivity and advancing neutron imaging. Dhruva operated at 70% availability, irradiating hundreds of samples and improving safety and cooling systems. The Heavy Water Upgrading Plant processed 11 tons of downgraded heavy water, while the Critical Facility supported diverse experiments. CIRUS moved towards decommissioning, producing defense illuminators, and commissioning new isotope facilities. Old Apsara is being converted into a Science Museum. At the National Facility for Neutron Beam Research at Dhruva, more than 75 research groups performed neutron scattering experiments.

**In Accelerator, Laser and Plasma** innovations, the 10 MeV electron RF Linac found new uses like bio-hydrogel production and radiation testing of nuclear waste materials. A novel cryo-cooled CO laser achieved stable, high-power emission without toxic gases. A six-electrode gliding arc discharge torch was developed for applications including gas purification and catalytic processes. Magnetic Pulse Welding proved effective for joining metals in nuclear fuel applications, ensuring strong, leak-tight bonds.

**Advancements in Sensors, Detectors, and Specialized Instruments** include indigenous thermocouple sensors for reactor coolant monitoring and enhanced PLC systems with redundant CPUs for reliability. A novel fiber optic dual ring network improved real-time data communication. X-ray detectors for baggage scanners and small He-3 neutron detectors were fabricated. High-temperature boron-coated ion chambers and an automated PHWR fuel pellet scan system improved nuclear safety. The indigenous PuCAM monitors airborne plutonium continuously. Polystyrene pellets for plastic scintillators and a laser-based VibroSense instrument for vibration measurement were developed. BARC-developed X-ray scatterer has been integrated into ISRO's XPoSat mission.

**In Radiopharmaceuticals**, large-scale production of Lutetium-177, Iodine-131, and Molybdenum-99 supported clinical use. Innovative formulations like BhabhaSpheres for liver cancer and Er-labeled microparticles for arthritis showed promising results. Novel radiolabeled compounds enhanced cancer detection and therapy, including radioimmunotherapy targeting breast cancer.

**In the realm of Water Purification**, Groundwater Management & Solid Waste Management, electron beam treatment drastically reduced textile wastewater pollutants. Radiation-assisted adsorbents and cellulose-based materials efficiently removed dyes and mercury. Superhydrophobic jute fabric achieved over 95% microplastic removal. Water purification units equipped with BARC technology know-how were widely deployed across India, including prominent railway stations and border outposts. The Nuclear Desalination Demonstration Plant supplied millions of liters of pure water to power stations.

**Radiation technology** helped release new, high-yielding crop varieties, taking the total count to 70 varieties, and BARC's storage protocols enabled the successful marketing of 1,000 tons of onions after long-term storage. Certified Vikram Trombay Chhattisgarh Rice seeds were distributed to farmers, bringing hope for better harvests.

**In pursuit of clean energy**, a bench-scale integrated facility for the Copper-Chlorine cycle was operated continuously for more than 165 hours, advancing hydrogen production — a key step toward a net-zero future. High-purity calcium metal was extracted, and a Probabilistic Safety Assessment Software Tool was developed to quantify plant risks. In collaboration with NALCO, BARC produced the first indigenous certified reference material of alumina, strengthening industrial quality standards.

These advancements contributed to health, environmental sustainability, and technological self-reliance.



## BASIC AND DIRECTED RESEARCH

**BARC's directed research** efforts form a synergistic model where foundational science drives technological innovation, and targeted research benefits from a strong scientific base. This integrated approach ensures sustained progress in India's nuclear and scientific capabilities.

**BARC inaugurated Asia's** most extensive and the world's highest MACE Imaging Cherenkov Observatory in Hanle, Ladakh in October 2024. This state-of-the-art observatory will significantly enhance research in astrophysics, particularly in detecting high-energy gamma rays, and is expected to inspire future generations of Indian scientists while strengthening India's standing in global scientific research.

**BARC made notable advances in Solid-state Physics**, including explaining Vanadium's anomalous thermal expansion through phonon behavior and MLMD simulations. Key developments also include the creation of LiPON solid electrolytes for stable thin-film batteries and discovering pressure-induced semiconductor-to-metal transitions in  $\text{TiS}_3$  and insulating N-doped  $\text{LuH}_3$  phases. In technical physics, BARC developed a 50 cc HPGe detector, which achieved an energy resolution of 0.39% at 662 keV, making it suitable for high-precision gamma spectroscopy. Additional breakthroughs in this area include neutron tomography for heritage studies, the creation of high-reflectivity X-ray supermirrors, in-house mass spectrometers for nuclear fuel analysis, and the development of compact electronics and high-stability high-voltage modules for scientific instruments.

**Nuclear Physics** has also seen significant strides, with BARC-TIFR researchers discovering a new mass-asymmetric fission island in pre-actinide nuclei, challenging current models. Studies confirmed the role of shell effects in slow quasi-fission, and new proton emission patterns were observed in heavy-ion fission. Advancements in neutrino, gamma, and synchrotron-based studies further expanded our understanding of nuclear science. BARC successfully assigned stable structures to small lanthanide metal and oxide clusters in quantum physics using an indigenous laser-vaporization setup. In quantum sensing, enhanced two-photon coherent population trapping in rubidium atoms was demonstrated using bichromatic circularly polarized light with orthogonal magnetic fields, contributing to advancements in quantum sensing applications.

**In Chemical Sciences** arena, BARC made new strides in finer aspects of nanotechnology and drug delivery. Cucurbituril-Functionalized gold nanoparticles (CB7AuNPs), which enhance antibiotic activity, and SCx6AuNPs, which show promise for targeted drug delivery and bioimaging were developed. BARC also made significant progress in sensing and catalysis, developing sensors for serotonin and  $\text{NO}_2$  detection, along with vanadium composites for hydrogen generation and photocatalytic improvements using Ag-MOF/g- $\text{C}_3\text{N}_4$  materials. Studies using micro-Raman spectroscopy revealed that the depletion of iodide in sodium iodide-malonic acid aerosols is accelerated with increasing humidity, highlighting the significant role of relative humidity in atmospheric iodine chemistry.

**BARC, in collaboration with NALCO**, released BARC-B1301, a certified alumina reference material that meets ISO standards. This development was complemented by BARC's support of analytical services for DAE projects. BARC also pioneered protocols for research purposes for selectively leaching Lu isotopes from copper substrates. Environmental and sustainability research at BARC resulted in the development of polymeric adsorbents for rapid uranium estimation in urine, ZIF-67 composite beads for uranium extraction from water, and solvent extraction methods for niobium separation from zirconium alloys. Additionally, modified graphene oxide and carbon nanotubes were explored for radionuclide remediation, and a catalytic system using gold nanoparticles was developed for organic pollutant degradation.

**Using Computational Fluid Dynamics (CFD)** and Molecular Dynamics (MD) models, BARC studied various phenomena such as bubble movement in pulsatile flow, droplet formation at submerged nozzles, grain flow dynamics, and seawater desalination using nanotube membranes. Other simulations included examining the thermal conductivity of actinide metals and ion transport through membranes.

**In Healthcare and Cancer research**, by combining dihydroxystilbene with talazoparib, researchers synergistically induced DNA damage and killed ovarian cancer cells. Other advancements include the development of PSMA-targeted doxorubicin to enhance prostate cancer cell death and the identification of CHK1 and ATR regulation of TOP1 in cancer cells. TFEB knockdown has increased pancreatic cancer sensitivity to PARP inhibitors, while mitocurcumin has demonstrated effectiveness in targeting both breast and pancreatic cancer cells.

**BioScience** research in agriculture has also yielded valuable insights, identifying a groundnut mutant with a 70% higher seed weight, linked to the downregulation of a specific gene. 53 ammonium transporter genes in millets have been discovered, and it found that MusaDREB1-like proteins enhance banana stress tolerance. Other studies have shown that biochar can reduce arsenic levels in rice, and *Trichoderma virens* can alleviate potassium deficiency in soybeans.

**BARC's healthcare and drug discovery research** has explored thorium's effect on lung surfactants and investigated mechanisms of radioresistance, leading to the development of radioprotective agents. In the area of cancer research, BARC has focused on novel fluorescent, biodegradable compounds and anticancer agents, including protein binders, CPL-active dyes, and gamma dosimeters, showcasing advancements in diagnostics, therapeutic applications, and environmental remediation.

## **HUMAN RESOURCES, SCIENTIFIC INFORMATION AND TECHNOLOGY MANAGEMENT**

**Dr. Homi J. Bhabha** had conceptualized the creation of Training School system in DAE, and the first training school was established in 1957 in Bombay (now Mumbai), as a centre of excellence for training of professionals through in-house efforts. Over the years, around 11,000 well-rounded individuals graduated from the ramparts of training schools with flying colors.

**A total of 177 graduating TSOs** of the 67th batch of BARC Training School OCES/DGFS-2023 programme (73 Engineering + 58 Sciences, including 12 Radiological Safety & Environmental Science (RSES) among others) after successful completion of one-year training, were placed in various divisions of BARC. There were 10 Trainee Defence Officers, who passed out with this batch and were assigned to different Divisions/Units for undertaking project for M. Tech. Two NTPC officers also completed their training in the OCES/DGFS-2023 Batch.

**BARC orchestrated the Trombay Colloquium**, a forum that hosted five eminent speakers from diversified scientific domains who shared insights on topics ranging from the future of our universe to Indian vaccine development. The speakers include Prof. Ashoke Sen, Honorary Fellow at NISER Bhubaneswar; Prof. Balram Bhargava, Chief of Cardiothoracic Centre, AIIMS New Delhi; Shri Raj Chengappa, Group Editorial Director at India Today Group; Dr. Soumya Swaminathan, Former Chief Scientist at World Health Organization and Shri A.S. Kiran Kumar, Member of the Space Commission, Government of India.

**BARC also conducted Chintan Baithak**, a collaboration platform for the BARC community focusing on R&D activities with discussions on proton accelerators and alignment with Amritkaal Targets.

**BARC published three books** - "IMPACT 2019-2024" documenting scientific activities, "Beneficial Effects of Ionizing Radiation in Biological Systems," and "The Miniature Marvels" about BARC's bonsai collection.

**BARC maintains a robust a vast collection of knowledge and information resources**, organizing exhibitions of scientific books and regularly issuing newsletters and souvenirs focusing on interesting themes to showcase the center's scientific and technological outcomes in tandem with information bulletins and nuclear web digests.

**The academic resources** include access to over 1,400 journals via subscriptions, with BARC researchers producing around 1500 publications in 2024. It has proactively implemented the One

DAE One Subscription (ODOS) architecture to expand the reach of journal resources to its scientific community.

**In Official Language (Hindi) implementation,** BARC conducted quarterly workshops and language courses for 198 officials, awarded cash prizes to 81 officials excelling in Hindi usage, celebrated World Hindi Day and Hindi Month with competitions and cultural activities, published new Hindi works including NUCDECA and technical article summaries, and launched BARC's official Hindi website in January 2025. The Committee of Parliament on Official Language inspected BARC's Official Language implementation on January 19, 2024.

**For Technology Management,** BARC established 60 agreements with 53 firms for licensing 43 technologies, released 9 new technologies into the public domain, established Atal Incubation Centers with 11 technologies undergoing incubation, and expanded the AKRUTI Program for rural and urban technology implementation through 8 new agreements with academic institutes.

## SCITECH OUTREACH

**BARC conducts extensive outreach programs** to engage citizens and promote science and technology. The center hosts students from various institutions across India, providing facility tours at the Trombay campus to showcase multidisciplinary research activities and inspire scientific careers. Participating institutions during the period include colleges from Mumbai, Maharashtra, and neighboring states such as SVNIT Surat, Carmel College Goa, and several Mumbai-based institutions, including Wilson College and Podar International School.

**BARC** conducted an outreach program in August 2024 in Raipur, Chhattisgarh, engaging approximately 1,200 students and faculty from five colleges to enhance their understanding of nuclear technology.

**As part of Campaign-IV** of the novel school outreach programme, Parmanu Jyoti, Scientific Officers of BARC, visited 48 JNV schools and Atomic Energy Central schools across four North Indian states, reaching over 18,000 students.

**National Science Day 2024**, themed “Atoms for Society: Securing Water, Food, and Health,” was celebrated with Professor K. Vijayraghavan (Homi Bhabha Chair Professor and former Principal Scientific Adviser to the Government of India) as chief guest, while National Technology Day 2024 featured General Anil Chauhan. These events showcase BARC’s contributions to national development and provide platforms for students to interact with renowned scientists.

## SAFE AND SECURED WORKPLACE

**The BARC Safety Council (BSC)** has demonstrated a strong commitment to workplace safety through comprehensive facility reviews. In 2024, the BSC and its committees held 8 council meetings and 178 committee sessions, resulting in 92 facility clearances, 65 radioactive waste management authorizations, and 109 radiation source approvals. It also conducted 124 regulatory inspections, approved 30 radioactive shipments, and oversaw 46 emergency preparedness exercises.

**Beyond operational work,** the BSC published a new safety guide on regulatory processes, drafted documents on event reporting and inspection procedures, and organized training courses across multiple locations. These efforts culminated in a December 2024 theme meeting on radiation facility regulatory measures, highlighting BARC’s dedication to maintaining exceptional safety standards throughout its operations.

## INFRASTRUCTURE DEVELOPMENT

**BARC** has implemented numerous infrastructure projects to enhance its facilities and sustainability.

**A state-of-the-art Digital Studio** was established at the HRDD Training School Complex in Anushakti Nagar, featuring precision acoustic design and advanced audio-visual equipment for broadcast-quality e-learning content in Nuclear Science & Engineering. The studio supports various functions, including video recording, editing, web streaming, remote teaching, and interviews. Additionally, six lecture halls at the Training School Complex were modernized with state-of-the-art AV systems.

**A 250 kLD sewage treatment plant** was established for BARC Hospital to meet zero-discharge requirements and address potential water shortages. This plant utilizes BARC's Sequential Batch Reactor technology to produce manure-usable solid waste and treated liquid, meeting Maharashtra Pollution Control Board standards.

**The Bhabha Botanical Garden** was re-developed to serve as a living repository for plant species and biodiversity preservation, featuring a meditation area with 70-year-old twin wells planned for solar-powered irrigation and trellised climbers for shade.

**At OSCOM in Odisha**, a seawater intake system was developed for a 5.0 MLD desalination project to test indigenous technologies while meeting water requirements.

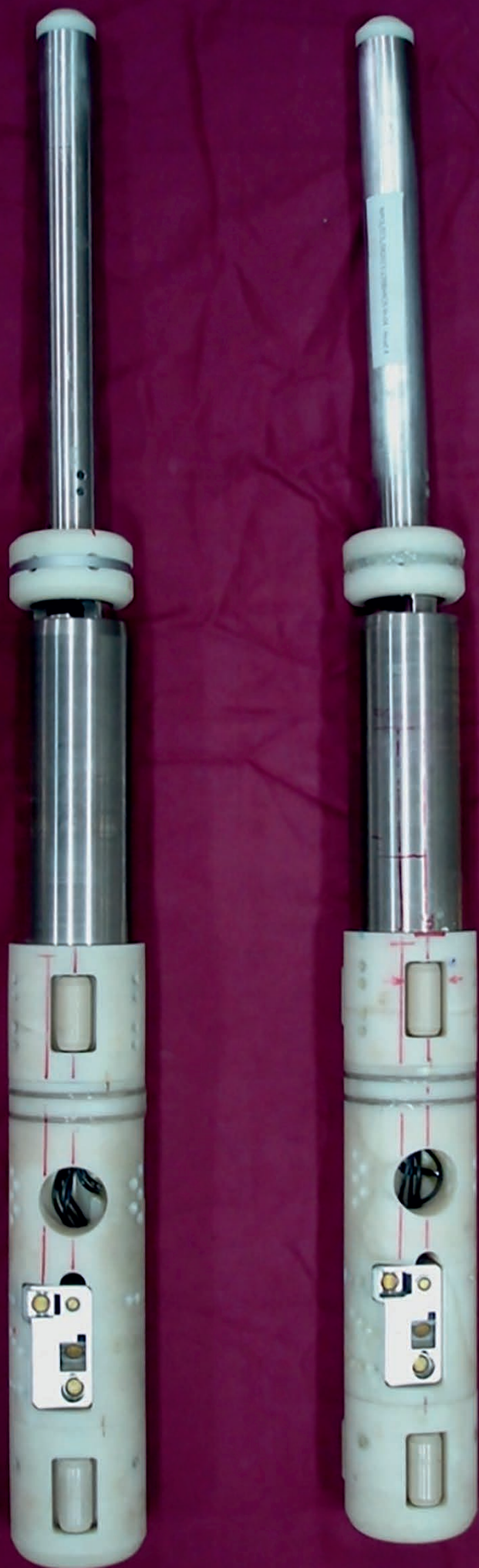
**A portable Nisargruna biogas** plant with a 50kg daily capacity was commissioned at the Training School Hostel Complex, featuring a compact design with spiral pipe construction that eliminates the need for conventional pits and produces enriched organic manure.

**A high-altitude guest house** was constructed in Ladakh for officials visiting the MACE facility at 14,000 feet elevation, incorporating solar-passive design elements to prevent freezing.

**A 15kW micro hydro power** unit was established at Plutonium Plant lake to generate electricity from harvested rainwater.

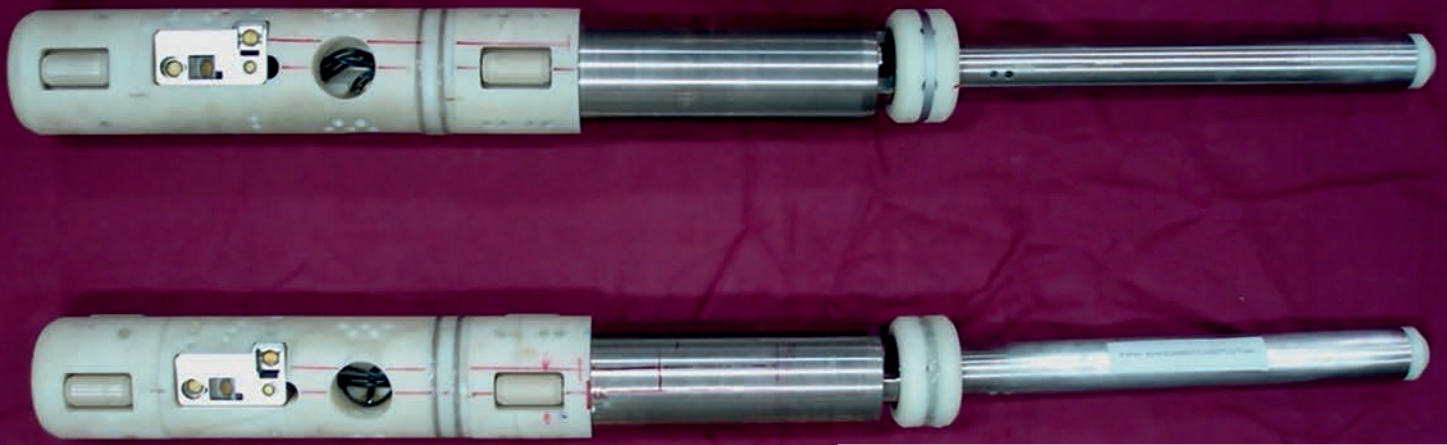
**Three fully automated polyhouses** were developed at BARC Trombay to cultivate exotic flowers and tropical orchids while supporting plant propagation, conservation, and acclimatization of new species.





# INDIAN NUCLEAR POWER PROGRAMME

BARC is engaged in multi-disciplinary and multi-scale activities leading to the development of technologies related to India's nuclear power program. These include fuel fabrication, quality assurance, in-service inspection, post irradiation examination, inspection tools for research reactors, Pressurized Heavy Water Reactors (PHWRs). The technologies related to front and back end of the nuclear fuel cycle, which includes spent fuel reprocessing and nuclear waste disposal, are within the ambit of forefront research areas of this centre. The activities under these thrust areas cover the first three vision programmes of BARC, the highlights of which are sketched in this section.



BARC Inspection Heads (BARCIS) deployed in various Pressurized Heavy Water Reactors.

# Indian Nuclear Power Programme

## Development of Inspection Systems

### BARCIS Inspection Heads for inspection of PHWR coolant channels

BARCIS Inspection Heads (2 units, manufactured by ECIL) were prepared and deployed at RAPS-3 to perform volumetric inspection of 18 coolant channels and adjacent rolled joint area inspection of 24 rolled joints. BARCIS was also utilized for pressure tube volumetric inspection at KAPS-1. The system successfully completed Pre-Service Inspection (PSI) of coolant channels at RAPP-7 on June 24, 2024, a critical milestone before fuel loading.



BARCIS Inspection Heads deployed in various PHWRs.

### Software for ECT-based ID inspection of SG tubes

An Auto Decision Assist Software has been developed and deployed at Nuclear Fuel Complex for identifying defects in Steam Generator (SG) tubes from ECT signals. Testing on 1398 SG tubes of 700MWe PHWRs achieved 92.7% accuracy with no false acceptances. The software is now deployed at Nuclear Fuel

Complex (NFC) Hyderabad for in-situ inspection of SG tubes for upcoming PHWR fleet.

### ECT technique-based flaw detection tool for Pressure Tubes of 540MWe Indian PHWRs

An Eddy Current Testing (ECT) based inspection tool compatible with BARCIS system has been developed to complement existing UT-based tools for detecting ID surface opening flaws in 540MWe PHWR pressure tubes. Testing in BARC's horizontal calibration facility demonstrated successful detection of flaws ranging from 91 to 455 micron depth. The tool is now ready for deployment in Indian 540MWe PHWRs.



Set-up for Testing of Eddy Current based Inspection Tool in Horizontal Calibration Facility.

### X-Ray based automatic PHWR fuel pellet scan system

Software for automatic detection of uranium fuel pellets in zirconium tubes has been developed and commissioned at NFC Hyderabad. The



system ensures fuel pellet stack completeness in PHWR fuel pins, streamlining workflow through state-machine based control for fuel tray scans and barcode-based lot number reading.

### Development of compact IDMT for 220 MWe PHWRs

A new Inside Diameter Measurement Tool (IDMT) was developed for faster, remote deployment, measuring pressure tube diameters without de-fueling. The tool uses FM Ram-C travel, taking about 2 hours per channel, and was calibrated to within  $\pm 10\mu\text{m}$ . Successful trials were conducted at Kaiga Generating Station II, with the tool set for deployment soon.

### Quantification of thermal ageing effects on fracture behavior of austenitic stainless steel pipe weld joints

Fracture tests on thermally aged pipe welds (aged at  $400^\circ\text{C}$  for 10,000–20,000 hours) showed higher fracture resistance than as-welded joints. This unexpected result may be due to the presence of ferrite phase and residual stress relaxation during thermal ageing.



Fracture tests being carried out on full scale pipe weld with crack.

### Reactivity control mechanisms for PWRs

Design of Magnetic Jack type Reactivity Control Mechanism has been completed, including pressure housing, motion unit, groove shaft, electromagnetic coil unit, and sensor unit. Manufacturing technology has been established with two mechanism components manufactured and assembled using available materials. A control unit has been integrated with the mechanism, and functional testing is underway at BARC. This technology will support Indian Pressurized Water Reactors (IPWRs) and future Small Modular Reactors (SMRs).



The Magnetic Jack type Reactivity Control Mechanism.

## Recovery of Nuclear Minerals

### Recovery of Rare Earth elements & by-products from Dantala ore of Siwana Ring Complex, Rajasthan

The Dantala hard rock deposit of REE in Siwana Ring Complex (SRC) of Rajasthan has gained importance & attention for occurrence of REE deposits along with Nb, Hf & Zr. Host rocks in Dantala area are of tuffaceous nature, which originates from consolidation of volcanic ash. Total REE conc. in the ore is about 0.5%, 38% of which is Heavy REE (HREE). Significant conc. of Nb (506 ppm) & Zr (1.13%) are noted for their recovery. U was not detected & Hf (240 ppm) is present. A comprehensive process flow sheet was developed for recovery of REE, Zr, Hf & Nb. It mainly consists of comminution of ore, froth flotation, followed by roasting-leaching with sulphuric acid for extraction of REE, Zr, Hf & Nb, purification by solvent extraction & precipitation. Solvent extraction scheme developed consists of selective extraction of Zr & Hf from REE bearing leachate using PC88A & D2EHPA leaving most of the REEs in raffinate from which mixed REE product is precipitated.

### Uranium Pulsed Disc & Doughnut Column based pilot plant for Uranium refining

A pilot-plant with extraction, scrubbing and stripping columns was designed and installed to demonstrate complete uranium refining through solvent extraction. The system uses pulsed disc and doughnut columns for all operations. Water and two-phase trials are complete, and uranium refining trials have begun.

### Scale-up of Pulsed Disc and Doughnut Column

A 6-inch diameter glass Pulsed Disc and Doughnut Column (PDDC) facility has been installed to quantify scale effects on liquid-liquid two-phase hydrodynamics and mass transfer.

### CFD analysis

Two-phase Euler-Euler Computational Fluid Dynamics (CFD) simulations quantified axial dispersion in a 3-inch PDDC across different throughputs, pulsing velocities and phase flow ratios in aqueous continuous operation. Experimental validation using radiotracer data showed good agreement with CFD-predicted E-curves.

A 2D CFD-population balance model studied scale-up effects on liquid-liquid hydrodynamics in air pulsed columns with nozzle plates. Simulations for columns from 2-16 inches in diameter determined dispersed phase hold-up and Sauter mean drop diameter for organic continuous operation with varying aqueous phase velocities at constant O/A ratio. Results showed dispersed phase hold-up increases with dispersed phase velocity, and flow patterns in the continuous phase change with column diameter, providing insights for hydrodynamics and mass transfer performance.

### Direct denitration of Uranyl Nitrate in Nuclear Fuel Cycle Front-end operations

Technical specifications were completed for a demonstration setup for direct denitration of pure uranyl nitrate solution. The bench-scale system includes a fluidized bed reactor, off-gas system (filter housing, heat exchangers, alkali scrubbers), tanks, control panel, and required instrumentation. Utility requirements, equipment layout, P&ID, BOM, 3D layout, GA drawings, and safety documentation have been prepared.

### Uranium recovery

Nano-crystalline hydroxyapatite (HA) synthesized from egg-shell (a natural bio-waste

material) was tested for the recovery of Uranium from processed stream effluents. Uranium removal efficiency was estimated by measuring it (using LED fluorimetry) in eluent solutions and was found to be 99%.

### Post synthetic modification of Metal Organic Framework for boosting Uranium capture from aqueous solution

UiO-66-NH<sub>2</sub>(Ce) was synthesized at room temperature and post-synthetically modified to phosphorous-functionalized UiO-66-NHPOPh<sub>2</sub>(Ce). Both materials were evaluated for uranium extraction from aqueous solutions. Some of the key findings are that both MOFs achieved high uranium sorption (95% for NH<sub>2</sub>, 99% for NHPOPh<sub>2</sub>) in pH 3-9, with optimal performance at pH 5. Phosphinic amide functionalized MOF demonstrated superior uranium sorption across all tested pH ranges. Rapid kinetics observed with >95% uranium uptake within 1 minute. Effective uranium sorption demonstrated in tap water, drinking water, and seawater. Desorption studies confirmed potential for material reuse. EXAFS analysis revealed efficient coordination between uranyl(VI) ions and both MOFs, explaining the capture mechanism.

### Zirconium extraction

Zirconium extraction was evaluated using a 3-inch diameter glass PDDC with 1.5m active column at 15 LPH feed flow rate (O/A=3/1). Using 5.5M acidity ZNCS feed (21 gpl Zr, 1 gpl impurities) and 0.3M APO in 50:50 ID:DD organic phase, 17% extraction of Zr was achieved with selective extraction over impurities.



Extraction of Zr is in Pulsed Disc and Doughnut Column (PDDC) of 3-inch diameter.



## Environment Monitoring

### Development of Sample Oxidation System

A semi-automatic system was developed for combusting large biota samples (40-60 g dry) to measure Organically Bound Tritium (OBT) and C-14. The system achieves better MDA (1.0 Bq/L for OBT, 8.0 Bq/kg C for C-14) and offers a cost-effective, high-sensitivity solution for environmental monitoring.



Semi-automatic oxidation system.

### Environmental surveillance

Environmental Survey Laboratories (ESLs) monitor radioactivity around nuclear facilities, analyzing samples within a 30 km radius. ESLs also participate in public awareness programs and act as Emergency Response Centers. Pre-operational data collection has begun for new Nuclear Power Plants.

### Personnel Monitoring

TLD personnel monitoring services were provided to approximately 23,000 radiation workers using  $\text{CaSO}_4:\text{Dy}$  based TLD badges. Neutron monitoring is conducted for about 3700 radiation workers using CR-39 detectors.

### Retrospective Dosimetry

TL and OSL techniques were used on household items (quartz, soil, electronics, salt, medicine) to reconstruct radiation doses in radiological incidents. Doses in the range of 20 mGy – 5 Gy can be estimated with  $\pm 5\%$  accuracy.

### Dose measurements in phantoms

Head & Neck and Prostate phantoms were 3D printed and tested. Dose values calculated by Treatment Planning System were compared to TLD-100 powder measurements, with deviations of  $< 1\%$  for target volume, 1-5% for Organ At Risk (OAR), and 7-9% for distal exit points.

### $\text{Fe}_3\text{O}_4$ -TPP hybrid particles for Uranyl removal

Hybrid  $-\text{O}-(\text{PO}_2)_3-\text{O}-\text{NH}_3^+-\text{SiO}-\text{Fe}_3\text{O}_4$  magnetite particles (10 mg) removed 70.2% of uranyl from water and 65.0% from blood serum at 100 ppm, while pure  $\text{Fe}_3\text{O}_4$  showed negligible absorption. These particles address uranium toxicity concerns associated with nuclear power operations.

### Iodine sorption with Silver-impregnated Zeolite

Silver-impregnated zeolite (8.5% w/w  $\text{Ag}^0$ -zeolite) was developed to capture radioactive iodine emissions from nuclear fuel reprocessing and accident scenarios. The material demonstrated  $\sim 100$  mg/g iodine adsorption capacity (vs. 9 mg/g for pristine zeolite), excellent stability under gamma irradiation (4.32 kGy total dose over 6 months), with no significant physicochemical changes post-irradiation and no desorption of iodine from silver iodide bonds.

### Cosmic Ray measurement at North Pole

Tissue Equivalent Proportional Counter (TEPC) was used to measure secondary cosmic rays at Himadri, Ny-Ålesund, Svalbard, correlating them with solar weather. Gamma detectors measured minimal terrestrial radiation, highlighting the location's suitability for cosmic ray studies.



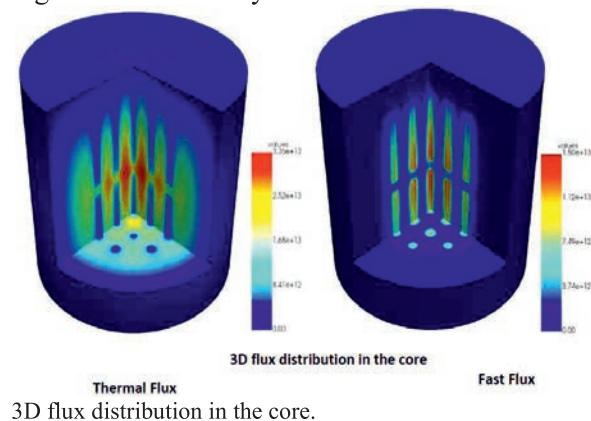
Detector placed in Gruevebadet laboratory, near North Pole.

## Nuclear Hydrogen

### Physics design of Small Gas Cooled Reactor (GCR) for high-temperature applications–Hydrogen

A small GCR core, graphite-moderated and  $\text{CO}_2$ -cooled, has been designed with a long refueling cycle and an outlet temperature of  $650^\circ\text{C}$ , aimed at hydrogen production. Core life, reactivity, xenon and samarium loads, and power distribution were estimated using in-house codes

PATMOC and ARCH, and open-source codes Dragon and OpenMC. Core reactivity coefficients remain negative throughout burn-up. Fuel loading schemes, criticality approach, neutron flux, and detector placement for regulation were analyzed.



## Advanced Reactors & Associated Materials

### Reactor Physics design of Experimental Indian Molten Salt Reactor (IMSR)& related physics experiments

The first phase of MSR experiments at BARC Critical Facility has been successfully completed, showing good agreement with computed results. Experimental analyses of a small Indian MSR with fuel salt flowing through graphite channels were carried out. Parameters like reactivity, fuel cycle length, and neutron emission rate based on fissile loading were assessed using OpenMC.

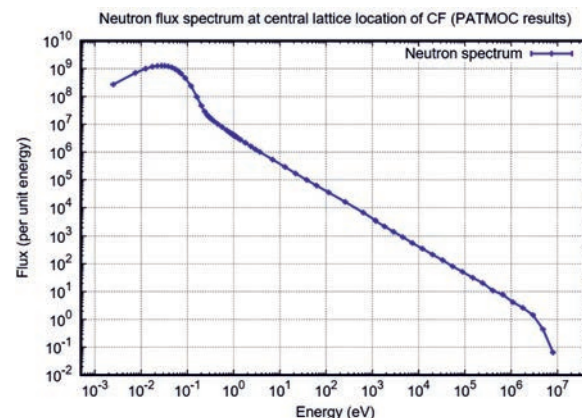
### Fabrication of NiMoCrTi-C alloy plates for MSBR loop

MSBR loop is required to study the thermal hydraulics, corrosion attack from liquid fuel & structural integrity up to  $650^{\circ}\text{C}$ . NiMoCrTi-C alloy plates are needed to fabricate MSBR loop facility. To optimize thermo-mechanical processing parameters for producing plates from as-cast ingots, various lab-scale hot deformation & heat treatments were performed. Lab-scale experiments revealed that the range  $1200\text{--}1250^{\circ}\text{C}$  is the optimum hot deformation temperature for achieving a desirable microstructure. Using optimized parameters, large-sized forged ingots were hot-rolled into plates of different thicknesses. After hot rolling, annealing trials were conducted to determine the temperature & time required to achieve a fully recrystallized microstructure. Based on these, annealing was carried out at  $1080^{\circ}\text{C}$  for 30 min,

resulting equiaxed grains. Using flow sheet developed for NiMoCrTi-C alloy, 14 & 12 mm thick plates were produced.

### Development of Full-Core Monte Carlo Neutron Transport Code - PATMOC

PATMOC, an indigenous Monte Carlo code for reactor physics and neutron transport, simulates reactor parameters such as  $k\text{-eff}$  and neutron flux. It uses WIMS-D fine group nuclear data and can handle complex geometries. The code supports both eigen and fixed-source mode simulations and has been validated against reactor benchmarks. New modules for geometry visualization, parallel execution, and full-core burn-up analysis have enhanced its capabilities.



PATMOC computed neutron flux spectrum at central cluster of CF.

### Simplified Complex Frequency Transfer Function Method for generation of Floor Response Spectra for nuclear structures

A computationally efficient Transfer Function Method was developed to generate Floor Response Spectra using complex frequency transfer functions from modal time history analysis, reducing the need for repetitive site-specific seismic analyses in PHWR designs.

### Leakage experiment in BARCOM Containment at BARC, Tarapur

A scaled-down containment model (1:4) of the 540 MWe PHWR at Tarapur was pressurized to evaluate leakage rates. Results showed a 7.7% increase in leakage over 12 years, attributed to losses in pre-stressing from creep and shrinkage.

### Experimental study on adequacy of Spray Cooling System for RAPS/MAPS for Design Extension Conditions scenario

Experiments confirmed that the spray cooling system effectively removes decay heat during LOCA scenarios in older PHWRs like RAPS-2



and MAPS-1/2, maintaining channel coolability and sufficient flow rates for quenching.

#### Development of ML Models for identification of Accident Scenarios in Nuclear Power Plants

AI techniques like Artificial Neural Networks (ANN) and Random Forest (RF) were used to identify accident scenarios such as LOCA and MSLB in real-time sensor data from 220 MWe PHWRs. The Model, without Principal Component Analysis, performed well in identifying these scenarios for quicker decision-making.

#### Development of Cr coating on Zircaloy-4 by Magnetron Sputtering as Accident Tolerant Fuel cladding

A 20-30  $\mu\text{m}$  thick pore-free highly adherent Cr coating on Zry-4 coupons was carried out successfully by DC magnetron sputtering for the first time; cross-section microstructure confirmed pore-free nature of deposit. Excellent adhesion of Cr coating on Zry-4 has been established. Steam oxidation of Cr-coated Zry-4 at 1000°C for 3h & 1200°C for 30 min was carried out & compared with bare Zry-4 substrate oxidation behaviour. In Cr-coated samples, weight gain measured was ~15 times & ~10 times lower than bare Zry-4 samples after steam oxidation at 1000°C/3h & 1200°C/30 min, respectively. Cr-coated Zry-4 showed formation of less than 10  $\mu\text{m}$  thick  $\text{Cr}_2\text{O}_3$  layer on top of Cr coating. This provides oxidation resistance at elevated temperature. This study highlights sputter deposited Cr coated Zry-4 can be a plausible solution towards ATF cladding application under LOCA situation in nuclear power reactors.

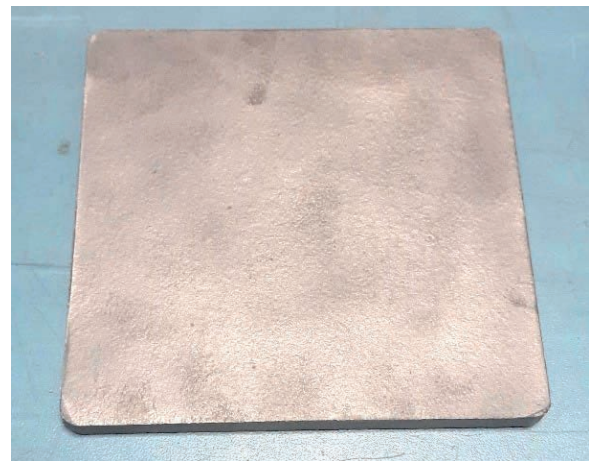
#### Optimization of Cold Spray Deposition Process parameters for depositing $\text{Cr}_2\text{AlC}$ MAX-phase coating onto Zr-4

Cold spray process parameters for depositing  $\text{Cr}_2\text{AlC}$  MAX-phase, such as temperature (T), pressure (P), stand-off distance (SOD) & number of passes ( $n_p$ ) were optimized to build up coating thickness ( $t$ ) > 100  $\mu\text{m}$ . Initial trials showed that increasing T & P to 975°C & 50 bar, respectively helped in increasing  $t$  & uniformity of coating. However, the coating still exhibited significant nonuniformity (in  $t$ ). In order to improve coating quality, SOD &  $n_p$  were varied. Microstructural study of Cr-MAX phase coated sample showed that  $t$  can be increased from an average of 30  $\mu\text{m}$  in single pass to up to 100  $\mu\text{m}$

in five passes. Additionally, increasing SOD from 40 to 60 mm helped in improving coating uniformity.

#### Synthesis, characterization & densification of nanostructured Boron Carbide

Nanostructured  $\text{B}_4\text{C}$  was synthesized via planetary ball milling of B-powder & CNTs, followed by high-temperature vacuum heat treatment at 1500°C. This successfully produced single-phase  $\text{B}_4\text{C}$  in spheroidal & flaky forms, scaled from grams to 500 g batches. Consolidation by hot pressing at 1950°C yielded 98% dense  $\text{B}_4\text{C}$ . Compared to coarse-grained  $\text{B}_4\text{C}$ , which typically exhibits a flexural strength of 360-400 MPa, the nanostructured  $\text{B}_4\text{C}$  demonstrated an improved flexural strength of 476 MPa, along with an elastic modulus of 450 GPa & notable reliability, as indicated by Weibull modulus. Additionally, room temperature thermal conductivity of nanostructured  $\text{B}_4\text{C}$  was better (43 W/m·K) than conventional coarse-grained  $\text{B}_4\text{C}$  (26 W/m·K). Combination of enhanced mechanical & thermal properties makes nanostructured  $\text{B}_4\text{C}$  a promising material for improving durability & performance of absorber elements in neutron irradiation environments.



Hot pressed square shape  $\text{B}_4\text{C}$  (115x115x6 mm; 98% dense).

#### Ductile fracture & microstructure of APURVA

APURVA, an indigenously developed ultra-thick (>350 mm) pressure vessel, is investigated *w.r.t.* microstructure in quenched-tempered condition, from SEM micrographs along R-C plane & ductile fracture features quantified from fractographs of RT quasi-static tensile experiments carried out using samples in axial orientation. Microstructural feature reveals that, except at internal diameter, generic microstructure of APURVA consists of either,

bainite or bainite + martensite, with the latter assuming a degree of refinement depending on location. Fractograph of the central fully bainitic region is quantified to have higher dimple sizes & lower areal density, suggesting larger void nucleation strain as compared to other locations. Fractographs show nearly spherical dimples for ID region having fully martensitic structure & elongated morphology for the regions having substantial bainite. Embrittling effects due to martensite in a bainitic microstructure are not manifested in dimple-morphology. Presence of shallow cluster of shear dimples (oval shape) is seen at both quarter & three-quarter locations having bainite + martensite. These trends suggest that central region is unlikely to be inferior in toughness.



**APURVA Steel Forging:** 750 mm thick Ring Forging for Flange Area of RPV-OD5300 x ID3800 x 700L.



Replica of APURVA grade steel forging.

### Comparison of irradiation response of indigenously developed & imported RPV steel forgings

BARC has developed shell forgings of eastern grade RPV steel for compact pressurized water reactors. During reactor operation, the

microstructure & mechanical properties of RPV altered significantly. Therefore, study of irradiation response of such steel under irradiation is extremely crucial for its qualification. Neutron irradiation induced damage in a material can be aptly simulated using proton irradiation. A comparative assessment of irradiation response of indigenous & imported eastern grade RPV steels was carried out. Specimens from Indian & imported forgings were irradiated with proton beam to a dose of 0.1 dpa at RT & were subsequently characterized using synchrotron XRD, positron annihilation spectroscopy (PAS) & microhardness. XRD indicated larger change in domain size after irradiation in imported steel (64%) as compared to indigenous steel (6%). The imported steel exhibited irradiation hardening, while hardness did not change much in the indigenous steel following irradiation. PAS study suggested presence of relatively more irradiation induced defects in imported steel. All results indicate better irradiation resistance of indigenous eastern grade RPV steel in comparison of imported eastern grade RPV.

### Threshold Stress for hydride reorientation under bi-axial load in Zr-2.5Nb Pressure Tubes

Hydrided PTs were subjected to heating to dissolve hydrides, followed by cooling under internal pressure using an experimental setup. Variation of hoop stress was obtained using tapered tubes & residual stresses induced near roll joint is computed using 3D nonlinear FEM. Effect of applied stress on radial hydride fraction was evaluated using images obtained from metallography & serial sectioning. Threshold stress for formation of radial hydrides (RHF-50%) was determined for both 220 & 700 MWe PTs under both biaxial & uniaxial loading conditions, revealing a threshold stress range of approximately 110-130 MPa. Remarkably, this threshold stress remains independent of state of applied stress.

### Hydride Embrittlement mitigation in Zr-alloys using Yttrium

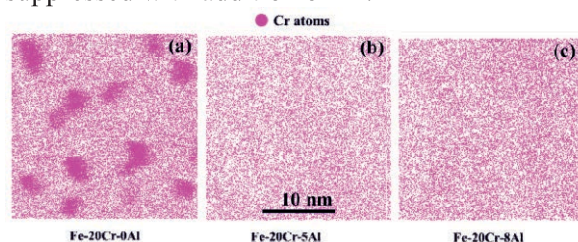
Hydride embrittlement is one of the life limiting factors in Zr-2.5Nb PT in PHWRs. In light of the importance of minimizing hydride precipitation related issues in PTs, a set of experiments were conducted to assess gettering action of yttrium in absence of a metallurgical bond between Zr-2.5Nb & Y. For this, two principal cases were studied, which include Quartz tube containing



hydrided Zr-2.5Nb piece (200 ppm) along with a physically separated Y (of similar dimensions); a quartz tube containing stand-alone Zr-2.5Nb hydride (200 ppm) piece meant to be a 'controlled sample' for assessing the gettering action of Y in case 1. The quartz tubes sealed to maintain 150 mm Hg of Ar pressure. These were subjected to a heat treatment (H/T) at 400°C for 30 days for enabling gettering by Y. Study of distribution of hydrides in Zr-2.5Nb controlled sample indicated no difference in hydride content (~27%) in post H/T condition compared to condition before H/T (~26%). Whereas a significant drop of hydride content (~7%) was observed in case of sample treated in presence of Y. This clearly demonstrated the efficacy of Y in acting as a getter in spite of not being metallurgically joined with Zr-2.5Nb. This paves way for new possibilities in hydride mitigation.

#### Effect of aluminium on nanoscale phase separation in Fe-20Cr-xAl Ternary Alloy System

FeCrAl alloys have seen increased interest for nuclear power applications including accident tolerant fuel cladding, structural components for fast fission reactors & as first wall & blanket structures for fusion reactors. These applications are limited by nano-scale phase separation occurring in these alloys either at elevated temperatures or due to neutron irradiation. To understand the effect of Aluminium (Al) on nanoscale phase separation, a systematic study on Fe-20Cr-xAl model alloy, thermally aged at 500°C for different durations was performed at near atomic resolution using Atom Probe Tomography (APT). Distribution of Cr atoms in alloy containing 0, 5 & 8 at.% Al, thermally aged for 120 hours showed a retardation in the process of phase separation with increase in Al-content. It was demonstrated that deleterious nanoscale phase separation of Cr could be suppressed with addition of Al.



Distribution of Cr atoms obtained from APT data for Fe-20Cr-xAl alloy aged at 500 °C for 120 h, (a) x=0, (b) x=5 & (c) x=8. Each single, color dot, in these images is a single Cr-atom.

## Spent Fuel Reprocessing & Radioactive Waste Management

### Treatment of ILLW at PHIX Facility

The Intermediate Level Radioactive Liquid Waste (ILLW) from spent nuclear fuel decladding was treated at the PHIX facility using an ion exchange system with a highly Cs-selective resin. Processing one tank achieved a Volume Reduction Factor (VRF) of 70 and a Decontamination Factor (DF) of 4000. The indigenously developed Resorcinol Formaldehyde (RF) resin performed well, with a Cs DF of approximately 10,000, effectively partitioning ILLW into Cs-rich eluate and dischargeable effluent, minimizing solid waste.



Ion Exchange column of 100 litre bed volume without shielding.

### Treatment of MWPF Raffinate at WIP Trombay

MWPF Raffinate, an alpha-rich, fluoride-bearing stream with high inactive salt concentration, was treated using the Partitioning System with CALmsu-30 mixer-settler units and TEHDGA solvent. A Decontamination Factor (DF) of 3300 was achieved, with the resulting product concentrated to a VRF of 23. The effluent was managed by pH adjustment and complexation.

### DTBDCH18C6 synthesis

A three-step process for synthesizing and purifying Strontium (Sr) selective crown ether DTBDCH18C6 was developed, scaled up, and evaluated for Sr extraction.

### Effluent Polishing System at WIP Trombay

A retrofitted Effluent Polishing System at WIP Trombay was used to treat secondary radioactive effluents from HLLW, MWPF Raffinate, and Th-lean Raffinate processing. It processed 550 L of eluate from TLR processing (VRF of 30) and

8.0 m<sup>3</sup> of in-house acidic secondary waste (DF of 20 with respect to  $\beta\gamma$ ). The system is currently used for MWPF waste raffinate treatment with indigenously developed resin.

#### Cesium Pencil manufacturing system

Cesium (Cs) Pencil making resumed with in-cell modifications, including a remotely operated linear trolley and a partially closed pouring system to reduce activity loading on ventilation filters. Approximately 3450 gm of Cs-rich glass (2.3 Ci/gm) was poured into 24 Cs pencils. 20 pencils were manufactured, qualified and collected by BRIT for use in irradiators.



Inactive demonstration facility for Cs pencil.

#### Upgradation of Radioactive Waste Management Facilities at Trombay

Augmentation/refurbishment is underway at WIP Trombay. Key achievements include equipment and piping installation, construction of an exhaust room, hot-cell alterations, additional low-level tanks, and delivery/installation of MHEs. Special equipment fabrication is in progress. Connectivity with existing process equipment is being established through piping works. A mockup facility was installed to validate design changes of Cs pencil making flowsheet.

#### Radioactive low level liquid waste management & Decontamination services

60,585 m<sup>3</sup> of radioactive liquid effluents were managed at ETP. 736 m<sup>3</sup> of LLW was treated chemically, and 1551 m<sup>3</sup> was treated using an ion exchange process. 1.2 m<sup>3</sup> of spent TBP was managed by Alkaline Hydrolysis, and 2.3 m<sup>3</sup> of recovered dodecane was incinerated. A SCADA-based control room was installed and commissioned. Also, 77,068 kg of protective wear was processed and recycled. 16.8 Te of cut-

end rods were decontaminated, and 168 Aluminium shields and 204 SS plugs were recycled.



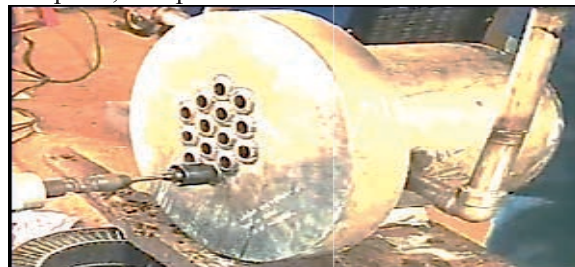
New control room of ETP-DC.

#### Development & process standardization for decontamination & volume reduction of metallic waste

An experimental setup for volume reduction by inactive Metal melting by Induction Furnace has been fabricated and installed. The Metal Melting System consists of an induction furnace, Ingot casting unit, and associated off gas treatment unit. It was tested for melting of different type of material CS, Al, SS at different temperatures i.e. from 600°C to 1700°C.

#### Thermosiphon Evaporators with new material of construction

Failure analysis of two Thermosiphon Evaporators (TSEs) led to the identification of root causes and a shift towards titanium and zirconium materials for critical components. Tube-to-tube sheet (TTS) weld qualifications are complete, and plant-scale trials will follow.



Tube-to-tube sheet Joint Mock Up for qualification.

#### Completion of ALLT construction

Additional Low-Level Liquid Waste Tanks (ALLT) with a capacity of approximately 1000 cubic meters have been constructed at the ETP&DC Complex. The reinforced concrete structures have passed leak-tightness tests.



### Solvent synthesis for radionuclide separation & Spent novel solvent management

Actinide – Lanthanide purification from Simulated Liquid Waste (SLW) using 0.1 M CA-BTP/1-octanol in counter current solvent extraction mode has been completed. The process development work on the recovery of spent CC6 (calix crown 6) has been completed

### Organic liquid waste incineration system at ETP

Setting up of Organic Liquid Waste Incineration System (OLWIS) for treatment of novel solvent was taken up at ETP site. Fabrication and installation of major components is completed and Electrical and instrumentation work is also nearing completion.

### Design fabrication & installation of Induction Levitation Melter

An Induction Levitation Melter (ILM) facility has been developed, installed and commissioned at BARC Trombay. The system has been tested for melting and homogenisation of SS, Al and Zr –SS alloys during commissioning trials.

### Indigenous development & manufacturing of RSW glass slab

Development work for RSW Glass slabs of different densities of large dimensions is ongoing. After multiple iterative trials, a glass slab of 800 mm x 800 mm x 230 mm thickness has been casted successfully without any cracks and optical defects.



Casted glass slab of 740mm x 740 mm x 200 mm thk (5.2 g/cc density).

### Development activities for Strontium based RHU for terrestrial use

Development has been initiated towards strontium based RTG. Heat transfer study for RTG with 84 watts heat source has been completed and R&D efforts are ongoing to improve efficiency of Thermo-Electric Generator from 0.16% to 3%.

### Geopolymer applications

Geopolymerization of mixed waste from NRB Tarapur exhibits lower leach rates compared to cementation. Synchrotron X-ray micro-tomography (SR-μCT) revealed that geopolymerized products require higher force for crack initiation than OPC vermiculite cements after 700 kGray gamma irradiation. This confirms the superior durability of geopolymerized products.

### Chemometry for online Uranium monitoring

An online monitoring setup, tested for continuous prediction of uranyl nitrate concentration (1-130 g/L), used a Partial Least Squares Regression model. The model was unaffected by corrosion product impurities (Cr, Ni, Fe) and acidity variations (2-4M HNO<sub>3</sub>). The PLS-R model uses absorbance spectra from 50+ laboratory-verified standard samples, using Davis Gray and spectrophotometry methods.

### Virtual Reality-based glove box operator training

A Virtual Reality training software allows Category-1 & Category-2 trainees to learn glove box repair, maintenance, and operations independently. The software provides an immersive VR experience of lab entry, PPE kit checks, and glove box inspection. Operators can practice decontamination, material movement, bag in/bag out procedures, fire-fighting, filter replacement, and other routine tasks in a 3D VR environment with real-time feedback.

### Back End Activities: Value Recovery

Ru-106 plaques are manufactured via selective separation of Ru-106 from radioactive waste, followed by electrodeposition on silver plaques. These plaques are used for eye cancer treatment and distributed to hospitals through BRIT. Improvements in electrochemical deposition and brazing enhance production efficiency. Continued Ru-plaque production meets the demands of hospitals, with notched, round, and pediatric eye plaques manufactured and leak-tested per regulatory requirements, and several delivered to BRIT for distribution. Yttrium-90 (<sup>90</sup>Y), the daughter product of Strontium-90 (<sup>90</sup>Sr), is a β emitter used for Neuro Endocrine Tumor (NET) treatment. A process to recover pure <sup>90</sup>Sr from HLLW has been standardized, with bulk <sup>90</sup>Sr separated using solvent extraction

at WIP, Trombay. Multi-step separation processes were developed to purify  $^{90}\text{Sr}$ , followed by milking carrier-free radiopharmaceutical-grade  $^{90}\text{Y}$  from the  $^{90}\text{Sr}$  -  $^{90}\text{Y}$  solution using a supported liquid membrane (SLM Generator) system. Four lots of clinical-grade Yttrium-90 were supplied to RMC for radiopharmaceutical applications.

## Ru- eye plaque



Round  
Ø15.8 mm



Notched  
Ø21 mm



Pediatric  
Ø12 mm



Crescent Moon  
Ø16 mm

Various Ruthenium plaque configurations developed in BARC.





## ADVANCED TECHNOLOGIES, RADIATION TECHNOLOGIES & APPLICATIONS

Research and Development program in BARC is focused on achieving self-reliance. Over the years, this approach has resulted in development of advanced technologies indigenously in the areas of Research Reactors, Accelerators, Lasers, Sensors, Detectors, Radiopharmaceuticals, Materials for Energy Storage, Management of Surface Water and Groundwater Resources, Solid Waste Management, Agriculture, Food, Healthcare and various niche domains.



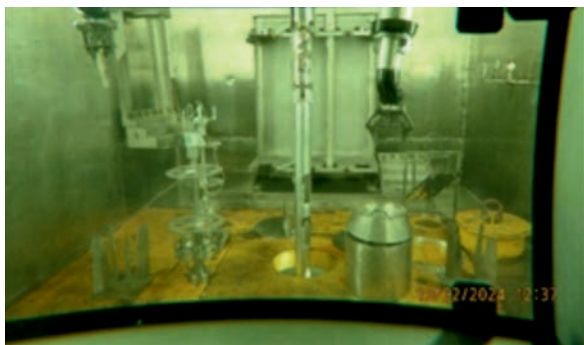
Heated Junction Thermocouple based discrete level sensors.

# Advanced Technologies, Radiation Technologies & Applications

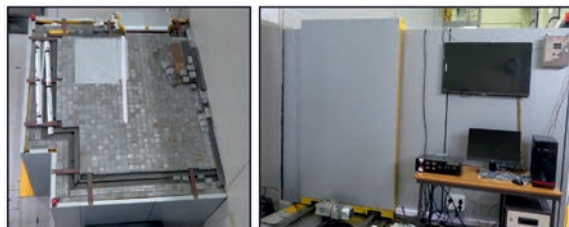
## Research Reactors

### Apsara-U Reactor

Research Reactor Apsara-U operated with 88% availability to meet user requirements. 12 cans in tray rod were irradiated and 25 samples were processed for neutron activation analysis. Plans to irradiate Fission Moly target plates progressed with successful qualification of newly fabricated tray rod and facility upgrades. The neutron imaging beam line at BT-7 port passed radiation surveys, produced encouraging test images.



Transfer of Fission Moly Tray Rod in shielding flask.



From left to right: Neutron Imaging and Depth Profiling

### Dhruva Reactor

Research Reactor Dhruva operated throughout the year with 70% availability for isotope production and research. About 450 samples were irradiated, and antimony pins were fabricated for a neutron source for TAPS-1. An on-power Fission Moly Tray Rod was developed with successful testing and flow optimization. Several monitoring systems were implemented, including differential temperature monitoring for Failed-Fuel-Detection, continuous position monitoring for Shut-off-rods, and a new Radiation Data Acquisition System. Safety modifications included larger size Reactor structure cooling line strainers and an alternate emergency cooling pathway.

Surveys for a new seawater intake

system were completed, with a sunken pond design selected. Physical protection systems were upgraded and the aging jetty was rehabilitated.

The Heavy Water Upgrading Plant (UGP) operated continuously throughout the year to process downgraded heavy water from the Dhruva reactor. Approximately 11 tons of downgraded heavy water were processed at the UGP, and the upgraded heavy water was supplied to meet Dhruva's operational requirements during this period.

## Critical Facility

Operated 62 times for various purposes including surveillance, experiments, and testing. Activities included neutron flux measurements, sample irradiation for activation analysis, detector testing for RAPS and TAPS, worth measurement of hafnium plates, activation of solid-state nuclear track detectors, and criticality experiments for Molten Salt Reactor fuel testing.

## CIRUS

Remained under deferred decommissioning. Dismantling of Primary Coolant & Seawater system components was completed with 11 tons of non-active metallic scrap removed. A new ventilation duct for the Rod Cutting Building was constructed and commissioned. Material samples were extracted from test components for characterization. The Special Illuminators Production Facility produced 890 illuminators for defense applications, and a new I-131 processing facility was commissioned with 100 Ci/batch capacity. A Rod Cutting Gadget was deployed for underwater cutting of damaged spent fuel rods, completing 83 cutting operations.

## Old Apsara

Preparation for conversion of the facility into a Science Museum is underway. Reactor pool revamping was completed, including repairs to the liner, support structure, beam tubes, closure of the thermal column, and qualification through non-destructive checks and water testing.

## Accelerator, Laser and Plasma

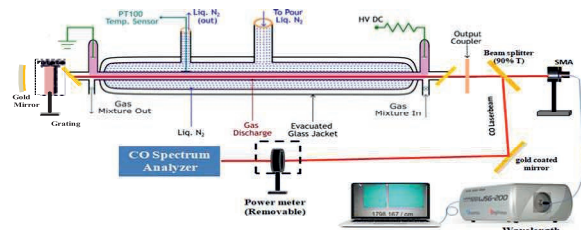
### Applications of 10 MeV, 3 kW Electron RF Linac

New applications of the 10 MeV, 3 kW electron RF Linac include a bio-hydrogel created by irradiating chitosan composites for its high

efficacy. Radiation sustainability tests were conducted on new materials (Olivine and Hydroxyapatite powders) being developed for nuclear waste depositories.

### Novel cryo-cooled CO Laser operating with CO<sub>2</sub> laser gas mixture

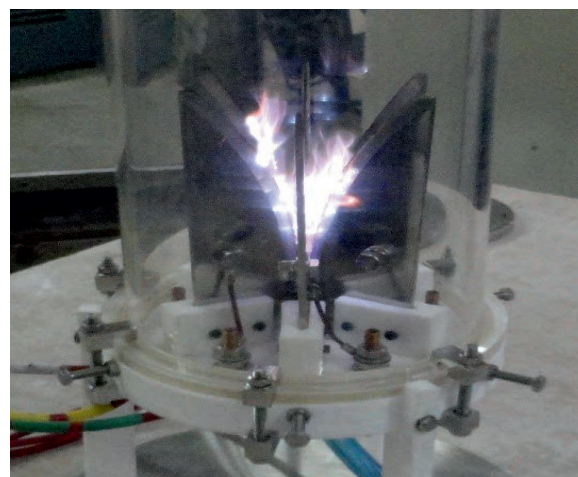
The emission spectra and performance characteristics of a novel cryo-cooled CO laser system that uses CO<sub>2</sub> laser gas mixture under varying operational conditions was studied and some of the findings are that Nitrogen addition provided multiple benefits such as Enhanced discharge stability, improved excitation efficiency, increased output power and enriched emission spectrum. Lowering the coolant temperature shifted trapping levels to lower vibrational quantum numbers, which theoretical calculations support. The system achieved lasing on over 20 transitions in grating-tuned mode, with several lines delivering output power exceeding 100 mW. A key advantage of this system is that it produces CO laser emission without requiring any toxic CO gas.



The schematic of experimental setup of indigenously developed novel CO laser.

### Design & development of six electrode large volume Gliding Arc Discharge Torch

A six-electrode gliding arc discharge torch with a power source (15 kV, 0.3 A @ 50 Hz) was designed, fabricated and operated. The arc glides forward from the narrowest gap between the



Six electrodes GAD torch.



electrodes and expands along the plasma gas flow direction. Key features of the torch are variable electrode gap (15 mm to 100 mm), production of large volume atmospheric pressure non-thermal plasma. It was successfully tested with both argon and air as plasma gas. The potential applications include exhaust gas purification from plants, methane reforming, nitrogen fixation and in plasma catalytic processes.

### Applications of Magnetic Pulse Welding

Magnetic Pulse Welding (MPW) technique was successfully applied in joining SS304 Tube to AA5052 tube as an alternative method for rotary friction welding. MPW reduces number of machining and forming processes in addition to mitigating thermal stress. It has also been used for joining D9I clad to SS316LN end plug for PFBR fuel application. The welds were qualified for HLD, UT and found to have bonding in 3 to 5mm range at 6-degree tapered angle. Furthermore, MPW has been applied in joining Ti-SS dissimilar metal joint for FBRs. The welded samples have qualified a helium leak rate up to  $10^{-9}$  mbar. lit/s, revealed a continuous lap bond of ~ 3-4 mm and exhibited a hardness of ~330 HV indicating the formation of intermetallic at the joint interface.

## Sensors, Detectors and Specialized Instruments

### In-vessel level & temperature sensor assemblies

Indigenous Heated Junction Thermocouple based discrete level sensors have been developed for PWR type reactors to directly measure coolant level and temperature within the reactor pressure vessel. These sensors detect water presence at up to 3 critical locations and withstand harsh Reactor Pressure Vessel (RPV) conditions. Despite manufacturing challenges due to dimensional constraints (fitting six thermocouples and a three-zone heater inside a 9mm tube) and stringent qualification requirements as part of the RPV pressure boundary, functional sensor assemblies were successfully designed, manufactured and tested for upcoming PWRs.



Heated Junction Thermocouple based discrete level sensors.

### Servo Control System for defence sector applications

BARC has developed a Ku band 0.6M Airborne Satcom Terminal (AST) to meet the requirements of indigenous aerial surveillance program of defense sector. The AST is equipped to stabilize the Satcom antenna against the roll, pitch and heading motions and latitude, longitude and altitude changes of the aircraft. Designed to operate at up to -54°C ambient temperature and up to an altitude 40,000 feet AMSL, it supports multiple mode of operations viz., standby, pointing, slew and manual mode. The test results of the integrated AST were found to be in line with the user requirements. The fitment trials of 0.6M AST ET with UAV (TAPAS) were also completed.



The 0.6M Airborne Satcom Terminal ET with ACU.

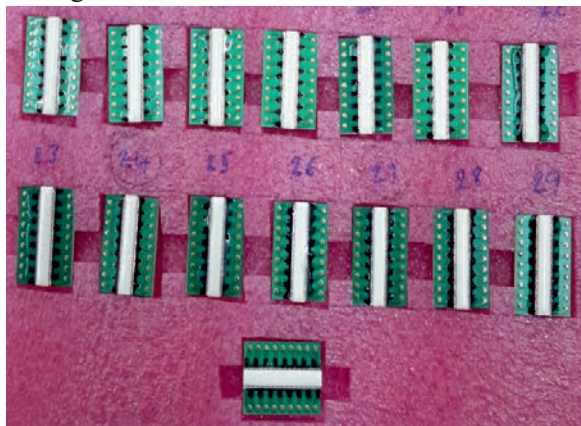


### Implementation of redundant CPUs in remote I/O nodes of NUCON PLC

The indigenously developed NUCON PLC platform has been enhanced with redundant CPU capability in Remote I/O nodes to improve fault tolerance, reliability and availability. This enhancement allows two CPUs on the same backplane in hot standby configuration within a single RIO node. The implementation uses customized FPGA firmware for fault detection and seamless switchover between redundant CPUs. The design has been fully documented according to development processes and successfully tested.

### Daisy Chain Protocol for fiber optic dual ring RIO network of NUCON PLC

A switchless, dual ring, real-time data communication protocol has been developed for NUCON PLC network modules, eliminating commercial network switches in distributed control systems. This Dual Ethernet Ring Network with Fiber Communication provides high-speed, fault-tolerant, EMI-free communication over long distances. The daisy chain protocol efficiently handles data communication from RIO nodes over the dual ring network, incorporating path rerouting algorithms for node or segment failures. Redundant paths ensure seamless failover during link or node failures, verified through rigorous testing with three Remote I/O nodes.



16-pixel photodiode linear array with  $3.2 \times 1.4 \text{ mm}^2$  pixel size.

### Detectors for X-ray based imaging systems

A production lot of 750 detectors for X-ray baggage scanner systems has been fabricated. Each detector features a 16-pixel photodiode linear array with a pixel size of  $3.2 \times 1.4 \text{ mm}^2$ , coupled with a CsI scintillator array. The detectors were characterized using an in-house developed test setup to evaluate their forward and reverse characteristics. Additionally, noise

performance was tested by integrating the detectors with readout electronics. All detectors demonstrated satisfactory performance for implementation in X-ray baggage imaging systems.

### Small size He-3 REM Detectors

Five indigenous small-size He-3 neutron detectors for Roentgen Equivalent in Man (REM) monitoring have been successfully developed and qualified, reducing import dependency. These one-inch diameter detectors have a 1cm sensitive length with ~6cm overall length including gas filling tube. They feature a cylindrical cathode with a  $50\mu\text{m}$  diameter tungsten wire anode mounted axially. After evacuation to  $10^{-6}$  bar vacuum, the detectors are filled with high-purity He-3 gas for neutron detection and 35% Kr to reduce wall effect, achieving acceptable average neutron sensitivity of 0.5 cps/nv for REM monitoring applications.

### High temperature tolerant Natural Boron coated Parallel Plate Ion Chamber Detector

A parallel plate gamma uncompensated Boron lined Ionization Chamber with enhanced boron coating has been developed through a joint collaboration exercise in BARC. Unlike the conventional brush coating method, this technique uses an inorganic binder providing superior adhesion on any cathode surface and temperature tolerance up to  $600^\circ\text{C}$ . The detector measures 50mm in diameter with 300mm overall length and 128mm sensitive length, filled with Nitrogen gas at 700mm Hg pressure. Qualification tests confirmed neutron sensitivity of 2.05fA/nv, gamma sensitivity of 0.98 pA/R/h, and signal linearity within 1%.



Natural boron coated parallel plate ionization chamber.

### X-Ray based automatic PHWR fuel pellet scan system

A software system has been developed for the automatic detection of missing uranium fuel pellets from zirconium tubes placed in fuel trays. This X-Ray based Automatic PHWR Fuel Pellet Scan System has been commissioned at Nuclear Fuel Complex in Hyderabad and is currently being used to ensure the completeness of fuel pellet stacks in PHWR fuel pins. The automation of missing pellet detection has streamlined the

workflow at NFC Hyderabad and the system has significantly improved the efficiency and reliability of the fuel pin inspection process.

### Indigenous PuCAM

A Plutonium Continuous Air Monitor (PuCAM) has been developed to detect airborne plutonium in real time and trigger alarms when activity exceeds preset thresholds. The system uses a locally developed Ion-implanted Planar Silicon detector with 450 mm<sup>2</sup> active area coupled to a Multi-Channel Analyzer. BARC developed the detector heads including detector, biasing and signal conditioning systems, while IGCAR handled the remaining hardware and software development. Production was completed by ECIL.



Detector Head of PuCAM.

### Polystyrene pellets for large plastic scintillator detectors

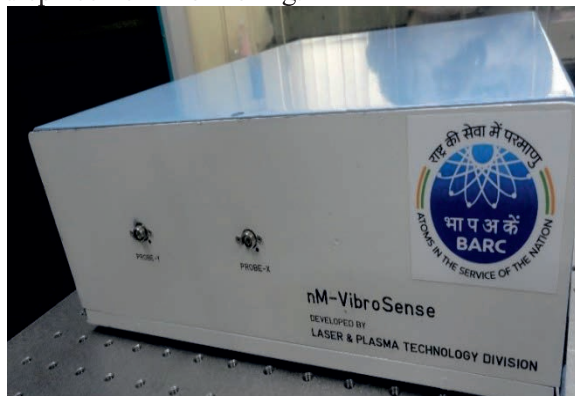
Small plastic scintillators (5 cm × 5 cm cylinders, thin films, and sheets) from styrene monomer that match imported equivalents in quality were successfully developed through in-house efforts. To advance to larger rectangular slab scintillators, we needed technology to fabricate polystyrene pellets for cell casting. A polystyrene reactor with extruder system featuring a hot oil-based temperature controller, devolatilizer, and polymerization vessel was designed and built in BARC. The extrusion system forms polystyrene strands, later cut into custom-sized pellets. The reactor is now operational, with ongoing trials to optimize polymerization parameters.



Polystyrene developed in BARC.

### Development of nMVibroSense

The nMVibroSense is a compact, laser-based instrument that measures tiny vibrations without physical contact. Designed to work in harsh environments, it uses Fabry-Perot Interferometry technology. This device can detect vibrations in the frequency range of 0.2 Hz to 1 kHz with a resolution of 0.25 Hz, and can measure movements from 0.2 μm to 15 μm with precision down to 12 nanometers. The instrument has several potential applications, including structural vibration monitoring, pump and motor vibration measurement, flow-induced vibration monitoring, and low-level shaft displacement monitoring.



nMVibroSense Instrument.



## Radiopharmaceuticals

38.6 TBq of Lutetium-177, 25.4 TBq of Iodine-131, 18.3 TBq of Molybdenum-99, 925 GBq of Samarium-153, 260 GBq of Iodine-125, and 7.4 GBq of Yttrium-90 were produced. A total of 580 consignments of radiochemical products were supplied for human clinical applications.

Five ready-to-use doses of  $[^{90}\text{Y}]$ Yttria Alumino Silicate Glass Microspheres or BhabhaSpheres were formulated and supplied for liver cancer treatment.

$^{169}\text{Er}$ -Labeled Mesoporous Hydroxyapatite Microparticles ( $[^{169}\text{Er}]\text{Er-HA}$ ) was developed for arthritis treatment, showing near-exclusive retention at the administration site in preclinical studies.

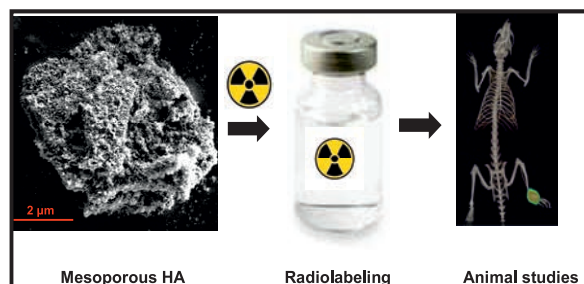
A single-vial kit for  $[^{68}\text{Ga}]\text{Ga-NODAGA-JR11}$  was prepared and evaluated in neuroendocrine cancer patients, showing high uptake in primary and metastatic sites.

A novel radiolabeled rituximab-chlorambucil (Antibody-Drug) conjugate was prepared, showing higher cell toxicity and increased tumor uptake compared to individual counterparts.

Novel  $^{99\text{m}}\text{Tc}$ -Labeled Lactoferrin-Based Nanoparticles (LF-NPs) were developed for Sentinel Lymph Node (SLN) detection, with PEGylated LF-NPs showing improved properties and increased SLN uptake.

Novel DNA aptamers were developed for detecting Tri-iodothyronine (T3) and Thyroxine (T4) hormones, capable of detecting picogram levels in human serum.

A patient dose formulation of  $^{177}\text{Lu}$ -DTPA-Pertuzumab was optimized for radioimmunotherapy of HER2-overexpressing breast cancers. The formulation exhibited strong HER2 receptor affinity and specificity, with improved tumor uptake and retention in preclinical SPECT imaging.



Preparation and localization of  $^{169}\text{Er}$ -hydroxyapatite.

## Water Purification, Water Resources Management & Solid Waste Management

### Electron Beam treatment of textile wastewater

The treatment of 10,000 litres of industrial textile effluent using electron beam technology (10 kGy) combined with induced coagulation achieved a significant reduction in Chemical Oxygen Demand (COD) levels, decreasing from 761 mg/l to 204 mg/l.

### Textile effluent decolouration

Radiation-Assisted Adsorbent Technology for Textile Effluent Decolouration (RAD-TED), developed for treating textile dye effluents, has been installed at a 75 KLD plant in Jodhpur. Over 800 KL of wastewater has been treated, and the technology has been transferred to two licensees. Rajasthan State Pollution Control Board approved its application.

### Radiation-grafted functional adsorbent for mercury remediation in water

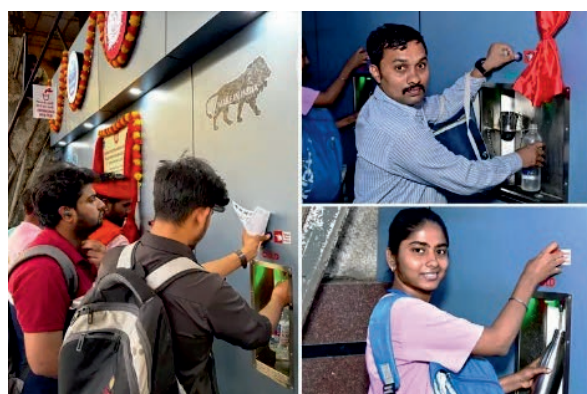
A cellulose-based adsorbent was developed for efficient mercury (Hg) removal from water. The adsorbent demonstrated fast uptake kinetics, with a removal capacity of 175 mg/g, and could be reused for over 5 cycles.

### Microplastic separation using superhydrophobic jute fabric

Superhydrophobically modified jute fabric was used for efficient microplastic removal from water, achieving over 95% removal efficiency for polyolefin microplastics.



## Deployment of BARC-developed water technologies



A large 750 LPH UF-based water purification-cum-dispensation unit based on BARC technological know-how installed at the busy CSMT station in Mumbai. Commuters making good use of the water facility installed at CSMT.

Five 1000 litres per hour (LPH) BWRO-based water treatment units have been deployed in Tamil Nadu, Assam, and Odisha. Additionally, 5000 UF-based water purifiers have been installed in Chengalpattu, Tamil Nadu. In Mumbai, 10 UF-based water units are operating at Central Railway platforms. Two 60 LPH UF units were installed in Northern Railways' Deen Dayalu coaches. Five BWRO plants have been set up at BSF Border Outpost, Rajasthan. More than 200 villages in country have received these technologies.

### NDDP, Kalpakkam

The Nuclear Desalination Demonstration Plant (NDDP) continued operating in 2024, supplying 213.23 million liters of pure water to Madras Atomic Power Station and 280.6 million liters to IGCAR. Membrane performance evaluation and pipeline replacement work were completed for efficient operation.

### 2.0 MGD WRO Plant at NDDP, Kalpakkam

The CRZ proposal for Kalpakkam desalination plants has been approved, and the NIT for constructing the 2 MGD SWRO plant is

released. The Consent to Establish (CTE) is submitted to TNPCB.

### 5 MLD seawater desalination plant, OSCOM, Odisha

A 5 million litres per day (MLD) seawater desalination plant, including 4.5 MLD SWRO and 0.5 MLD multi-effect distillation, has been commissioned. The plant provides essential process and potable water for OSCOM operations and was inaugurated by the Prime Minister of India in March 2024.

### Setting up MED-based nuclear desalination plant at MAPS

Tendering for a 2 million litres per day (MLD) Nuclear Desalination Plant at MAPS using MED technology has been initiated. Factory evaluation and recommendations were completed.

### Humidification-Dehumidification Desalination Unit (HDDU)

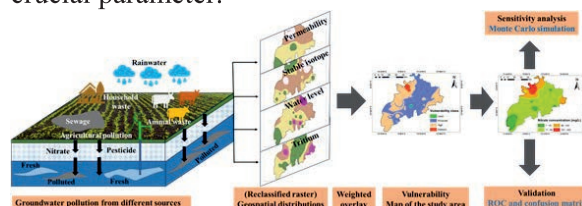
A 70 litres per day (LPD) portable HDDU, designed to extract water from high-humidity coastal air and saline feedstocks, was developed. It produces 3 LPH of pure water and is powered by a 5 KVA off-grid solar system.

### Isotopic reconstruction of paleo-recharge history in Northwest India

Environmental isotopic analysis of groundwater recharge in Northwest India reveals that deeper aquifers are sustained by meteoric recharge from the Himalayas, with groundwater residence times ranging from modern to 28,000 years. This study aids in groundwater resource management and planning.

### Aquifer vulnerability assessment using Isotope-Geospatial Modelling

Isotopic tools were used to assess aquifer vulnerability in Northern Gujarat, revealing that 97% of the area is at moderate to high risk. The model was validated using nitrate data, achieving 82% accuracy. Sensitivity analysis highlighted aquifer permeability as the most crucial parameter.



Aquifer vulnerability assessment using isotope-geospatial modeling in Northern Gujarat.

### Radiation technology for sewage sludge hygienization

Approximately 650 cubic meters of municipal sewage sludge were irradiated at SHRI Vadodara, producing 14 tons of irradiated sludge during the year. Large-scale dry sludge hygienization plants at AMC Ahmedabad and IMC Indore also continued operations.

### Commissioning of 250 kLD sewage treatment plant for BARC Hospital

A Sewage Treatment Plant was implemented at BARC Hospital to meet zero-discharge requirements. The plant uses Sequential Batch Reactor technology to process sewage in controlled batches within a single tank. The fully organic waste produces manure (solid component) and treated water (liquid component) that meets MPCB standards. This treated water supports the hospital's cooling towers and gardening needs, reducing dependence on limited municipal water supply.



250 kLD STP of BARC Hospital.

### Reuse and recycle of kitchen waste water by Membrane Bio-Reactor (MBR)

An open-channel spiral wound UF membrane system with 200 LPD capacity has been used to treat kitchen wastewater. The system achieved 100% reduction in suspended solids and 75% COD reduction, providing treated water for non-potable uses.



Kitchen waste water treatment skid in operation in BARC.

## Agriculture and Food Technologies

### Mutation breeding

BARC has released eight new crop varieties using radiation-based mutation breeding, bringing their total to 70 varieties. These climate-resilient, non-GMO crops include five cereals and three oilseeds (wheat, rice, sesame, mustard, and groundnut) developed in a joint collaboration with state universities. Seed distribution is active, with 78 quintals of rice seed in Chhattisgarh, 7 quintals in Maharashtra, and 320 quintals of groundnut seed supplied across eight states.



Chhattisgarh Trombay Mungfali

Trombay Jodhpur Mustard 2

Trombay Latur Til 10

### Registration of wheat germplasms with NBPGR, New Delhi

Three wheat germplasms have been successfully registered with the National Bureau of Plant Genetic Resources (NBPGR), New Delhi, enhancing the genetic diversity and resilience of wheat varieties in India. Trombayaestivum wheat 41 (TAW41), a novel mutant genotype that exhibits resistance to spot blotch and terminal heat, has been assigned the registration number INGR23081 and IC0648495; Trombayaestivum wheat 185 (TAW185), which is characterized by a high thousand kernel weight, has received the registration number INGR23080 and IC0648496; Trombayaestivum wheat 186 (TAW186), noted for its tolerance to both heat and drought conditions, has been registered under the number INGR23079 and IC0648497. These registrations signify an important step in improving wheat cultivation, addressing challenges posed by climate change, and enhancing food security.

### Onion preservation

An integrated technology combining irradiation (60 Gy) with controlled storage conditions maintains onions' nutritional properties for six months. A successful 250 MT trial was completed in Maharashtra.

### Novel plasma-based fertilizer

A novel thermal plasma-based compact portable catalytic system has been developed for fast synthesis of nitrate and nitrite fertilizer using



only air and water. The system offers several advantages, including portability, ability to operate with renewable energy and suitable for small-scale distributed production.

### Commercial feasibility of chilled irradiation in marine irradiator

Pilot trials have confirmed the commercial viability of Chilled Irradiation in a Marine Irradiator, enhancing the shelf life and safety of whole fish and flesh foods. Typically, meat and fish are sold fresh or frozen, with fresh products having a limited shelf life and frozen options being costly and less appealing to consumers. India, a leading exporter of frozen fish and meats, could benefit significantly from marketing these products in a chilled state, which would reduce energy costs and improve export potential. In trials conducted at BRIT's newly commissioned marine irradiator in Navi Mumbai, whole fish varieties such as Indian Mackerel, Seer fish, and Hilsa exhibited a shelf-life extension of 3-4 weeks when irradiated at 4 kGy and stored at 1°C. Additionally, research indicated that irradiated buffalo and goat meat could be stored at 0-3°C for up to 30 days, compared to just 3-6 days for non-irradiated samples. This demonstrates the effectiveness of irradiation in prolonging the freshness of meat and seafood products.



Whole fish varieties undergoing pilot trials.

### Enhanced mango exports

Radiation treatment has boosted mango exports to 3,000 tons in 2024, reaching markets in the USA, Australia, Malaysia, and South Africa. A new technology for extending Kesar mango shelf life has been commercialized.

### Bread preservation

Gamma radiation (5 kGy) extends puffed bread shelf life from 3 days to 12-14 days while maintaining quality and preventing fungal contamination.

### Dosimetry innovation

In the realm of food irradiation, accurate measurement of absorbed doses is vital. Traditionally, dosimeters like Fricke and Ceric-cerous sulfate have been used, but India lacks a cost-effective option for measuring doses between 25 to 1000 Gy. "Anudose," a cost-effective dosimeter for the 25-1000 Gy range, offers 10-month stability and minimal sensitivity to environmental variables. It is user-friendly, requiring only single distilled water for preparation, and remains stable for up to 10 months. Anudose is unaffected by irradiation temperature, dose rate, or gamma energy, and shows minimal variability between batches. Now ready for commercial deployment, Anudose promises to enhance food irradiation practices by providing reliable dose measurement, supporting food safety, and extending shelf life while adhering to global standards.



Anudose - A cost-effective dosimeter for the 25-1000 Gy range.



### Mushroom Storage

A combination of cold water washing, ultrasonication, and irradiation preserves white button mushrooms for over 20 days with quality retention.

### Expanding irradiation facilities

India has 28 operational food irradiation plants (6 government, 22 private) and seven more under commissioning, but these are insufficient for domestic and export needs. To address this, the Union Budget announced financial support for 50 multi-product food irradiation facilities under the Pradhan Mantri Kisan Sampada Yojana. A National Workshop on Food Irradiation, held in September 2024 by BARC and MoFPI, garnered strong interest, with 12 applicants already seeking support. MoFPI, in collaboration with BARC and DAE, plans to expand the initiative further.

## Technologies for Health Safety

### Remotely operated Iodine-131 vial handling system

A remotely operated system has been developed for the safe handling of Iodine-131 vials. This system consists of an articulated slave arm mounted on a movable trolley and a master arm located at a remote control console. Its primary



The Master arm at remote control console of Iodine-131 vial handling system.

function is to place I-131 vials into shielded casks for transportation to BRIT, thereby minimizing radiation exposure and contamination risks to human operators at the Iodine Production Facility. The system is designed to be deployed on-site, allowing for the retrieval of I-131 vials from shielded hot-cells. Operators use the master arm at the remote control console to perform handling operations, guided by real-time video feedback. This setup ensures a safer and more controlled environment for handling radioactive materials.

### Table-top fluorescence based Heparin Analyser

In critically ill patients, precise monitoring of anticoagulant Heparin is essential for improving outcomes. A newly developed compact Heparin Analyser offers a standardized method for real-time and accurate detection of anticoagulant activity in clinical settings. Some of the key features of the analyser include Limit of Detection (LOD) of 0.5 U/ml, Linear Detection Range of 0–5 U/ml and provides results within 1 minute. This analyser is particularly beneficial for patients undergoing cardiovascular surgeries, hemodialysis, intensive care, and post-operative care, ensuring that healthcare providers can effectively manage anticoagulation therapy in these vulnerable populations.

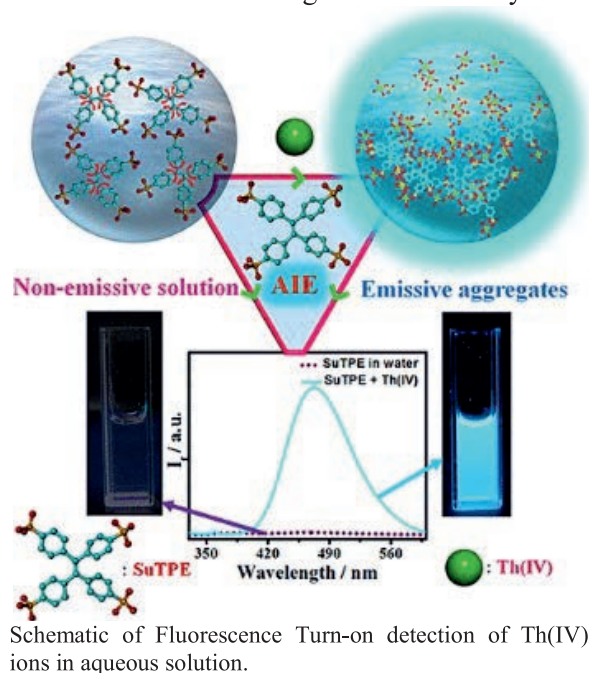


Heparin Analyser.

### Selective sensing of Thorium in aquatic systems for health safety

A turn-on detection method for thorium (Th(IV)) using aggregation-induced emission (AIE) of the fluorophore tetra (4-sulfophenyl) ethylene (SuTPE). The aggregation of Th(IV) enhances the emission properties of SuTPE, enabling selective detection in 100% aqueous media. The sensing mechanism was investigated through various techniques, including ground-state

absorption, steady-state and time-resolved emission spectroscopy, FTIR, DLS, SEM, AFM, and quantum chemical studies of the SuTPE-Th(IV) complex. The probe's selectivity for Th(IV) was confirmed by assessing interference from other metal ions, such as lanthanides and uranyl. The limit of detection (LOD) for Th(IV) was found to be 240 nM (56 ppb). The probe's performance was validated in both tap water and diluted seawater, marking a significant advancement for Th(IV) detection in aquatic environments, with implications for environmental monitoring and health safety.



### Multi-cuvette LED fluorimeter system for uranium concentration measurement in bioassay samples

A multi-cuvette LED fluorimeter system (LF-3) with automated sample processing and analysis has been developed to measure uranium concentration in bioassay samples. The system uses fluorescence measurement technique and is capable of analyzing 16 samples in a duration of 2-3 minutes, significantly reducing the sample counting time. The excitation source for the LF-3 system consists of a bank of pulsed LEDs that emit light at 340 nm, which excite the uranyl ions, and upon de-excitation the ions emit fluorescence at 496, 516, and 540 nm which is detected by a photomultiplier tube. The LF-3 system has been standardized and validated. The compact design of LF-3 makes it suitable for use as a portable uranium analyzer in case of radiation emergency situations.



Multi cuvette LED fluorimetry system.

### Fluorescence sensor for Protamine & Trypsin

A novel fluorescence sensor utilizing (4-(1,2,2-tris(4-phosphonophenyl)vinyl)phenyl) phosphonic acid octasodium salt (TPPE) was taken up. The sensor employs aggregation-induced emission (AIE) and electrostatic interactions for the selective and sensitive detection of protamine and trypsin. The interaction mechanisms and aggregation dynamics of TPPE with these biomolecules were analyzed through optical characterization. The sensor demonstrates high sensitivity, with limits of detection (LOD) of 1.45 nM for protamine and 32 pM for trypsin. It maintains selectivity and stability while functioning effectively in complex biological matrices such as human serum and urine. This design highlights the synergy between AIE phenomena and biomolecular interactions, offering a promising alternative for analytical applications in biomedical research and clinical diagnostics. The principles established could pave the way for developing other AIE-based sensors for various biomolecules.

### Area Radiation Monitors for Accelerator Facilities

Accelerators generate pulsed and scattered radiation, increasing dose rates in surrounding areas during operation. To ensure safety, an Area Radiation Monitor (ARM) using plastic scintillator detectors in charge accumulation mode has been developed. These detectors offer near tissue-equivalent energy response without external filters, fast response, and high saturation dose rates, making them ideal for pulsed radiation monitoring. The system integrates an ARM processor-based single-board computer



with efficient data acquisition electronics, features a local real-time dose rate display, and provides radiation data over Ethernet via MODBUS TCP/IP for facility-wide integration.

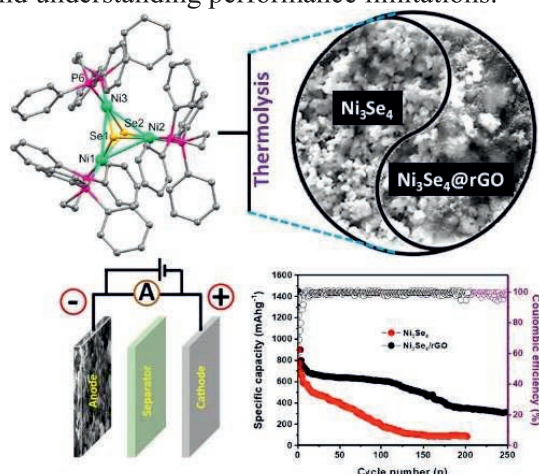


Area Gamma Monitor.

## Energy Storage Materials

### Nickel Selenide synthesis for LIB anodes

Nickel selenides ( $\text{Ni}_x\text{Se}_y$ ) demonstrate promising potential as electrode materials for energy applications due to their unique chemical and physical properties. A trinuclear nickel selenolate complex has been synthesized which functioned as an effective molecular precursor for producing  $\text{Ni}_3\text{Se}_4$  nanostructures. These nanostructures were characterized using pXRD and electron microscopy techniques. Band gap measurements were conducted to evaluate electronic conductivity. While the nanostructures were tested as LIB anode materials, they exhibited low lithium uptake. Current efforts focus on enhancing electrochemical performance and understanding performance limitations.



Schematic representation of  $\text{Ni}_3\text{Se}_4$  based supercapacitor performance.

### $\text{V}_2\text{O}_5$ -Polypyrrole-Graphene Oxide Hybrid for enhanced solar evaporation & thermoelectric power generation

A novel hybrid photothermal structure (PPy- $\text{V}_2\text{O}_5$ -GO) was developed by intercalating  $\text{V}_2\text{O}_5$  and polypyrrole into graphene oxide layers. This multifunctional assembly achieved a  $1.9 \text{ kg m}^{-2}\text{h}^{-1}$  water evaporation rate with 92% conversion efficiency under 1 Sun, reaching surface temperatures of  $64 \pm 2^\circ\text{C}$ . Field testing demonstrated  $15 \text{ kg m}^{-2}$  daily water output. When integrated with a  $\text{Bi}_2\text{Te}_3$  thermoelectric module, the system generated 2.8 mW power with  $1.24 \text{ mW/cm}^2$  power density. The stable, recyclable assembly effectively purifies seawater without leaching, offering a sustainable solution for both water treatment and off-grid power generation.

### $\text{MnO}_2$ -doped Graphene Oxide hydrogel for efficient photothermal applications

A composite material consisting of GO and  $\text{MnO}_2$  embedded in an alginate matrix ( $\text{MnO}_2@\text{GO}@\text{Alg}$ ) was synthesized and evaluated for photothermal applications. Under 1 Sun illumination, the material reached  $55^\circ\text{C}$  within 5 minutes, demonstrating 91% light-to-heat conversion efficiency and a high-water vaporization rate of  $4 \text{ kg m}^{-2} \text{ h}^{-1}$ . The stable composite showed no component leaching and effectively purified both dye-contaminated water and real seawater. When coupled with a commercial thermoelectric module, it generated 350 mV voltage and 1.2 mA current, confirming its dual functionality for clean water production and power generation.

### Rare earth element doped Prussian Blue analogs for electrochemical energy storage

Prussian Blue and its analogs (PB/PBAs) offer excellent properties for energy storage applications, including stability, electrical conductivity, abundant catalytic active sites, and large specific surface area. A reduced graphene oxide/Ni-Fe PBA nanocomposite was synthesized via hydrothermal method. Rare earth metal ion doping created additional redox sites in the RGO/Ni-Fe PBA, enhancing electrochemical performance. Testing in 1M KOH solution demonstrated good cyclic stability through 500 cycles in both cyclic voltammetry and galvanostatic charge-discharge measurements. The material's redox properties also enabled detection of important biomolecules, including dopamine, ascorbic acid, and uric acid.



## Hydrogen Energy Technologies

### Commissioning of alkaline water electrolyzer Plant

A compact alkaline water electrolyzer plant capable of producing 3 Nm<sup>3</sup>/hr of hydrogen gas has been commissioned. The facility underwent leak testing, with necessary adjustments made to ensure integrity. Utility systems, including chilled water and nitrogen generation, were integrated, along with in-house developed control and instrumentation systems. Aqueous potassium hydroxide was prepared for performance testing.

### Tank-type water electrolyzer design and installation

The skid-mounted tank-type water electrolyzer with a gas purification system has been designed and fabricated. It features a compact four-tank cell configuration with a hydrogen generation capacity of approximately 1 Nm<sup>3</sup>/h. The design and installation of a PLC-SCADA-based control system have also been completed.



Tank type water electrolyzer system.

### MW Scale Alkaline Water Electrolyzer cell stack design

Following the successful demonstration of a 500-kW prototype stack, a 1 MW alkaline water electrolyzer cell stack was fabricated using indigenous technology. CFD studies evaluated pressure drops and ensured uniform electrolyte flow within the cell. A numerical technique was developed to assess intra-half-cell and stack performance, incorporating two-phase flow hydrodynamics.



1 MW Prototype Alkaline Water Electrolyzer cell Stack under operation.

### Proton Exchange Membrane (PEM) development

Proton Exchange Membranes (PEMs) are essential in PEM water electrolyzers and fuel cells, playing a significant role in the hydrogen economy. Currently, PEMs are primarily imported, but efforts for indigenous development are underway. Sulfonated poly(ether ether ketone) (PEEK) membranes, stable up to 80°C, are being optimized for quality. In-situ small-angle X-ray scattering (SAXS) experiments conducted from room temperature to 300°C aim to understand the evolution of pore structure with temperature.

### Anion Exchange Membrane (AEM) development

Anion exchange membranes (AEMs) selectively transport anions while blocking cations. Two approaches for AEM development are being pursued. These include Chloromethylation and Radiation Grafting. As part of this, chloromethyl ethyl ether (CMEE) was synthesized and characterized via NMR. Polymers were modified with CMEE to introduce halide groups and subsequently quaternized using trialkyl amines. The Radiation Grafting of Vinyl Monomers method yielded graft percentages ranging from 11% to 39%. The resulting polymers were also quaternized and characterized, achieving a maximum conductivity of approximately 19 mS/cm at 60°C.

### Indigenous PEM Hydrogen Generator Development

The polymer electrolyte membrane (PEM) electrolysis system utilizes a solid polymer electrolyte for high-pressure water splitting. A test membrane and membrane electrode assembly were designed for a multi-cell electrolyzer system with an active electrode area of 63 cm<sup>2</sup> per cell. The end plates were reinforced to withstand gas pressure, while porous electrodes optimized for 80% porosity utilized IrO<sub>2</sub> and Pt-based catalysts with a loading of about 1 mg/cm<sup>2</sup>.

### Hybrid natural circulation water electrolyzer

The hybrid electrolyzer is a natural circulation alkaline water electrolyzer that produces high-purity gases directly from the cell module, eliminating the need for a Balance of Plant (BOP) typically required for gas conditioning. This robust and durable system features no moving parts and includes an internal gas-liquid separator in each half-cell, enhancing dynamic response. A single cell stack has been designed and tested at 3000 A/m<sup>2</sup>, achieving a hydrogen production rate of approximately 40 NL/h with over 99.9% purity. Additionally, a 10-cell stack is designed for a capacity of 500 NL/h.

### Copper-Chlorine thermochemical cycle process development

An integrated pilot-scale Copper-Chlorine (Cu-Cl) thermochemical cycle facility was installed with a design capacity of 150 NL/h hydrogen production. This facility demonstrated hydrogen production over 225 hours, marking the highest operational duration for any thermochemical cycle globally. Key features include novel cycle integration, efficient multiphase reactors, and systems for handling high-temperature solids and molten salts, all within an intensified plant footprint.

### Membrane Electrode Assembly (MEA) for Cu-Cl Cycle development

Systematic experiments were conducted to optimize a Proton Exchange Membrane (PEM)-based Membrane Electrode Assembly (MEA) for the electrolyzer step of the Cu-Cl thermochemical cycle. This involved selecting and testing various materials, including PEM membranes, catalysts, and gas diffusion electrodes, under different process parameters such as pressure, temperature, and catalyst loading. Significant improvements in material structure and operating conditions were

achieved. An optimized MEA with an active area of 256 cm<sup>2</sup> (16 cm x 16 cm) was successfully developed and tested.



Integrated pilot scale Copper-Chlorine (Cu-Cl) thermochemical cycle facility with design capacity of 150 NL/h hydrogen.

### Pd-Ag metal membrane reactor for ammonia decomposition

A Pd-Ag metallic membrane reactor was fabricated using a DC magnetron sputtering machine. Ammonia decomposition studies with a commercial Fe-Co/C catalyst achieved approximately 90% conversion at 500°C and 1 bar, surpassing the ~80% conversion in conventional packed bed reactors. The membrane reactor produced pure hydrogen (99.9%) and is expected to reduce capital costs by about 30% in ammonia cracker units. CFD simulations determined an optimal reactor diameter of 400 mm for a length of 1000 mm. Comparisons between ceramic and metallic membrane reactors showed that the metal membrane reactor could achieve ~100% conversion at 450°C (1 bar), while the ceramic reactor achieved only ~85% with significant ammonia loss. Efforts are underway to commercialize this technology.

### Gamma irradiated Bi/V/Mo Ternary Oxides for PEC water splitting

BiVO<sub>4</sub>/CoBi composite electrodes were synthesized and irradiated with 50-100 kGy gamma radiation for photoelectrochemical water splitting. Gamma irradiation reduced surface recombination states, enhancing performance by 170% under AM 1.5 sunlight. Hematite photoanodes were also developed with thickness optimization, showing 1 μm films achieved optimal charge transfer efficiency and donor density. Results were validated using IMPS and Gartner equation analysis.



### Magnesium Hydride for enhanced hydrogen storage

Magnesium Hydride ( $\text{MgH}_2$ ) is a promising solid-state hydrogen storage material due to its high gravimetric capacity (7.6 wt%) but is limited by a high dehydrogenation temperature of  $430^\circ\text{C}$ . To enhance its hydrogenation-dehydrogenation kinetics, mesoporous  $\text{V}_2\text{O}_5$  was added as a catalyst. Results showed that  $\text{MgH}_2$  with 5 wt.%  $\text{V}_2\text{O}_5$  began releasing hydrogen at  $220^\circ\text{C}$  and completed at  $290^\circ\text{C}$ , significantly lower than uncatalyzed  $\text{MgH}_2$ . A compact hydrogen storage device with a capacity of 100 normal liters was fabricated for laboratory applications, providing ultra-pure hydrogen for various processes.



Prototype of portable hydrogen storage gas dispenser for laboratory applications.

### High temperature glass sealant for HTSE hydrogen production

A high-temperature glass sealant has been developed for use in high-temperature steam electrolyzer (HTSE) systems for hydrogen production. Its thermal and chemical compatibility with HTSE cell components was tested, demonstrating long-term stability up to 500 hours under thermal cycling. The glass sealant was tested in tubular HTSE single cells at  $800^\circ\text{C}$  for over 300 hours with 14 thermal cycles from room temperature to  $800^\circ\text{C}$ , indicating its suitability for long-term HTSE operation. The synthesis of the glass sealant has been successfully demonstrated in batches of 100 grams.

### Enhancing $\text{TiO}_2$ photocatalytic activity through strategic doping

Titanium Dioxide's photocatalytic activity for hydrogen generation and  $\text{CO}_2$  conversion under visible light was studied. These processes

represent promising approaches to combat global warming and develop sustainable energy. Our research focuses on modifying anatase  $\text{TiO}_2$ 's electronic structure through strategic doping. Pure  $\text{TiO}_2$  has a 3.13 eV bandgap, restricting its photocatalytic activity to UV light. Cu-doping creates unoccupied midgap states that divide the bandgap into smaller regions (0.96 and 1.75 eV), reducing the effective excitation threshold. However, these impurity states accelerate electron-hole recombination, decreasing photo conversion efficiency. Notably, co-doping with W or Mo eliminates these impurity states, producing a clean band structure that enhances photoconversion efficiency through extended light absorption range and reduced electron-hole recombination.

## Specialized Technologies

### Development of Post Quantum Cryptography in BARC networks

BARC has implemented a StrongSwan VPN using Open Quantum Safe (OQS) algorithms to enable post-quantum cryptography (PQC) in its networks. An IPsec tunnel was successfully demonstrated for live video streaming and network performance testing, utilizing Raspberry Pi devices and a network server as the VPN gateway. The configuration uses CRYSTAL-Dilithium for digital signatures and CRYSTAL-Kyber for key encapsulation. Internet Key Exchange (IKE) conformance was validated with tools such as conf-test, IKE-Scan, and load-tester.

### Scanning Electron Microscope equipped with Thermionic Electron Emitter

A tungsten filament-based Scanning Electron Microscope (SEM) with a thermionic electron emitter was developed by BARC, which enables microscopy and microanalysis with spatial resolution down to 20 nm. SEM uses a finely focused electron beam, generated by heating a tungsten filament, to image and analyze the surface morphology and composition of specimens. It is widely used across scientific and engineering fields due to its versatility and minimal sample preparation requirements. Despite high demand, India previously lacked domestic SEM manufacturers, leading to reliance on costly imports. The indigenous SEM technology from BARC is expected to provide a cost-effective, customizable alternative for Indian research institutions, universities, and



industries, supporting import substitution and local innovation.



Tungsten filament-based SEM.

## Silicon Carbide hydrothermal corrosion resistant coating

The technology for creating silicon carbide (SiC) thin films ( $\sim 1 \mu\text{m}$ ) using Plasma Enhanced Chemical Vapour Deposition (PECVD) from a non-toxic, single-source precursor - polycarbosilane - was developed. Tests on SS316 tubes (254 mm diameter, 200 mm height) demonstrated successful conformal coverage over the entire tube length. The coating achieved proper SiC stoichiometry as confirmed by XPS and XRD analysis, with strong adhesion (LC1  $\sim 12\text{N}$ ), excellent ambient stability lasting 12 months, and superior wear resistance when tested against 5 different counterface materials.



SiC thin film deposited on SS Tube via PECVD.

## Automated Guided Vehicle for PHWR fuel pellet plant

An Automated Guided Vehicle (AGV) has been developed for automated transfer of PHWR fuel pellet boats between the compaction and

sintering areas of the pelletization plant at Nuclear Fuel Complex, Kota.



Automated Guided Vehicles.

## Fabrication of silicon pad detectors

Silicon pad detectors were made using locally produced high-purity silicon wafers and tested them at TIFR's Pelletron facility with Am-241 and Th-229 lab sources. The in-house detector achieved an energy resolution of about 2.2% with the Am-241 source, which comes close to the 1.8% resolution of the best commercial wafer-based detectors of the same design.

## Pilot scale crude Trichlorosilane production plant at HWBF, Talcher

The design calculations for precoolers using cooling and chilled water systems. These precoolers reduce both low-temperature refrigeration requirements and the needed surface area for the main Trichlorosilane condenser were completed. The process flow diagrams for both the Crude Trichlorosilane production and Silicon Tetrachloride recycle plants by adding precoolers, knockout drums, hydrogen compressors, and surge vessels have been updated. The electrical and instrumentation work on the silicon tetrachloride to trichlorosilane conversion test setup was updated, finishing cable installation and panel wiring for heaters and thermocouples. The  $\text{H}_2$  and STC mass flow controllers were installed, two in-house fabricated resistive heaters on the fluidized bed reactor for silicon tetrachloride conversion experiments, and an in-house fabricated condensate storage tank.

## Purification of germanium for HPGe detector

The germanium used for the HPGe detector has been purified using zone refining under optimized conditions. Measurements of the refined germanium's physical properties showed

a purity level of approximately 12N. A total of 2 kg of this purified material has been earmarked for in-house efforts for crystal growth.



Zone refined germanium ingot.

### Removal of carbon dioxide from air by adsorption

Removing CO<sub>2</sub> from the atmosphere is essential. Adsorption is a promising approach due to its relatively low energy use and operating costs. While physical adsorption processes operate under mild conditions, they have limited capacity. Chemical adsorbents like alkali metals, calcium oxides, and magnesia form stronger bonds but require high temperatures (above 200°C) for regeneration. A novel macro-porous polymer resin-based chemical adsorbent that can capture CO<sub>2</sub> at room temperature and regenerate

at lower temperatures (below 100°C) while maintaining reasonable capacity is being studied. This material was tested in a recirculating packed bed batch reactor to measure its adsorption kinetics.



The adsorbent used for removal of carbon dioxide from air.





# BASIC AND DIRECTED RESEARCH

BARC has a highly competent workforce which is ingrained in pursuing specialized research in fundamental aspects of sciences, to complement inherently complex nuclear technologies. Over the years, research in basic sciences has expanded significantly from the traditional domains into new and emerging areas with a clear emphasis on ensuring directed outcomes that would contribute immensely towards improving the overall standard of living. In line with this philosophy, sustained efforts are underway in physical sciences, chemistry, biology, water resources management, radiotherapy and radiopharmaceuticals, mutation breeding for improved crop varieties, food preservation approaches and waste management, to achieve the desired outcomes.





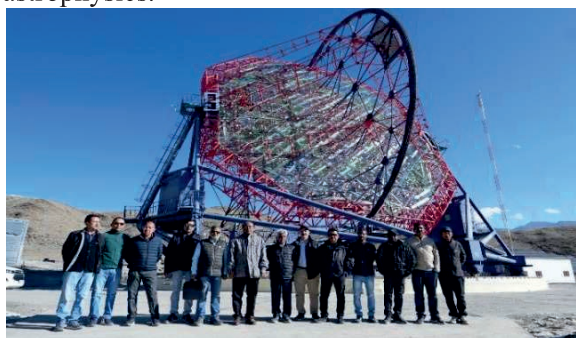
Inauguration of MACE observatory at Hanle, Ladakh on October 4<sup>th</sup> 2024. Senior officials of DAE and BARC accompanied Dr. Ajit Kumar Mohanty, Chairman, AEC and Secretary, DAE and Dr. S.M. Yusuf, Director, Physics Group, BARC during the event.

# Basic and Directed Research

## Astrophysical Sciences

### Inauguration of MACE Observatory

Asia's largest and world's highest MACE Imaging Cherenkov Observatory at Hanle, Union Territory of Ladakh was inaugurated on October 4<sup>th</sup> 2024. The inauguration of MACE Observatory was a part of the Platinum Jubilee year celebrations of the DAE. The MACE observatory will serve as a beacon of inspiration for future generations of Indian scientists, encouraging them to explore new frontiers in astrophysics.

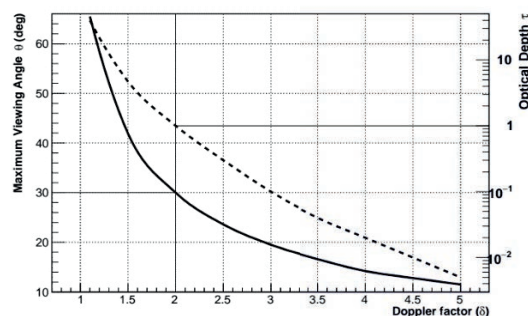


The MACE Telescope at Hanle in Ladakh.

### MACE observations & results

The Major Atmospheric Cherenkov Experiment (MACE) telescope observed more than 25 galactic and extragalactic sources in the year 2024. The telescope has detected a nearby blazar, Markarian 421 in the flaring state on March 16, 2024, with an integral flux of ~70% of the Crab Nebula. Preliminary analysis of the recorded data shows that the differential energy

spectrum extends below 50 GeV. Detection of these low energy photons by ground-based experiment uncovers key scientific insights on the radiative processes in astrophysical sources.



The maximum viewing angle of NGC 1275 jet (solid line) and optical depth (dotted line) for different Doppler factor values.

A detailed analysis of the MACE data, collected from the radio galaxy NGC 1275 on December 21, 2022, and January 10, 2023, along with other multi-wavelength observations, has helped estimate the maximum viewing angle of its jet as 30 degrees. This is the first robust estimation of the viewing angle of NGC 1275 jet, based on very-high-energy gamma-ray observations, challenging earlier estimates of 30–60 degrees using radio observations.

### Phenomenological studies in Astrophysics

An expanding fireball model has been developed to explain the prompt emission spectra of gamma-ray bursts (GRBs). The model can explain the peculiar peak observed in the

spectral width distribution of a sample of GRBs which could not be explained by earlier blackbody emission models. A time-dependent leptonic model was developed considering various turbulence scenario for electron acceleration. The model explains observed multi-wavelength variability properties of blazars.

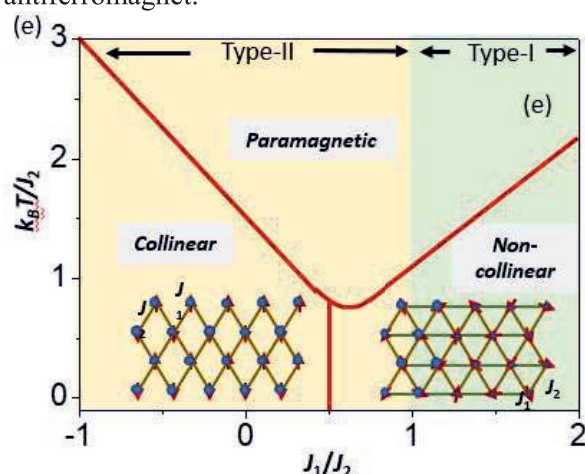
### Silicon photomultiplier camera for TACTIC

One of the elements of TACTIC telescope array at Mount Abu has been upgraded with silicon photo-multiplier (SiPM) camera developed by TIFR. The SiPM has improved quantum efficiency (~50%) in comparison with the conventional PMT. The camera has 225 pixels of size 22 mm including light guides. It will help in improving the sensitivity of the telescope and to increase its duty cycle.

## Solid State Physics

### Magnetic properties of distorted triangular lattice antiferromagnet $\text{Na}_3\text{Fe}(\text{PO}_4)_2$

A combined study of neutron diffraction, inelastic neutron scattering (INS), and density-functional-theory (DFT) calculations reveals a collinear antiferromagnetic magnetic ground state and the spin Hamiltonian involving interactions  $J_1$ - $J_2$  confined within the triangular lattice planes of the compound  $\text{Na}_3\text{Fe}(\text{PO}_4)_2$ . The ongoing study provides a benchmark for a quantitative description of the magnetic properties of distorted triangular lattice antiferromagnet.

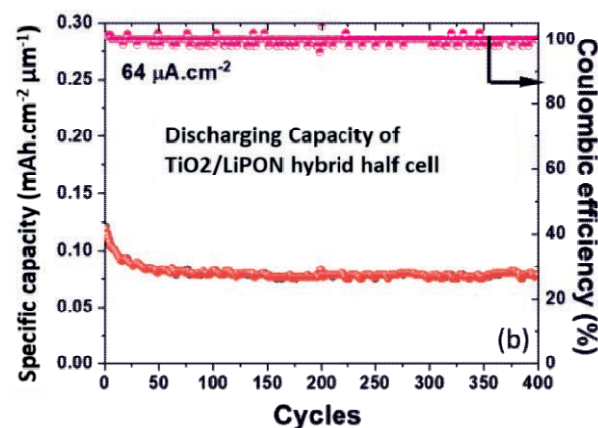


Magnetic phase diagram for isosceles distorted triangular lattice [type-I ( $J_1 > J_2$ ) and type-II ( $J_1 < J_2$ )].

### Solid electrolyte for solid-state thin film battery

Solid-state batteries with solid electrolyte have distinct advantage over conventional liquid electrolyte-based batteries in terms of safety as

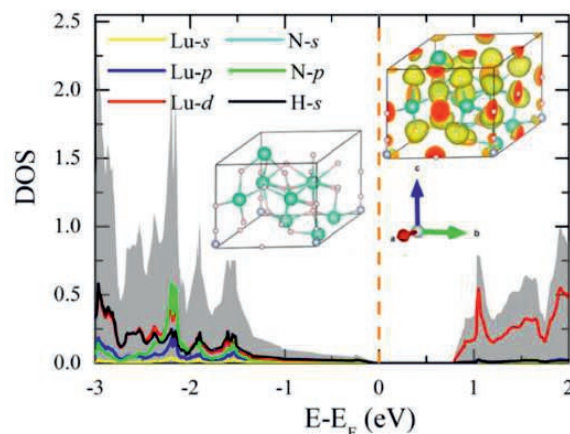
well as higher density of storage and compactness with potential use in micro-devices. As a step in this direction, a  $\text{Li}_{3+x}\text{PO}_{4-x}\text{N}_x$  (LiPON) thin film solid state electrolyte was developed by reactive radio frequency magnetron sputtering of  $\text{Li}_3\text{PO}_4$  target under nitrogen ambience. The half cells of LiPON solid state electrolyte with thin film  $\text{TiO}_2$  anode and LiPON solid state electrolyte with thin film of  $\text{LiNi}_{0.33}\text{Mn}_{0.33}\text{Co}_{0.33}\text{O}_2$  (LNMC) cathode were fabricated, which exhibited good cyclic stability in their galvanostatic charge discharge profiles.



Discharge capacity of half cells over 400 cycles of charging discharging.

### Novel ground state structures of N-doped $\text{LuH}_3$

Ab initio crystal structure searches have played a pivotal role in the recent discovery of high-temperature superconducting hydrides. The theoretical findings from novel ground-state structures for nitrogen-doped  $\text{LuH}_3$  at ambient conditions showed that approximately 1.0 wt.% N-doped  $\text{LuH}_3$  adopts an insulating ground state, in contrast to all earlier studies that proposed metallic structures. This insulating behavior persists up to around 49 GPa. The calculations also uncovered a metallic state in an H-deficient



The electronic density of states (DOS) for the ground state trigonal phase.



variant of N-doped  $\text{LuH}_3$ , which may support superconductivity. This observation establishes a clear link between the formation of N-H bonds and the insulating behaviour of N-doped  $\text{LuH}_3$ .

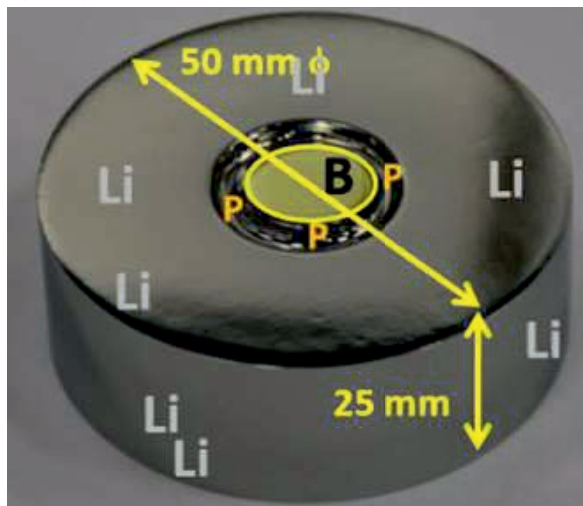
### Semiconductor to metal transition in $\text{TiS}_3$ under high pressure

Through Density functional theory and orbital-based bonding descriptors, it was found that Solid titanium trisulfide ( $\text{TiS}_3$ ) develops multicentre interactions under high pressure, mainly due to charge transfer from the  $3s^2$  lone electron pair to the antibonding  $pp$  orbitals of the S-S dimer, leading to structural instability. The study reveals a novel mechanism for the semiconductor-to-metal transition near 22 GPa, which may offer valuable insights for understanding metal-to-insulator transition in a broad range of 2D layered materials.

## Technical Physics

### Development of 50 cc volume HPGe detector

A HPGe detector (of volume 50 cc) was developed in-house from a procured single crystal. The detector diode was coupled to low noise electronics comprising pre-amplifier and feedback circuit housed in a compatible dipstick cryostat and tested for gamma spectroscopy. The energy resolution achieved at 662 keV for  $^{137}\text{Cs}$  gamma source was 0.39% as compared to 0.20% for commercial HPGe detector of similar volume.



The 50 cc HPGe diode.

### Neutron Tomography studies using Advanced Neutron Imaging Facility at Dhruva

The Advanced Neutron Imaging Facility at Dhruva research reactor has found new applications viz., studies on characterization of very old artefacts symbolizing cultural heritage

such as metallic statues, coins, weapons etc for understanding their upkeep and long-term preservation. Neutron Tomography studies on reactor materials, material science, agriculture and palaeontology are routinely conducted at Neutron Imaging Facility.



Neutron imaging of rare and vintage brass artefacts.

### Supermirror for high energy X-ray Optics

Thin multi-layered supermirrors comprising high density (viz., W, Pt) and low density (viz., Si, C) materials deposited in 36 layers were designed using dual ion beam sputtering system. The high energy (25 KeV) X-ray reflectivity of the supermirrors were measured at BL-02 beamline, Indus-2 synchrotron source at RRCAT, Indore. A continuous high reflectivity was observed up to  $0.28^\circ$  glancing angle of incidence, which is almost 1.5 times of the cut-off angle for W single layer film. The supermirror deposited with 0.3 nm carbon buffer layer shows 2% higher average reflectivity compared to the supermirror deposited without buffer layer.

### Installation of Thermal Ionisation Mass Spectrometer

The in-house developed Thermal Ionisation Mass Spectrometer (TIMS), fully customized to meet the requirements associated with precise isotopic



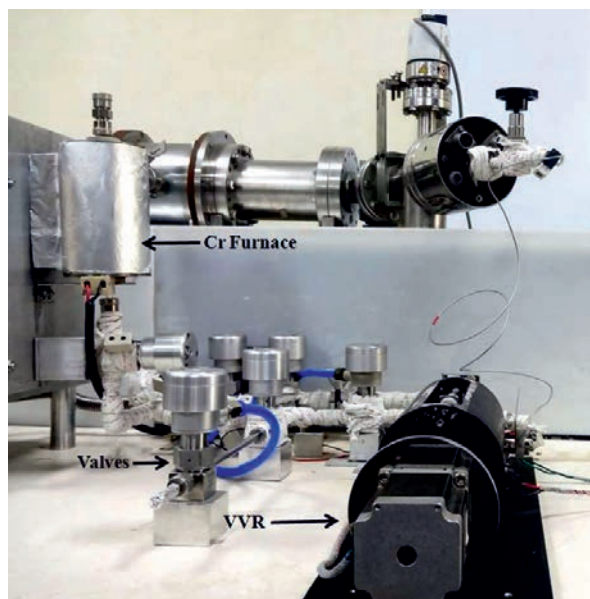
Thermal Ionisation Mass Spectrometer.



analysis of Uranium and Plutonium fuel of fast breeder reactors, was commissioned at FRFCF, Kalpakkam, and also at BARC. The salient features of the TIMS include mass range - 400 amu; resolution - 300 and precision in measurement of natural U isotopic ratio ( $^{235}\text{U}/^{238}\text{U}$ ) at 0.1%.

### System for accuracy in D/H analysis of water samples using Mass Spectrometer

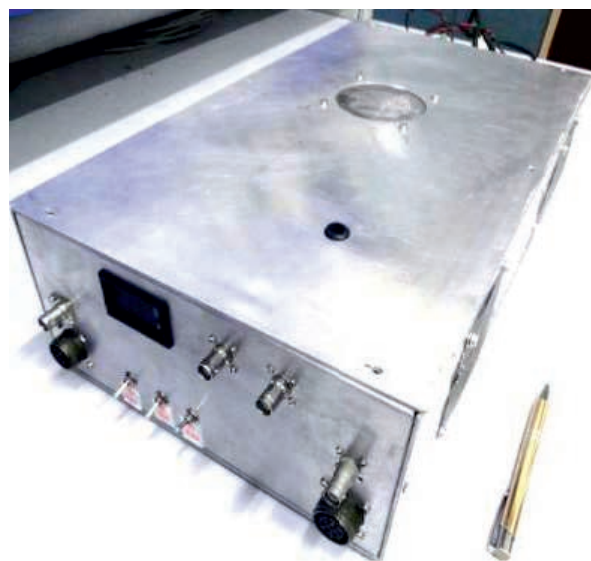
Accurate and precise measurement of deuterium content in water and heavy water is crucial for heavy water production & upgrading facilities. The D/H mass spectrometers developed by BARC employ a uranium reduction-based sample inlet system to convert water samples into gaseous form before analysis by Mass Spectrometry. To overcome challenges involved in this, a chromium reduction-based system, equipped with high-temperature chromium reactor-based Sample Inlet System and Variable Volume Reservoir was integrated for analyzing samples up to  $\pm 0.25$  ppm levels.



System Interface with Mass Spectrometer.

### Electronics package for Hydrogen-in-Steam concentration measurement system

A newly developed, highly compact QMS electronics package has been tested for implementation in Hydrogen-in-Steam Concentration Measurement System (HSCMS).



Compact QMS Electronics for HRTF/HSCMS.

### High stability modules for analytical instruments

Compact and stable HV modules with ratings of 20kV/0.5mA and 30kV/0.3mA, operating off 24Vdc, load regulation of 0.001% and ripple of 0.001% (p-p) were developed for applications analytical instruments like Mass Spectrometers, Scanning Electron Microscopes and Electron Spectroscopy.

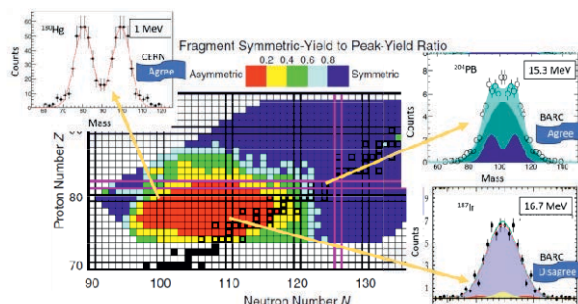


HV modules developed in BARC.

## Nuclear Physics

### Charting new mass asymmetric fission island in pre-actinide region

The fragment mass and total kinetic energy (TKE) in fission of several pre-actinide nuclei were measured using the BARC-TIFR Pelletron LINAC facility, which showcased discrepancies between the experiments and predictions of the widely accepted state-of-the-art Brownian shape Motion Model.



Nuclear chart showing the Brownian Shape Motion (BSM) model predictions.

### Experimental evidence of shell effects in Slow Quasi-fission

Signature shell effects in Slow Quasi-Fission (SQF), observed in the  $^{19}\text{F} + ^{238}\text{U}$  reaction, was studied using the BARC-TIFR Pelletron-Linac Facility, Mumbai. The experimental fission fragment mass distributions arising from the SQF process, derived by comparing the measured data with theory for several reactions, show distinct features. It was found that, irrespective of the fissioning systems, the peak corresponding to lighter fragments in the SQF mass distribution is always at  $A \approx 96$ , providing a clear evidence of shell effect in the slow quasi-fission process.

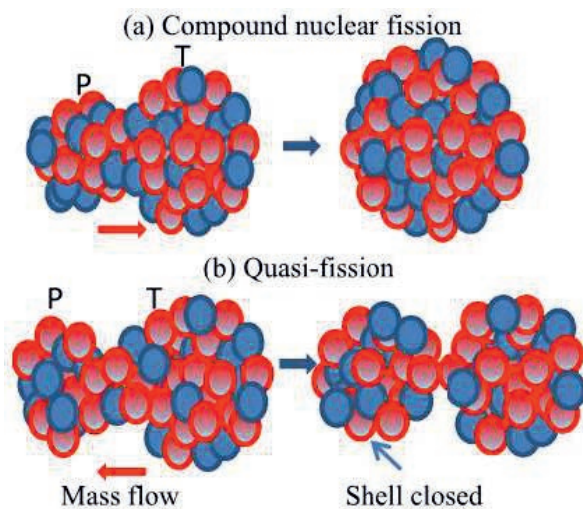


Illustration of (a) compound nuclear fission process, (b) Quasi-Fission process.

### Observation of near scission “Polar” and “Equatorial” protons emission in Heavy-ion Induced Fission

For the first time, “polar” and “equatorial” near scission protons were observed in heavy-ion induced fission reactions. These near-scission protons are observed to have similar intensities ( $\sim 20\%$ ) for perpendicular (“equatorial”) as well as parallel (“polar”) components. Around 40% of total pre-scission protons are emitted near the scission stage, whereas the same fraction for alpha particles is only around 10%. The observed results open new avenues to study the heavy-ion induced fission dynamics.

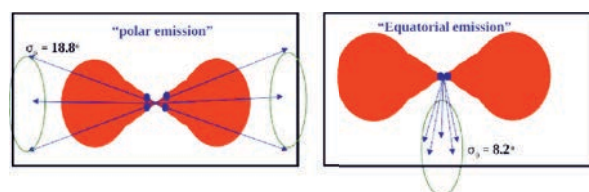


Illustration of polar and equatorial near scission emission.

### Coherent Elastic Neutrino Nucleus Scattering Studies using Antineutrinos

Measurement of Coherent Elastic Neutrino Nucleus Scattering (CEvNS) process using reactor antineutrinos provides unique opportunities for study of several neutrino fundamental properties. The CEvNS process has never been observed experimentally for the low-energy reactor neutrinos. Calculations have been performed for the India based Coherent Neutrino Nucleus Scattering Experiment (ICNSE) detector setup using p-type point contact high purity Germanium detectors (PPC-HPGe). Calculations show that the CEvNS measurements are feasible with moderate size ( $\sim \text{kg}$  scale) detectors.

### Measurement of Prompt Fission Gamma Spectrum in $^{238}\text{Np}$ ( $^6\text{Li} + ^{232}\text{Th}$ Reaction)

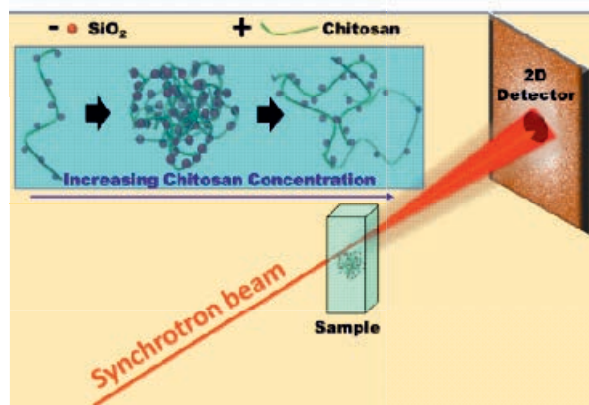
The Prompt Fission Gamma Spectrum (PFGS) of  $^{238}\text{Np}$  was measured using the  $^6\text{Li} + ^{232}\text{Th}$  reaction at the Pelletron facility in Mumbai. A pulsed  $^6\text{Li}$  beam with 40 MeV energy bombarded a  $^{232}\text{Th}$  target, and gamma rays were detected in coincidence with fission fragments. The nuclide  $^{238}\text{Np}$  was formed through a threshold (n,2n)(n,2n) reaction on  $^{239}\text{Np}$ . This study is relevant to Accelerator-Driven Systems (ADS) and the production of  $^{238}\text{Pu}$ , a key isotope for Radioisotope Thermoelectric Generators (RTGs). The results contribute to nuclear data for the uranium fuel cycle and enhance understanding of fission reactions.



## Synchrotron Beamline

### Structural collapsing & relaxation in Polyelectrolyte–Colloid complexes

Polyelectrolyte–colloid complexes exhibit remarkable phase transitions, mimicking intricate biological assemblies. SAXS experiments using the beamline BL-18, Indus-2 unveil a fascinating electrostatically driven phenomenon in such complexes, with anionic silica colloids and cationic chitosan as a model system. It unveils the formation of highly-collapsed structures (with volume fraction  $\sim 0.62$ ) until 3 wt. % of chitosan, followed by the swelling of the dense collapsed assembled structures at further higher concentrations.



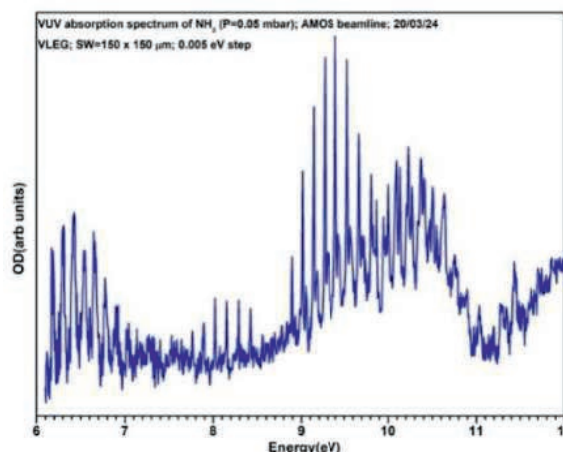
Schematic showing SAXS experiment on polyelectrolyte–colloid complexes.

### Evaluation of structural stability of Zircon at EXAFS Synchrotron Beamline

Effect of Nd incorporation on structural stability of zircon was evaluated using XRD, EXAFS, FTIR and Raman spectroscopy at EXAFS Synchrotron Beamline at Indus-2. Results indicated that apart from minor distortion in Zircon structure there were no major changes in it, making it one of the suitable host material for nuclear waste immobilization applications.

### Experiments on Atomic Molecular and Optical Science Beamline

Preliminary gas phase photo absorption studies of molecules in the VUV region and Soft X-ray absorption on solid samples were carried out at the newly commissioned AMOS beamline at Indus-2. The VUV photo absorption spectrum of ammonia - a molecule of environmental, astrophysical and industrial importance - and Naphthalene were recorded in the 6 - 11.8 eV region.

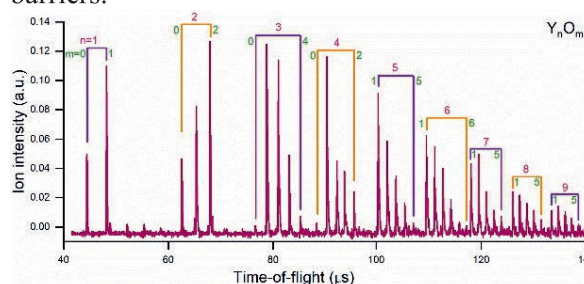


The VUV photoabsorption spectrum of ammonia in the energy region 6–11.8 eV.

## Atomic & Molecular Physics

### Experimental studies of Lanthanide metal & Metal Oxide clusters

The indigenous laser-vaporization metal cluster setup has led to the experimental assignment of density functional theory calculated stable clusters of small ( $<15$  metal atoms) lanthanide metal ( $M = Y, La$ ) and metal oxides. Monoxide clusters ( $MnO$ ) adopt the geometry of the corresponding metal clusters with the oxygen atom capping a triangular face. For the metal dioxide clusters, and also for higher oxygen content,  $M_nO_m$  ( $m \geq 2$ ), the  $O_2$  molecule–adsorbed configurations are either unstable or unfavourable in energy. The  $O_2$  activation occurs by charge transfer from the metal atoms to the molecule. The dissociation of  $O_2$  on the  $Y_2O_2$  cluster is an exothermic process with low barriers.



Time-of-flight mass abundance spectrum of  $Y_nO_m$  ( $n = 1-9$ ,  $m = 0-9$ ) clusters.

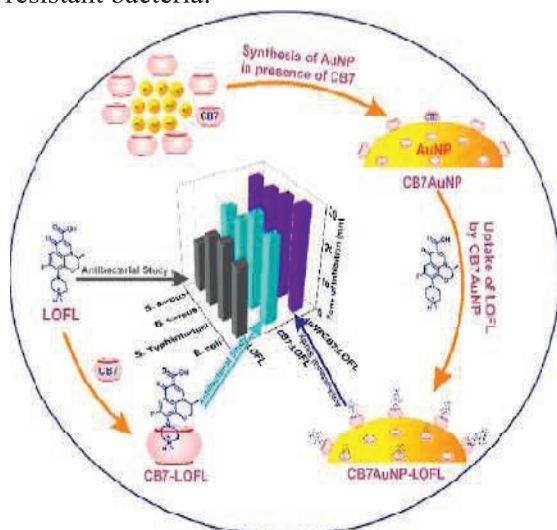
## Chemical Sciences

### Antibacterial efficacy of Levofloxacin with Cucurbituril-Functionalized gold nanoparticles

Synthesis of CB7AuNP, its interaction with LOFL & comparison of antibacterial activities of LOFL, CB7: LOFL & CB7AuNP:



LOFL.Cucurbit[7]uril (CB7)-functionalized gold nanoparticles (CB7AuNPs) have been synthesized to modulate activity of an antibiotic - Levofloxacin (LOFL). It is observed that LOFL forms 1:1 host-guest complex with CB7AuNP, leading to upward shifts of  $pK_a$  as well as photostability of LOFL, amounting to enhanced availability of active form for antibacterial activity at physiological pH. Antibacterial studies of LOFL with & without CB7AuNP were carried out using food-borne pathogens (*E. coli*, *S. Typhimurium*, *B. cereus* & *S. aureus*), which revealed a creditable enhancement of antibacterial property, irrespective of bacterium strain. These results are quite promising for development of drugs customized for multidrug-resistant bacteria.

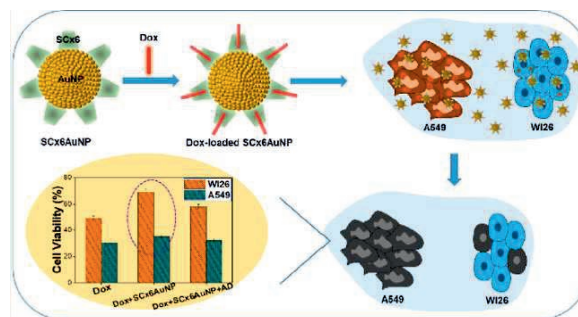


Schematic of uptake of doxorubicin by SCx6AuNPs & cell viability studies using drug loaded nanoparticles in both cancerous (A549) & non-cancerous (W126) cell lines.

### Applications of *p*-Sulfonatocalix[6]arene-functionalized gold nanoparticles in drug delivery and bioimaging

Stable *p*-sulfonatocalix[6]arene-functionalized gold nanoparticles (SCx6AuNPs) were synthesized and efficient uptake & stimuli-responsive release of doxorubicin (Dox) - an anticancer drug - by SCx6AuNPs had been established for targeted application. Decreased cytotoxicity of Dox loaded on SCx6AuNPs, towards normal cell lines & its multi-stimuli responsive release validated in both cancerous (A549) & normal (W126) cell lines find promising for selectively targeted applications toward cancer cells. At cellular level, efficient uptake of SCx6AuNP nanoconjugates was confirmed, by bioimaging using thioflavin T (ThT) dye loaded on to SCx6AuNPs instead of Dox as fluorescent tracking probe. Bright fluorescence microscopic image of ThT-

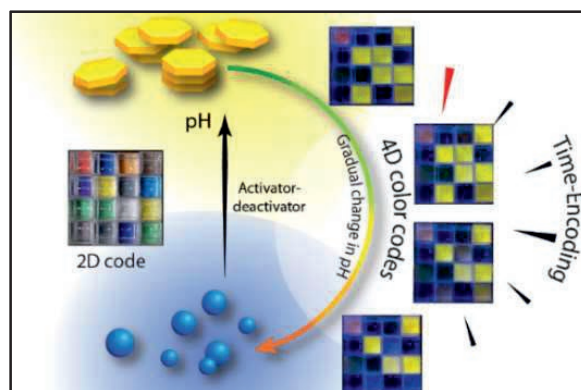
SCx6AuNP-stained cancerous cell lines corroborates uptake of SCx6AuNPs by cell lines & its projected utility for drug delivery & bioimaging.



*p*-sulfonatocalix[6]arene-functionalized gold nanoparticles (SCx6AuNPs).

### Time-encoded information encryption with pH clock guided Broad-Spectrum Emission

Development of smarter patterns with hierarchical security levels alongside dynamic display poses significant challenges. To screen out such complication, a pH switchable fluorescent assembly of a cyanostillbene derivative & myristic acid was developed. Further, molecular assembly was temporally directed with the aid of a chemical trigger-regulated pH clock, generating a transitory multicolor emission, including transient white light generation. Time-gated emissive system was also utilized to develop an advanced multi-dimensionally secure data encryption strategy.

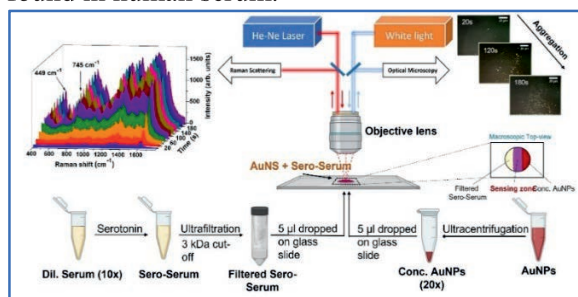


Schematic of anti-counterfeiting displays generated by cyanostillbene derivative & myristic acid under influence of pH clock.

### Rapid & sensitive detection of Serotonin in human blood serum matrix

Serotonin monoamine neurotransmitter acts as a feel-good hormone in brain. Fluctuations in serotonin levels can often lead to anxiousness, panic disorders, depression, etc. A study involving fabrication of novel gold nano surface (AuNS) platform for rapid sensitive detection of traces of serotonin in human serum matrix by

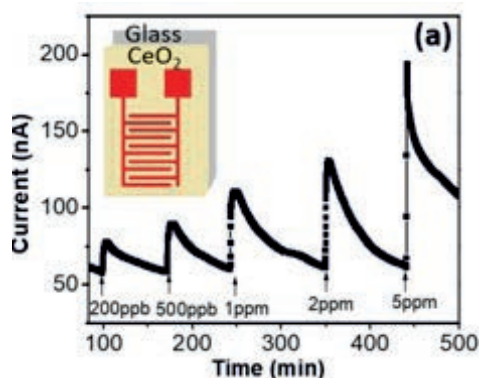
surface enhanced Raman scattering was carried out. Human serum was spiked with varying concentrations of serotonin and incubated with AuNS. Within minutes of incubation, serotonin Raman marker bands were observed at 449 (indole rotation) & 745 (indole in-phase breathing)  $\text{cm}^{-1}$ . Intensity variation of marker bands with serotonin concentration, determined limit of detection (LOD) of serotonin in serum matrix. The LOD was found to be 9 ng/ml lower than normal levels of serotonin (50-200 ng/ml) found in human serum.



Detection of serotonin (sero) in human serum matrix by Raman Scattering.

### Highly sensitive & specific detection of $\text{NO}_2$

Ultrathin  $\text{CeO}_2$  nanostructured films were deposited by Langmuir-Blodgett (LB) technique to develop a high-precision, low-cost room temperature (RT) operated  $\text{NO}_2$  sensors. The size of the nanoparticle size was estimated to be 3-4 nm by XRD & Raman spectroscopy. X-ray photoelectron spectroscopy revealed presence of  $\text{Ce}^{3+}$  (12%) & a large quantity of surface adsorbed oxygen species (33%) in  $\text{CeO}_2$  nano-ultrathin films. These films were used to develop a RT-operable highly sensitive  $\text{NO}_2$  gas sensor (200% for 1 ppm). Reduced cerium ( $\text{Ce}^{3+}$ ) on  $\text{CeO}_2$  surface forms oxygen defect sites leading to more surface adsorbed oxygen, resulting in high  $\text{NO}_2$  sensitivity. Self-doped  $\text{CeO}_2$  at particle surface with oxygen vacancies gives rise to p-type conductivity. Little response with other toxic gases indicated high selectivity of  $\text{CeO}_2$  film.



Room Temperature sensing of  $\text{NO}_2$  at various concentrations.

### Radiolytically synthesized $\text{Te}/\text{TeO}_x$ nanosheets for anticancer, photothermal & $\text{NO}_2$ gas sensing applications

Work on development of a highly rapid one-pot synthesis of  $\text{Te}/\text{TeO}_x$  nanosheets *via* high-energy electron beam irradiation was carried out. No external reducing agent was used as in-situ generated solvated electrons reduced the precursors. Extensive pulse radiolysis provided insights into formation mechanism of Te-based nanomaterials. A notable aspect is that an exceptional anticancer efficacy (>80%) was demonstrated by  $\text{Te}/\text{TeO}_x$  nanosheets against A549 lung cancer cells while exhibiting negligible cytotoxicity towards normal WI38 cells. Further,  $\text{Te}/\text{TeO}_x$  nanosheets were explored as gas sensors, displaying outstanding sensitivity & selectivity towards  $\text{NO}_2$ , with a detection threshold as low as  $\leq 1$  ppm at room temperature. Reusability tests highlighted their remarkable stability & sustained heating efficacy, underscoring immense potential of  $\text{Te}/\text{TeO}_x$  nanosheets as versatile photothermal nanoagents.

### Vanadium composites for electrocatalytic hydrogen generation

Vanadium chalcogenide has been evaluated for its electrocatalytic activity for hydrogen evolution reaction (HER).  $\text{VS}_2/\text{VO}_2$  composites were prepared by  $\text{NaVO}_3$  (VSO1) &  $\text{VOSO}_4$  (VSO2) (different precursor sources) via hydrothermal synthesis. Electrochemical hydrogen evolution was evaluated in acidic medium & catalyst supported glassy C-electrode. The overpotential at 10  $\text{mA}/\text{cm}^2$  current density for VSO1 & VSO2 were found to be 309 & 270 mV respectively. However, overpotential drastically reduces for both composites with repetitive linear sweep voltammetry scans between -0.5 to -1.5 V vs. RHE. The overpotential for VSO1 & VSO2 reduces to 65 & 112 mV respectively with repeated scans. Electrochemical impedance spectroscopy revealed very low charge transfer resistance of activated form of both composites. Dynamic stability suggested VSO1 is a better candidate than VSO2 in terms of survivability in experimental medium.

### Ag-MOF enhanced g- $\text{C}_3\text{N}_4$ for $\text{H}_2$ Generation

For improving charge separation and photocatalytic activity, a study was carried out by dispersing Ag nanoparticles as co-catalysts on g- $\text{C}_3\text{N}_4$  using Ag-BTC MOF. This approach controls nanoparticle size and ensures better



Ag/g-C<sub>3</sub>N<sub>4</sub> interfacial contact. Ag-g-C<sub>3</sub>N<sub>4</sub> photocatalysts were synthesized using post-synthesis and in-situ MOF modification methods with varying Ag amounts. Characterization showed enhanced visible light absorption in Ag-g-C<sub>3</sub>N<sub>4</sub> samples due to surface plasmon resonance of Ag nanoparticles. SEM and TEM confirmed homogeneously dispersed spherical Ag nanoparticles on g-C<sub>3</sub>N<sub>4</sub>. High-resolution Ag<sub>3d</sub> spectra revealed peaks with signatures of both metallic and oxide silver. Notably, *in-situ* synthesized Ag/g-C<sub>3</sub>N<sub>4</sub> demonstrated nearly double the photocatalytic H<sub>2</sub> activity compared to *ex-situ* methods. The hydrogen evolution rate reached 10,100 mol/h/gAg, significantly higher than the 4,761 mol/h/gAg achieved using conventional silver chloride photo-deposition synthesis.

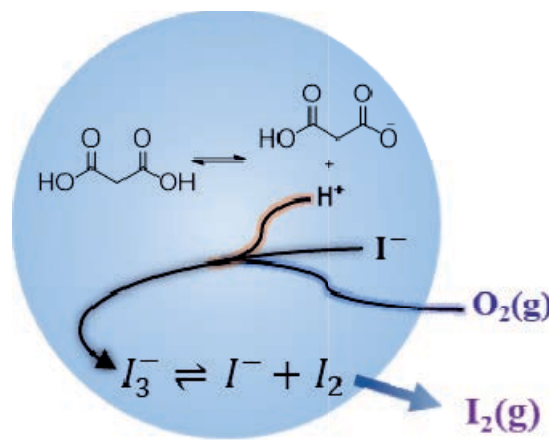
### Ni-based catalysts for water electrolysis

Nickel foam electrochemical activity for hydrogen evolution reaction (HER) in alkaline water electrolysis was enhanced by electrodepositing Ni-P, Ni-Mo, and Ni-Mo-P alloy coatings. XRD, FESEM, and EDS characterization confirmed uniform elemental distribution on the coatings. Electrochemical analysis in 1M KOH electrolyte showed all catalysts were active for HER in alkaline media, with Ni-Mo demonstrating superior activity and stability. To improve the oxygen evolution reaction (OER) kinetics, Ni-foams were coated with Fe-Co based layered double hydroxide via hydrothermal synthesis, followed by ultra-low Ru dispersion through precipitation. The catalyst was thoroughly characterized using multiple techniques. Electrochemical testing for OER in alkaline conditions achieved a current density of 10 mA/cm<sup>2</sup> at a remarkably low overpotential of only 0.21 V.

### In-situ observation of iodide depletion in ageing aerosols & role of humidity

A comprehensive analysis of humidity mediated changes in ageing aerosols using aerosol micro-Raman spectroscopy was carried out. Studies in model system and sodium iodide-malonic acid mixed aerosols unveiled depletion in iodide. Comparative studies conducted under inert & oxidative atmospheres revealed that iodide depletion occurs via oxidation to molecular iodine. Temporal evolution of reaction at three distinct RHs covering 30-80% revealed enhanced progression of reaction with increasing humidity. Given that geographical locations serving as major sources for atmospheric iodine

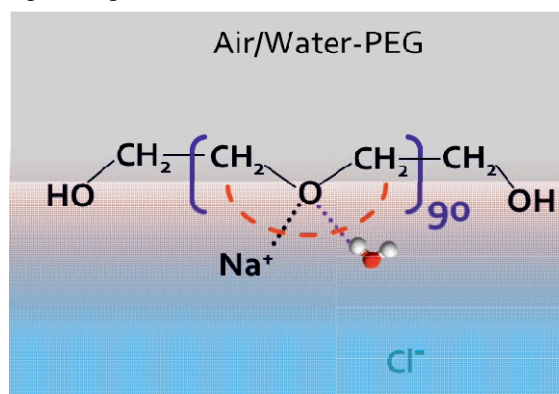
typically experience high humidity, these reactions could emerge as an additional process controlling iodine speciation in ageing aerosols.



Iodide depletion in mixed sodium iodide-malonic acid aerosols.

### Impact of electrolyte at air/water-polyethylene glycol polymer interface

Polyethylene glycol (PEG) is a water-soluble non-ionic polymer, having applications in drug delivery, protein precipitation, anti-biofouling, water-splitting, Li-ion battery & fuel cell. Using interface-selective spectroscopy, it was showcased that interfacial water adopts distinct structures & orientations depending on molar mass of PEG & they are perturbed differently by electrolytes in aqueous phase. At higher molar mass PEG (PEG4000)/water interface, water is H-up orientated  $\approx 3200$  cm<sup>-1</sup> & H-down orientated  $\approx 3470$  cm<sup>-1</sup>. Selective reorganization of interfacial water is assigned to disruption of asymmetric hydration around ether-oxygen of surface-adsorbed PEG4000 by Na<sup>+</sup> ion of the electrolyte. Interestingly, in case of low molar mass PEG (PEG200)/water interface, interfacial water neither showed such dual orientation nor they get affected by electrolyte (1.0M NaCl) in aqueous phase.



Impact of 1.0M NaCl on interfacial water at air/water-PEG4000 interface.



### Structural transformation of water at polarizable hydrophobic molecular interface

The water structure surrounding a hydrophobic yet polarizable molecular interface utilizing hydration shell spectroscopy was studied & compared with those around non-polarizable molecular hydrophobes. Dichloromethane (DCM) & chloroform (CHLF) as model polarizable hydrophobic molecules, ethanol & tert-butanol as polarizable hydrophobes were used. Analysis of OH stretch spectra of hydration shell water revealed strikingly distinct structural features in immediate vicinity of DCM & CHLF compared to those surrounding  $\text{CH}_3\text{CH}_2$ - or  $(\text{CH}_3)_3\text{C}$ - groups. Results revealed that polarizable hydrophobic molecules exhibit strong interaction with dangling-OH of water & diminishes water-water interaction in their proximity, while non-polarizable hydrophobes exhibit weaker interactions with dangling-OH & stronger water-water interaction in hydration shell.

### Detection of weak hydrogen bonds in aqueous medium & their dependence on charge polarity

Weak hydrogen bond interactions ( $\pi \cdots \text{HOH}$ ,  $\text{CH} \cdots \text{OH}_2$ ) of  $\pi$ -electron containing molecular ions (tetraphenylborate ( $\text{TPB}^-$ ) & tetraphenylphosphonium ( $\text{TPP}^+$ )) & uncharged benzene (Bz) were probed in aqueous medium using Raman-DS-SCF spectroscopy. The OH stretch spectra pertaining to hydration shells of structurally similar but oppositely charged molecular ions ( $\text{TPB}^-$  &  $\text{TPP}^+$ ) show distinct  $\pi$ -hydrogen bond ( $\pi \cdots \text{HOH}$ ) with  $\text{H}_2\text{O}$  molecule that approaches phenyl rings axially. Strength of such  $\pi \cdots \text{HOH}$  bond increases as  $\text{TPP}^+ < \text{Bz} < \text{TPB}^-$ .  $\text{H}_2\text{O}$  molecules that approach phenyl ring equatorially exhibit blue-shifted hydrogen bond with phenyl-CH ( $\text{CH} \cdots \text{OH}_2$ ), whose strength varies as  $\text{TPP}^+ > \text{Bz} > \text{TPB}^-$ . Unlike Bz &  $\text{TPB}^-$ , hydration shell spectrum of cationic  $\text{TPP}^+$  shows a unique band  $\approx 3200 \text{ cm}^{-1}$ , which is assigned to reinforced collective vibration of water in immediate vicinity of  $\text{TPP}^+$ . Results showed that charge polarity-dependent approachability of water & modulation of its collective nature as well as hydrogen bonding while hydrating  $\pi$ -electron containing hydrophobes in aqueous medium.

### Vitrification of Zr & Sr in Iron-Phosphate glass

Vitrification process is a preferred technology for immobilizing high-level radioactive waste.

Using Raman Spectroscopy, restructuring of iron phosphate glass (IPG) following addition of up to 20% (w/w)  $\text{ZrO}_2$  &  $\text{SrO}_2$  into glass matrix, respectively had been quantified. Original glass (IPG without Zr) displays three primary structural components within  $900\text{--}1250 \text{ cm}^{-1}$ , corresponding Q1, Q2 & Q3 structural units, where  $n=1, 2, 3$ , number of bridging oxygens. Introduction of Zr as well as Sr alters the relative proportions of Q1, Q2 & Q3 in glass matrix. With additional  $\text{ZrO}_2$  loading (20%), Qn bands of glass exhibit distinctly different band shapes, suggesting precipitation of Zr from glass. Similar results were obtained for  $\text{SrO}_2$ . Results revealed that Zr & Sr act as glass matrix modifiers & demonstrates that these elements can be effectively incorporated into glass matrix up to 15 wt.% without precipitation.

### Functional optical nanoscopy with chemical specific information

Fluctuations in fluorescence emission of immobilized single molecules (SM) are commonly attributed to intrinsic structural conformations of chromophore & influence of local environmental factors. Advanced single-molecule multi-dimensional tracking to simultaneously monitor both emission spectrum & 3D dipole orientation of individual fluorophores was employed and the findings demonstrate that spectral fluctuations are driven by variations in radiative relaxation probabilities among different vibronic emission bands, which are further influenced by interactions with associated vibrational modes. By analysing the separation between vibronic maxima in single-molecule spectral snapshots from a stack of images across various regions, the vibrational spectra of dye Rhodamine 6G was constructed. Ongoing studies are focused on assessing applicability & scalability of this methodology for functional super-resolution imaging, with implications for research in chemistry & biology.

### Glycosylated stimuli responsive Polyacrylamide microspheres for bacterial capture, detection & killing

The synthesis of a hitherto unknown glycosylated gel microspheres that can capture, kill & detect pathogenic bacteria had been demonstrated for potential applications in water treatment, wound dressing, etc. In-situ made covalently functionalized gel microspheres were made from acrylamide derivatives of glucose, mannose & galactose. Three glyco

functionalized microspheres namely; PAM-Glc, PAM-Man & PAM-Gal, were synthesized by inverse emulsion polymerization. The key highlight of the designed system was that the bacterial capture induced aggregation of gel microspheres & indicative colour change of AgNPs upon bacterial cell capture can be visually observed. Among AgNPs loaded glyco microspheres, silver loaded mannose microspheres (Ag@PAM-Man) exhibited greater inhibition against *E.coli* & antibiotic resistant *S.aureus* cells. Lysis of bacterial cells captured by PAM-Man exhibited pink coloration upon interaction with Resorufin  $\beta$ -glucuronide; an extension of detection capability of system in addition to capture & killing.

#### **Real time observation of anti-aromaticity relaxation using Ultrafast Spectroscopy**

Extremely large Stokes' shift ( $9100\text{ cm}^{-1}$ ) in a single benzene core-based para-diacylphenylenediamine (p-DAPA) molecule was demonstrated. Using femtosecond transient absorption spectroscopy, anti-aromatic-aromatic transition in p-DAPA was monitored. It was shown that such anti-aromaticity relaxation is extremely fast (0.5-5 ps) and largely depends on the nature of the solvent. Such relaxation is enhanced in presence of protic solvent, suggesting important role of solute-solvent H-bonding in relaxation of anti-aromaticity.

#### **Compositional characterization of paint using nuclear analytical techniques**

Elemental composition of paint was determined non-destructively by neutron activation analysis, charge particle activation analysis and EDXRF. Na, Si, Ca, Cr, Fe & Ba were found to be the major constituents and the concentration of chromium was the highest among all other constituents. NAA was chosen as primary method as it requires very small amount of sample, no requirement of matrix match standard, with detection capability down to ppb level and supported by self-validation.

#### **Uptake studies of Strontium on Resorcinol-Formaldehyde polycondensates**

Resorcinol-formaldehyde polycondensates - the well-established Cs-selective agents, along with their crown ether (18-crown-6) composite discs were synthesized, characterized & applied for strontium uptake from aqueous solutions. Effects of crown ether amounts, Sr in feed, pH, equilibration time, temperature, competing ions, sorption, along with re-usability of synthesized

sorbents were evaluated, followed by EDXRF spectrometry on both solution & solid phases. The pH (3-12) of the solution & temperature (up to  $100^{\circ}\text{C}$ ) had negligible impact on holding capacities. The sorption capacity was enhanced by  $\sim 33\%$  upon modification & followed pseudo-second order kinetics.

#### **Synthesis of Tannic Acid Functionalized Tb doped GO layered structure**

Tannic acid functionalized Tb doped GO layered structure was fabricated for potential photothermal application. Graphene oxide was produced using an improved version of Hummer's method. Tb solution in predefined conc. was added to crush GO powder; homogenized & placed into an ultrasonic bath. Measured quantity of tannic acid was used to functionalize Tb doped GO. Different ratio of tannic & Tb dopant was tried & composition was optimized. Optimum composition was 1% tannic acid doping into 5% Tb loaded GO layer. The synthesized materials were characterized by FTIR, Raman, XRD & SEM.

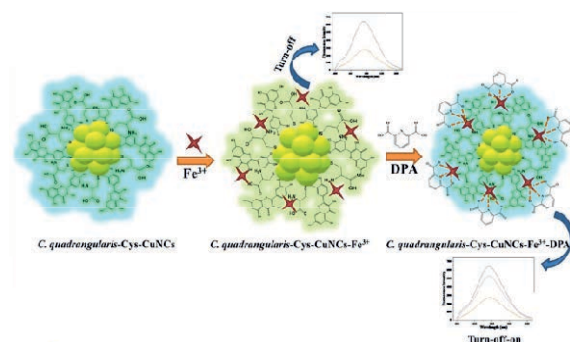
#### **MnO<sub>2</sub> doped GO loaded hydrogel for photothermal applications**

A composite material comprising GO & MnO<sub>2</sub> was synthesized & incorporated into an alginate matrix. Photo-thermal properties of material were evaluated, highlighting its dual functionality in clean water production & power generation. The material MnO<sub>2</sub>@GO@Alg, reached  $55^{\circ}\text{C}$  within an irradiation interval of 5 min under one Sun illumination. Also, the composite exhibited an exceptional light-to-heat conversion efficiency of 91% along with a notable water vaporization rate of  $4\text{ kg m}^{-2}\text{h}^{-1}$ . The composite effectively treated both simulated dye-contaminated water & real seawater samples, showcasing its potential as a robust interfacial water evaporator. Furthermore, when integrated with a commercially available thermoelectric module, material generated a stable voltage of 350 mV & a current 1.2 mA.

#### **Green synthesis of Cu nanoclusters using Cissus Quadrangularis**

The *Cissus quadrangularis*-Cys-CuNCs based fluorescence turn-off-on sensing platform showed remarkable performance for analyses of  $\text{Fe}^{3+}$  ion & DPA in real samples, revealing great potentiality of the method for practical applications. The Fluorescence intensity of *Cissus quadrangularis*-Cys-CuNCs was reduced

selectively to 63 % by  $\text{Fe}^{3+}$ , however it was restored with the addition of DPA.



Green synthesis of Cu nanoclusters using Cissus Quadrangularis.

### Amperometric sensing of urea using Metal Organic Framework modified electrode

Precipitation method was used for synthesis of Co-based metal organic framework & the microscopic & spectroscopic properties of the composite material were investigated. The non-enzymatic electrochemical method was developed under optimized condition for sub-micromolar detection of urea using Co-based MOF modified electrode. Amperometry scans were recorded for detection of Urea in 0.1 NaOH solution with linear dynamic range  $5\mu\text{M}$  -  $80\mu\text{M}$  & detection limit of  $0.93\mu\text{M}$  with  $\text{S/N}=3$ . The developed sensor showed very good repeatability as well good stability for detection of Urea in blood serum.

### Electrochemical sensing of As(III) using modified RGO/ $\text{NiCOFe}_2\text{O}_4$ glassy C-electrode

The RGO/ $\text{NiCOFe}_2\text{O}_4$  nanocomposite has been synthesized using hydrothermal method & microscopic characterization was carried out. The differential pulse anodic stripping voltammetry technique was used for determination of trace amounts of As (III) in phosphate medium at pH 7.2. This method showed a low limit of detection of 0.11ppb. Possible interferences were evaluated with the known concentration of Arsenic & the proposed method can be applied for quantification of As (III) in water samples.

### Electrochemical investigation & determination of Prednisone

Electrochemical property of prednisone - a synthetic corticosteroid drug - was investigated using carbon nano sphere modified glassy carbon electrode in neutral phosphate buffer medium at pH 7.2. The interaction of prednisone with transition metal ions ( $\text{Cu}^{2+}$ ) was investigated to understand the biological

functioning correlated with interaction of dsDNA & transition metal ion  $\text{Cu}^{2+}$ . An analytical method of determination of prednisone was developed using square wave voltametric techniques in 0.1 M PBS buffer solution at pH 7.2 & detection limit obtained was 73 nM.

### Molten salt electrochemistry of Magnesium

The molten salt electrolysis setup was augmented & several eutectic mixtures were investigated as media for selective electrolysis & deposition of metallic Magnesium. Temperature programming had been optimised for uniform solubilization of molten salt mixtures. The stability of MS media was also established over operations in batches. Electrolysis discharge conditions were established using multiple cyclic voltammetry scans & with constant potential electrolysis.

### Electrochemical determination of glycerol & heavy metal ions

A Voltammetric method was developed using Au-based bimetallic nano-composite modified electrode in alkaline medium for determination of glycerol. Bimetallic nano composite was electrochemically deposited under optimized conditions and the strength of the alkaline media had been optimized. Amine & carboxylate group functionalized C-dots were synthesized & impregnated into hydrogel matrix for fluorometric sensing & recovery of heavy metal ions, Pd & Hg. The detection limit of nano molar range has been achieved.

### Stability of $\text{Al}_2\text{O}_3$ thin films generated by atomic layer depositions in corrosive media

Neutron reflectivity measurements were carried out to measure thickness & surface roughness of  $\text{Al}_2\text{O}_3$  thin films generated using ALD technique. The corrosion property of SS304 was observed to be reduced on ALD deposition which was evident from polarization measurements & impedance data. Polarization resistance remained high even at high applied anodic potential of 0.7 V. The investigation supports the primary objective of the important role of protection of material through thin ALD- $\text{Al}_2\text{O}_3$  protective films.

### Studies on dielectric and conductivity properties of $\text{Ba}_3\text{V}_2\text{O}_8$ at high temperature

Alkaline-earth orthovanadates ( $\text{A}_3\text{V}_2\text{O}_8$ ) exhibit valuable properties like microwave dielectric response and high-temperature ferroelectricity.



While most show high dielectric constants but poor conductivity due to rigid  $\text{VO}_4$  groups,  $\text{Ba}^{2+}$ -containing compositions demonstrate notable oxide/proton conduction at moderate temperatures.  $\text{Ba}_3\text{V}_2\text{O}_8$  via solid-state ceramic method had been synthesized and confirmed its rhombohedral (R-3m) structure through XRD. Dielectric response studies (10Hz-10MHz, 623-1023K) revealed that thermally activated DC conductivity exhibits two distinct regions with different activation energies, transitioning near 800K. This change represents a shift from overlapping large polaron tunneling to small polaron tunneling mechanisms, supported by electrical modulus analysis showing increased non-Debye relaxation at higher temperatures.

#### Crystal structure and dielectric properties of $\text{Ln}_2\text{Ti}_2\text{SiO}_9$ (Ln = Pr and Nd)

Low-loss, high-dielectric-constant materials are crucial for electronics and communications applications. Two trimonsite-type titanosilicates ( $\text{Pr}_2\text{Ti}_2\text{SiO}_9$  and  $\text{Nd}_2\text{Ti}_2\text{SiO}_9$ ) were prepared via conventional ceramic methods and studied their properties from 203-673K. Their rigid structures restrict charge carrier movement, resulting in low conductivity ( $\sim 10^{-11}$  S/cm) at ambient temperature, increasing to  $\sim 10^{-7}$  S/cm at 400K. Both materials show promising dielectric properties: dielectric constants of 35 ( $\text{Nd}_2\text{Ti}_2\text{SiO}_9$ ) and 22 ( $\text{Pr}_2\text{Ti}_2\text{SiO}_9$ ), with low losses of 0.03 and 0.007 respectively. At 1MHz, losses decrease further to  $10^{-3}$  and  $10^{-4}$ , making them excellent candidates for device applications. Analysis indicates correlated barrier hopping of polarons as the dominant conduction mechanism.

#### Designing superior material for thermal barrier coating applications

Thermal barrier coatings (TBCs) protect materials from temperature gradient effects. The performance of zirconate pyrochlore ( $\text{Nd}_2\text{Zr}_2\text{O}_7$ ) was improved by modifying its stoichiometry rather than adding substituents. This approach increased linear thermal expansion coefficients from 9.89 to 11.44 ppm/K while decreasing thermal conductivity from 1.73 to 1.53 W/m·K. The local structure of zirconate pyrochlore was investigated through Raman and X-ray spectroscopies, with density functional theory providing deeper insights. The findings highlight the role of non-stoichiometry and coexisting fluorite-pyrochlore phases, offering a straightforward strategy to enhance TBC performance.

#### Photochemistry of Tetrahydropyran clusters upon interaction with intense laser pulse

Tetrahydropyran clusters ( $(\text{C}_5\text{H}_{10}\text{O})_n$ ) to 355 and 266 nm were subjected to pulses and analyzed the resulting ions using time-of-flight mass spectrometry to understand proton transfer in cyclic ethers—compounds with environmental and biological significance due to their role in pyranose sugars. At 355 nm, major ion signals ( $m/z$  55-87) corresponded to various fragments including  $\text{C}_4\text{H}_7^+$ ,  $\text{C}_4\text{H}_9^+$ ,  $\text{C}_5\text{H}_7^+$ ,  $\text{C}_5\text{H}_9^+$ ,  $\text{C}_5\text{H}_9\text{O}^+$ , and  $(\text{C}_5\text{H}_{10}\text{O})\text{H}^+$ , alongside cluster fragments  $(\text{C}_5\text{H}_{10}\text{O})_n\text{H}^+$  ( $n=2-4$ ). Notably, predominant signals from water-mixed clusters  $((\text{C}_5\text{H}_{10}\text{O})_4(\text{H}_2\text{O})_2\text{H}^+$  and  $(\text{C}_5\text{H}_{10}\text{O})_5(\text{H}_2\text{O})_3\text{H}^+)$  were detected, indicating higher clusters' tendency to form water adducts. Power dependency studies revealed a 3-photon absorption rate-limiting process, with tetrahydropyran clusters undergoing facile proton transfer like other cyclic ethers.

#### Speciation of ions produced upon SIMS analysis of pure Lu, Ta and Mo substrates

Secondary ionization mass spectrometric (SIMS) analysis of pure Lu, Ta, and Mo substrates was conducted using  $\text{Cs}^+$  ion sputtering to identify ion species crucial for qualitative and quantitative analysis in Lu-176 isotopic enrichment applications for targeted radiotherapy. For Mo, we detected  $\text{Mo}^+$  and  $\text{MoO}^+$  were detected in positive mode and  $\text{MoO}_2^-$ ,  $\text{MoO}_3^-$ , and  $\text{MoO}_4^-$  were detected in negative mode. Ta produced  $\text{Ta}^+$ ,  $\text{TaO}^+$ ,  $\text{TaO}_2^+$  (positive) and  $\text{TaO}^-$ ,  $\text{TaO}_2^-$ ,  $\text{TaO}_3^-$ ,  $\text{TaO}_4^-$ ,  $\text{TaO}_6\text{C}^-$  (negative). Lu substrate generated  $\text{Lu}^+$ ,  $\text{LuO}^+$ ,  $\text{LuO}_2^+$  (positive) and  $\text{LuO}^-$ ,  $\text{LuO}_2^-$ ,  $\text{LuO}_2\text{H}^-$  (negative). Oxide ions resulted from native oxide layers on these substrates. Notably, negative ion mode showed significantly higher ion yields, suggesting greater sensitivity for surface analysis of these elements.

#### Structural, Electronic and Mechanical Properties of $\alpha(\text{U})$ and $\alpha(\text{U-Zr})$ Alloy Fuels

Uranium-zirconium (U-Zr) alloys are promising fast reactor fuels due to their superior safety, high uranium density, and excellent thermal conductivity. The structural and mechanical properties of metallic uranium and U-Zr alloys was calculated using density functional theory with Hubbard U corrections. The analysis of lattice volume, elastic moduli, and electronic density of states across Zr concentrations (5-15 at%) revealed a linear relationship between volume and Zr content, with mechanical

properties varying according to Zr concentration. The electronic structure of  $\alpha(\text{U})$  remained largely unchanged with Zr addition. These computational insights enhance our understanding of U-Zr alloy fuel behavior under reactor conditions.

### **Direct capture of low-energy free-electron into delocalized $\sigma^*$ orbitals**

Chemically activating bonds through direct, resonant capture of low-energy free-electrons into  $\sigma^*$  orbitals presents a compelling approach for achieving bond-specific chemical control. This direct approach, previously unexplored experimentally due to low capture cross-sections, has now yielded successful defunctionalization and dehydrogenation reactions with remarkable efficiency. This may be due to quantum superpositions between  $\sigma^*$  orbitals and their vicinal or conjugated  $\sigma^*$ -CH orbitals. The ubiquity of such superpositions opens unprecedented possibilities for controlling chemical reactions using low-energy free-electrons.

### **Insight into structure of ethylene receptor proteins**

Ethylene, a key plant hormone regulating seed germination, growth, fruit ripening, and abscission, stimulates responses through Ethylene Response 1 (ETR1) transmembrane receptors. Despite its importance, the molecular mechanisms of ethylene signaling remain elusive, particularly how ethylene binds to receptor proteins with high affinity and specificity. Using the AlphaFold algorithm, we modeled the approximate structure of ETR1 with copper ions in different oxidation states. Through density functional theory-based tight binding methods and cluster-based models, we investigated the copper ion's oxidation state, quantity at the active site, and favorable coordination geometry (square planar versus trigonal bipyramidal). This work advances the understanding of ethylene perception, crucial for developing strategies to manipulate fruit ripening.

### **Geometric and electronic structures of high-valent metal ions strapped to novel macrocyclic amide ligands for small molecule activation**

The electronic structures of transition metal catalysts are typically short-lived intermediates difficult to characterize by X-ray crystallography, making spectroscopic techniques essential. High-

valent Co(IV) oxo and Ni(IV) species with non-innocent ligands using various spectroscopic methods, elucidating their electronic structures through density functional theory and ab initio calculations. These potent catalysts enable oxygen atom transfer, water oxidation, and C-H activation reactions.

### **Xanthate functionalized MOFs for highly efficient Hg(II) trapping from aqueous solution**

Xanthate-functionalized Ni-MOF-74 (MOF-74-XT) was synthesized via a two-step process: creating the base MOF from nickel(II) nitrate and DHDBC using solvothermal methods, followed by xanthation of free -OH groups. This material showed exceptional mercury ion removal capabilities with optimal performance at pH 4, 120-minute equilibration time, and following pseudo-second-order kinetics. The Langmuir adsorption capacity reached 833.30 mg/g, surpassing many new-generation adsorbents. Thermodynamic studies revealed an endothermic, spontaneous process ( $\Delta H=9.25\text{ kJ/mol}$ ,  $\Delta S=0.038\text{ kJ/mol}\cdot\text{K}$ ) with increasing effectiveness up to  $70^\circ\text{C}$ . MOF-74-XT demonstrated high selectivity for  $\text{Hg}^{2+}$  over competing ions ( $\text{Li}^+$ ,  $\text{Na}^+$ ,  $\text{Mg}^{2+}$ ,  $\text{Cd}^{2+}$ ) and maintained performance through multiple adsorption-desorption cycles with minimal capacity loss ( $<3\%$ ).

### **Aqueous partitioning data of TBP in solvent extraction process in different condition**

Tri-n-butyl phosphate (TBP), crucial in nuclear fuel reprocessing via PUREX process, exhibits variable aqueous solubility that requires careful monitoring to prevent undesirable reactions during evaporation. This study resolved conflicting literature values (ranging from 0.3-6.0 g/L) by measuring phosphorus content in aqueous phases using ICP-OES. Results showed TBP solubility increases with concentration (0.8 g/L at 30% TBP in n-dodecane; 2.3 g/L for pure TBP) and varies during actinide/lanthanide extraction, initially rising up to 200 mg/L before declining. Understanding these partitioning behaviors is essential for process optimization and safety in nuclear waste treatment.

### **Aqueous partitioning data of CMPO in solvent extraction process in different condition**

Carbamoylmethyl phosphine oxide (CMPO), used in TRUEX process for actinide/lanthanide

co-extraction from high-level waste, requires consistent partitioning behavior for effective solvent extraction. A validated HPLC-PDA method (linear range 10-200 mg/L,  $r=0.998$ ) was developed to accurately measure CMPO in aqueous media with  $\sim 100\%$  recovery. Partitioning studies revealed CMPO solubility increases up to 0.1M concentration before gradually decreasing. Similarly, nitric acid concentration initially enhanced CMPO solubility (maximum at 0.5M) before causing reduction up to 10M, likely due to nitric acid extraction behavior. This characterization supports process integrity monitoring during nuclear waste treatment operations.

## Analytical Services

### Certified Reference Material of Alumina: BARC - B1301

NCCCM-BARC in a collaborative exercise with public sector unit NALCO produced the first certified reference material (CRM) of alumina - BARC - B1301. The CRM is certified for six metallic impurities ( $\text{Na}_2\text{O}$ ,  $\text{CaO}$ ,  $\text{Fe}_2\text{O}_3$ ,  $\text{TiO}_2$ ,  $\text{Ga}_2\text{O}_3$  and  $\text{V}_2\text{O}_5$ ) after interlaboratory comparison exercise and statistical evaluation of data. Further, five indicative values ( $\text{MgO}$ ,  $\text{ZnO}$ ,  $\text{MnO}$ ,  $\text{LOI}$  and surface area) were also provided. The CRM was produced as per ISO 17034: 2016 and ISO guide 17035:2017 and the certified values are traceable to SI units. BARC-B1301 was released on 16.08.2024 at NRTC-NALCO Bhubaneswar by BARC and NALCO authorities. Alumina ( $\text{Al}_2\text{O}_3$ ) has very good mechanical properties and is chemically inert. By virtue of these characteristic properties, alumina is widely used in ceramic refractory



Certified reference material of alumina BARC - B1301.

industries and chemical industries as catalyst. However, presence of trace impurities severely affects the various physical and chemical properties of alumina leading to its poor performance.

### Analytical Services for DAE Projects

Analytical services were provided for various DAE projects and for those falling under non-power applications (societal). Large varieties of materials were analysed for chemical composition, trace constituent concentrations, structural, surface & thermal properties, totalling 3042 samples with 6525 determinations. Material samples analyzed include metals/alloys, environmental, biological, archaeological, industrial & process samples. Suitable analytical techniques were chosen based on analyte, matrix & concentration levels of analytes. Methodologies were optimized/ developed for characterizing new materials. Indigenous instruments were also deployed for analytical purposes.

### Up-keep of NABL Accreditation

The analytical chemistry laboratory facilities of BARC cater to the requirements not just to the constituent units of DAE, but also PSUs, law enforcement agencies & academic institutions. Supported by strict adherence to NABL standards, the ISO-17025:2017 accreditation for Analytical Chemistry Division laboratories has been extended up to 2026. The laboratory is accredited for analysis of metals in water and low alloy steels. A new methodology was optimized for steel analysis, which was audited separately by NABL & accepted for analysis.

### Selective leaching of Lu isotopes from copper substrate

Dissolution protocols were developed for selective leaching of Lu deposited over Cu substrate using magnetic sputtering. Since Lu atoms are engrossed inside Cu substrate, some amount of dissolution of Cu substrate was unavoidable. A separation strategy was also developed to remove Cu from Lu leach solution.

## Environmental and Separation Science

### Polymeric adsorbent for rapid estimation of uranium in urine matrix for personnel monitoring

A swift radiochemical separation technique was established for evaluating uranium levels in



urine samples by utilizing an in-house made amidoximated crosslinked polyacrylonitrile (ACPAN) adsorbent. ACPAN adsorbent demonstrated a remarkable uranium adsorption capacity of  $156.3 \text{ mg g}^{-1}$ , reaching equilibrium within 60 minutes at room temperature for urine samples adjusted to pH 2. Reusability of ACPAN adsorbent was confirmed, maintaining a consistent adsorption capacity for ultra-trace uranium levels across several cycles. Analysis of samples spiked with uranium concentration ranging 5 ppb-30 ppm revealed high measurement accuracy, excellent repeatability & strong linearity. These results meet ANSI 13.30 radio bioassay performance standards, affirming effectiveness of this innovative method for accurate quantification of uranium in urine matrices.

#### **ZIF 67-PES composite beads for extraction & recovery of uranium from aqueous waste**

Zeolitic imidazolate framework-67 (ZIF-67) was synthesized using a simple green chemical route & encapsulated polyether sulphone beads (ZIF-67@PES beads) were prepared by phase inversion technique. The synthesized beads had a surface area & average pore width of  $27.69 \text{ m}^2 \text{ g}^{-1}$  &  $2\text{-}4 \text{ nm}$  respectively. The composite was evaluated for its ability to sorb uranium from different aqueous wastes under various physical conditions. The obtained sorption data fit well with Langmuir isotherm model. The monolayer sorption capacity obtained was  $83.26 \text{ mg g}^{-1}$ , closely resembling experimental maximum sorption capacity of  $\sim 80 \text{ mg g}^{-1}$ . Importantly, ZIF-67 @PES beads showed promise in removing uranyl ions from various water samples, making them suitable for seawater treatment.

#### **Separation of Niobium from Zirconium-Niobium alloy**

Isolating Niobium-94 ( $^{94}\text{Nb}$ ) from discharged Zr-2.5Nb pressure tubes (PTs) could potentially reduce the volume of the radioactive waste, while the recovered Zr could be reused as PT material. A robust solvent extraction methodology for selective extraction of Nb from a mixture of Zr & Nb was developed. Nb was extracted from an aq. HCl solution using  $\alpha$ -benzoin oxime in chloroform. About 5 min of equilibration time & three separation cycles are sufficient for quantitative extraction. The temperature-dependent extraction studies suggest that the extraction is exothermic, spontaneous & enthalpy-driven. The method

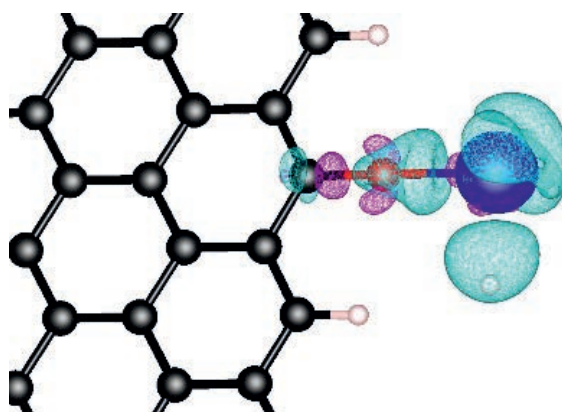
effectively separates long-lived  $^{94}\text{Nb}$  from discharged PTs, demonstrating its practical applicability.

#### **Remediation of uranium with treated Neem bark from environmental waters**

Treated neem bark (TNB) was successfully demonstrated as a sorbent for uranium from ground water collected from Punjab region. The sorption characteristics of TNB were affected by initial concentration of uranium, solution pH, equilibration time & temperature. Maximum sorption capacity was found to be  $10.42 \text{ mg g}^{-1}$  at optimized parameters of pH 7.0 & temperature  $27^\circ\text{C}$ . Sorption of uranium by TNB was not affected significantly with increase in T indicating a chemisorption mechanism. The fast sorption kinetics, reasonable sorption capacity & subsequent easy desorption of uranium make neem bark an alternative sorbent to synthetic materials. Further, TNB is an economical, readily available natural material having medicinal value.

#### **Thorium removal from aquatic environment using Phosphate-modified Graphene Oxide polymeric beads**

Highly selective adsorption of  $\text{Th}^{4+}$  on phosphate modified graphene oxide polymeric beads was investigated. Interaction of  $-\text{PO}_4$   $-\text{OH}$  &  $-\text{O}-$  functional groups of graphene oxide with  $\text{Th}^{4+}$  was thoroughly investigated using DFT. The affinity of  $\text{Th}^{4+}$  ions was obtained as  $-\text{PO}_4 > -\text{OH} > -\text{O}-$  group of phosphate modified graphene oxide. Phosphate modified Graphene oxide embedded in Calcium alginate matrix was characterized using ATR-FTIR, XRD, SEM & Raman spectroscopy. Highly efficient ( $> 93\%$ ) uptake of thorium with fast rate of sorption ( $< 5$  minutes) was observed in batch sorption studies.



The optimized structures of  $-\text{OH}$  functionalized (mode-2) graphene oxide after Th adsorption.

### Role of structure & organic contaminants on Cs sorption by clays

The role of structure & organic contaminants on Cs sorption performance of three clay geosorbents was investigated in a study. Structural characterization revealed modal mineralogical variation among three geosorbents. Cs retention facilitated by clay geosorbents was found to be rapid, concentration dependent & non-linear. The dominance of 2:1 clay geosorbent in Cs sorption over 1:1 clay geosorbents was clearly observed from batch sorption studies. In addition, the organic matter present in the clay was found to influence the sorption capacity of the geosorbent.

### Correlating shale geochemistry with metal sorption: Influence of Kaolinite content

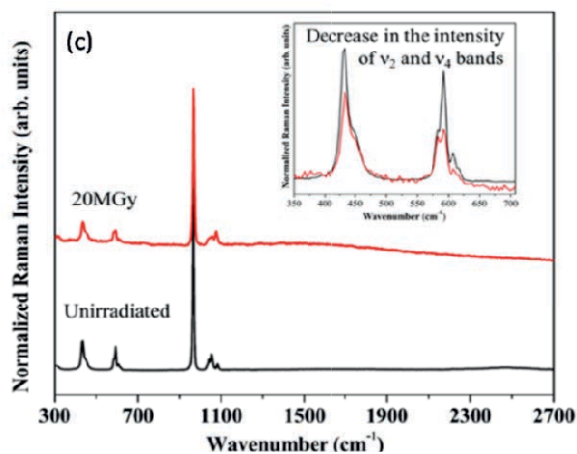
Two argillaceous rocks (shales) from different geological settings were characterized using various analytical techniques to evaluate textural attributes, mineralogical constituents & surface properties. The major mineralogical constituent of the surface & subsurface shale was quartz (62%) & kaolinite (56%), respectively. Fluorescence & UV-V spectra confirmed presence of polyaromatic hydrocarbons in subsurface shale. The higher Cs retention of kaolinite-rich subsurface shale as compared to surface shale can be directly correlated to its higher clay (kaolinite) content & surface area. The studies illustrate the radionuclides sorption potential of argillaceous rocks in view of nuclear waste management applications.

## Materials Science

### Exploring Fluorapatites for nuclear waste sequestration applications

Radiation stability of natural fluorapatites ( $(\text{Ca}_{10}(\text{PO}_4)_6\text{F}_2\text{Ca}_{10}(\text{PO}_4)_6\text{F}_2)$ ) was established by subjecting them to high-energy (10 MeV) electron beam (EB) to ascertain their capability in hosting high-level waste (HLW) generated in Molten Salt Breeder Reactors. As part of this, the structural stability of apatite over geological time, even with multiple cationic substitutions, was confirmed using XRD. Raman & FTIR spectroscopy indicated localized alterations in phosphate vibrational bands, attributed to minor radiation-induced damage. It was confirmed that fluorapatite exhibits excellent structural stability with no amorphization & radiation resistance under 20 MGy EB irradiation. These findings highlight the potential of fluorapatite for long-

term HLW immobilization in geological repositories.



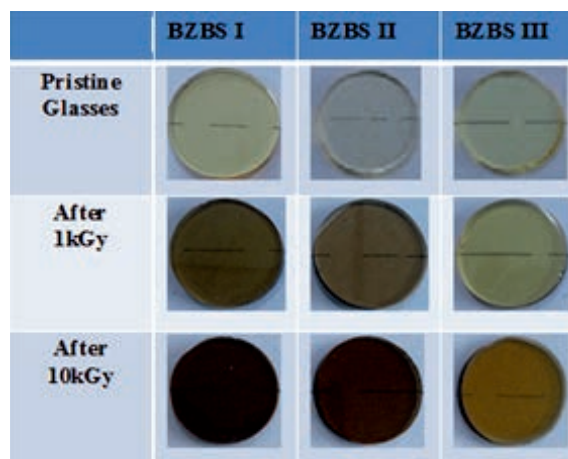
Comparison of Raman spectra for irradiated & unirradiated fluorapatite specimens.

### Development of ultrafine glass fibre for HEPA media

Pure silica glass fibers with nanometre dimensions were successfully synthesised by electrospinning for HEPA applications. The dimension of the fibers was confirmed from SEM. The average diameter stood at  $237 \pm 78 \text{ nm}$ .

### Post irradiation studies of lead-free BaO-ZnO-B<sub>2</sub>O<sub>3</sub>-SiO<sub>2</sub> glass for radiation shielding application

Lead free BaO-ZnO-B<sub>2</sub>O<sub>3</sub>-SiO<sub>2</sub> glasses were prepared with varying compositions as part of studies for their utilization in shielding applications. Glass composition with 10 mol.% Bi<sub>2</sub>O<sub>3</sub> (BZBS I); 5mol.% Bi<sub>2</sub>O<sub>3</sub> (BZBS II) & 0.1 wt.% CeO<sub>2</sub> doped glass (BZBS III) was characterized before & after irradiation. Optical transparency of all three glasses was ~80%, though cut-off wavelength was higher for BZBS\_III glass due to absorption of cerium ions.



Lead-free BaO-ZnO-B<sub>2</sub>O<sub>3</sub>-SiO<sub>2</sub> glass before & after irradiation.

Glasses were irradiated up to 10 kGy inside Co-60 gamma chamber. Post irradiation, undoped glasses were showing radiation induced absorption but BZBS III is radiation resistant against browning up to 1 kGy. However, all three glasses showed browning effect after exposure to 10 kGy radiation.

### Advancements in carbon nanomaterial synthesis & applications

The semiconducting properties of single-walled carbon nanotubes (SWCNTs) have made them indispensable in a variety of applications, including in electronics, sensors, & photovoltaics. However, their potential is hindered by metallic impurities from traditional synthesis methods & low carbon conversion efficiency (~4%) in Floating Catalyst Chemical Vapor Deposition (FC-CVD). To overcome these challenges, reactor modifications were introduced, including an annular flow plenum for controlled purge gas introduction, addition of water vapor & hydrogen during synthesis, which

semiconducting SWCNTs with over 90% purity were obtained, eliminating complex post-synthesis processing. Innovations like cascading facilitated selective etching & passivation of metallic SWCNTs, leveraging their lower oxidation resistance. The result was that the catalyst evaporation in multi-zone FC-CVD reactors enabled high-yield CNT aerogels with exceptional strength, conductivity & low iron content, suitable for advanced applications.

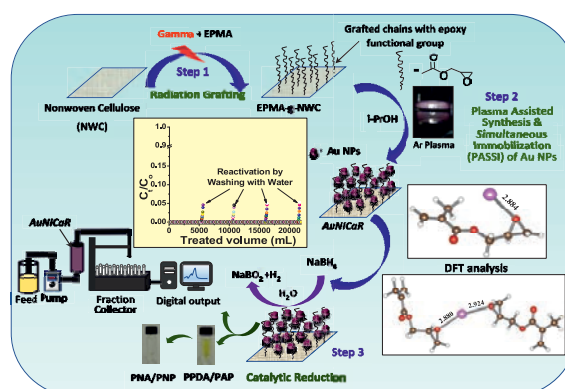
In graphene synthesis, a breakthrough Flash Joule Heating (FJH) method converted plastic waste into high-quality graphene. By subjecting plastic mixed with C-black to 3000 K, polymer chains were restructured into sp<sup>2</sup>-bonded graphene. This eco-friendly approach, supported by molecular dynamics simulations, highlighted the potential for sustainable material production.

### Reusable gold nanoparticles based catalytic system for remediation of organic pollutants

Gold nano-particles immobilized catalytic reactor (AuNICA<sub>R</sub>) was fabricated via Plasma Assisted Synthesis and Simultaneous Immobilization (PASSI). AuNICA<sub>R</sub> was used for catalytic reduction of p-nitroaniline (PNA), p-nitrophenol (PNP) and methyl orange (MO) azo dye in both batch and continuous flow mode on laboratory scale. Over 25000 mL of cumulative pollutant feed (0.06 mM – 2 mM) was treated using a single catalyst batch after intermittent reactivation by washing with water. AuNICA<sub>R</sub> displayed excellent storage stability of over 12 months and more than 90 % retention in catalytic activity post multiple cycles.



A snapshot of the CNT sheet developed in BARC.



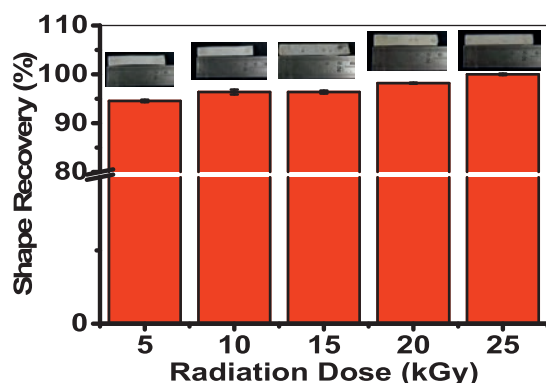
Schematic of fabrication of catalytic system and application of bifunctional cotton fabric.

### Radiation-crosslinked 3D printed polycaprolactone shape memory matrices

The shape memory properties of 3D printed polycaprolactone (PCL) matrices were enhanced through gamma radiation treatment. Enhanced



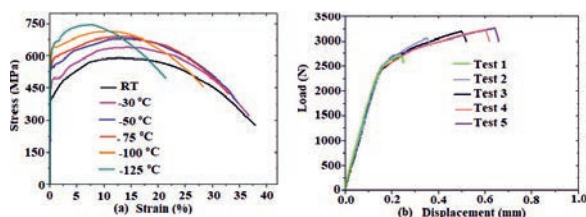
stability and complete shape recovery post-deformation were achieved through the incorporation of multifunctional acrylate and controlled radiation dose administration. Investigations demonstrated a positive correlation between radiation dose and shape recovery characteristics, with optimal performance being observed at 25 kGy exposure. These findings have established potential pathways for development of advanced materials exhibiting tailored properties, with prospective applications being identified in medical device fabrication and adaptive structural systems.



Gamma radiation dose effect on shape recovery of sensitizer-loaded PCL matrices.

### Loading rate effect on plastic deformation and fracture toughness of SA516Gr70 Steel

The effect of loading rate on the plastic deformation and fracture toughness of SA516 Gr.70 steel was investigated in a study. At a deformation rate of 500 mm/min, ductility decreases with lower temperatures, while flow and yield strength increase. Fracture toughness tests conducted at  $-100^{\circ}\text{C}$ , within the Ductile-to-Brittle Transition Temperature (DBTT) range, revealed significant variation in toughness due to the coexistence of ductile and brittle fracture mechanisms. Sudden crack growth occurs if critical stress is reached in the presence of flaws; otherwise, ductile crack growth continues via void nucleation and growth. This dual behavior results in large variations in the J-value at final fracture.



Stress-strain and load-deformation graphs for SE(B) specimen fracture tests at  $100^{\circ}\text{C}$ .

## Computation and Modelling

### CFD model for predicting bubble & drop movement in a pulsatile flow field

In a fundamental work related to air pulsed columns, a 2D axisymmetric model was developed that can simulate movement of a bubble in a pulsatile flow field of the continuous phase (water). The effect of the grid size was studied and an optimal grid density was obtained. Phase-field technique was used to capture the evolving interface. The simulations were validated against in-house experimental data. Absolute average relative error in prediction of time-period averaged rise velocity was less than 5%. The overall simulations showed that the upward movement of droplet is facilitated during the upstroke of the pulse while down stroke retards the upward movement.

### CFD model to predict formation of liquid drops at top-submerged nozzle

A 2D axisymmetric CFD model was developed to predict the size of the droplet of a liquid generated at a top-submerged nozzle immersed in a quiescent immiscible liquid, as part of a study related to air pulsed columns. Continuous and dispersed phases were considered to be uranium loaded 30% TBP in dodecane and uranyl nitrate solution, respectively. Phase-field method was used for tracking the interface and the model was validated with experimental data of drop size and drop detachment height for different concentrations of uranyl nitrate. The validated model was used to quantify drop size generated in a sieve plate vis-à-vis in a nozzle plate. The results showed that smaller drops are formed in a nozzle plate vis-à-vis sieve plate.

### Development & validation of a 3D CFD pseudo homogenous model for grain flow

A 3D CFD pseudo homogenous model was developed for simulating continuous flow of grain in a grain handling equipment (silo/irradiation chamber). The model will be useful to quantify residence time distribution in a grain irradiator. The model considers grain as a continuum pseudo fluid. A conservation equation for “granular temperature” was solved in a coupled manner so as to obtain apparent viscosity of fluid medium. The advantage of the model is that it is scalable and can be used for industrial scale equipment where millions of grain particles are expected and particle resolved technique like Discrete Element

Modelling will not be feasible. To validate the model, reported literature data for rectangular silos were used. Two types of silos – rectangular with an orifice at the bottom and a wedge-shaped silo – were considered. The stream-wise and span-wise velocities in these two shapes were compared and CFD predicted results matched well with experimental as well as analytical results.

### Large scale Molecular Dynamics Simulations for sea water desalination using nanotube membrane

Classical Molecular Dynamics simulations were conducted to demonstrate the potential application of nanotube membrane for sea water desalination. The nanotube membrane comprising  $18 \times 18$  array of CNT (9,9) in close hexagonal packing was connected to feed water with sea water composition. The simulation system comprised of 1.7 million atoms. The achieved permeation rate of  $2.5 \times 10^{-11}$  moles/cm<sup>2</sup>-sec-Pa was within the range estimated from single CNT(9,9) and two order higher than thin film composite membranes. A very high salt rejection efficiency of ~99% was achieved through the assembled membrane. The results shed light on the potential applicability of nanotube membrane for sea water purification at the engineering scale.

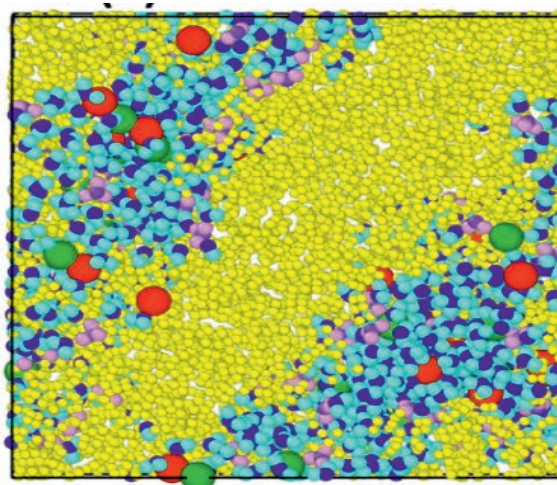
### ATOM GUI Module

Isotope separation module was incorporated in the ATOM GUI module and the testing of the isotope separation module was completed for Gd isotopes.

### Selective Ion ( $\text{H}_3\text{O}^+/\text{Cu}^+/\text{Cu}^{++}$ ) transport through Nafionmembrane for Cu-Cl Electrolyser

The performance of Nafion membrane in presence of external electric (E) field of strength 0.01, 0.05, 0.75, and 0.1 V/Å was evaluated. Water, being a polar solvent, tends to orient in the direction of the E field. However, the effect of the E-field was measured to be minor than that of hydration strength. The results suggest existence of a critical E field below which increasing hydration level improves the proton transport. Beyond the critical E field strength, water molecules begin to drift with the hydronium ions, thereby hinder proton transport rather than facilitating it. The presence of HCl medium was found to considerably enhance the ionic conductivity. However, with the addition

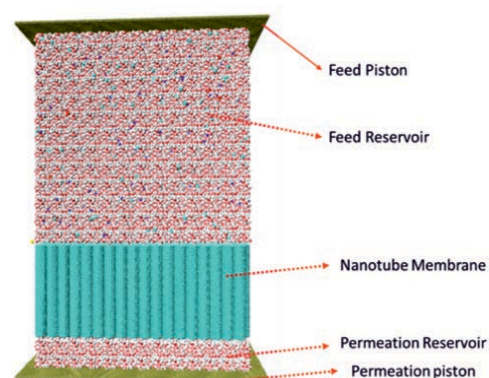
of Cu ions, the ionic conductivity of Nafion membrane was reduced



Snapshot representing the phase segregation of nafion-water channel.

### Large-scale sea water desalination through nanoporousmembrane

The nanotube membrane for employed sea water purification consisted of  $18 \times 18$  array of CNT(9,9) in close hexagonal packing was connected to feed water with real sea water composition. The simulation system comprised of 1.7 million atoms. It was found that a pressure gradient of 100 MPa or higher was desired to achieve the unidirectional flow of water from feed to permeate reservoir. Very high salt rejection efficiency of 99.9% was achieved through considered membrane. Notably, the water permeability of considered nanotube membranes was reduced by two order while considering sea water composition rather than pure water due to accumulation of salt ions at the



Representation of the system for sea water desalination using nanotube membranes.

water-membrane interface. Nevertheless, the achieved filtration rate of  $3.6 \times 10^{-13} \text{ m}^3/(\text{m}^2\text{-sec-Pa})^{-1}$  was within the range of thin film composite (TFC) membranes. The results shed light on the potential applicability of nanotube membrane for

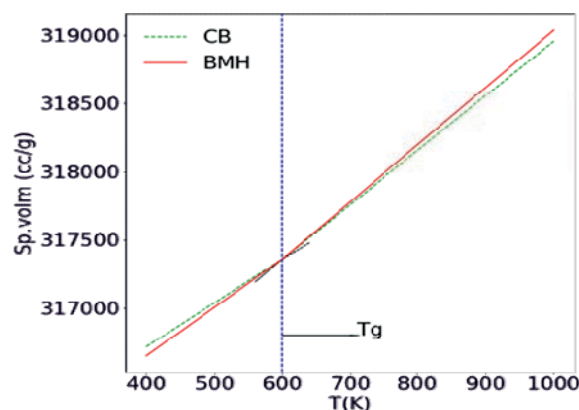
sea water purification at the molecular engineering scale.

### MD simulation study of water dynamics inside molecular cavity

Studies on molecular behaviour of water within confined spaces was carried out as part of efforts to understand Molecular recognition mechanisms and interactions between the host and guest molecules. Modified cyclodextrins (mCD) was chosen for this study as it can enhance the bioavailability and the stability of hydrophobic drugs inside living creatures, making it a crucial component in drug formulation and delivery. Understanding the behaviour of water in such confined spaces can aid efforts for development of environmentally responsive materials that can capture and release substances based on external stimuli. MD study using Gromacs force field showed the quantum of water molecules that are replaced when the host/sensor molecules come close-by cavity. This study also shows that solvation dynamics of the water becomes slower inside the cavity. It was earlier postulated that solvation dynamics of water slows down by virtue of its strengthening of hydrogen bond. However, present study shows that the restriction of translation and rotational motion of water is actually responsible.

### MD simulations for design of RSW Glass

Methodologies were developed for MD simulation of RSW glasses. Forcefield parameters were optimized and MD simulations were completed of RSW glass of composition  $64\text{PbO}-36\text{SiO}_2$  glass using BKS as well as BMH potential. Results showed good match of MD estimated density of RSW glasses with the available literature. The glass transition



The glass transition temperature computed from plot of specific vol. vs. temp.

temperature ( $T_g$ ) was measured to be 600 K, which is in good agreement with the reported literature. The computed Young's modulus was found to be 49.32 GPa which is comparable with the reported literature of 58.5 GPa.

### Interaction of H with Fe-Cr binary system with variation in Cr content using ab-initio simulation

The effect of Cr content on diffusion, permeation and solubility of hydrogen H in Fe-Cr system was studied. From the calculated values, it was observed that the diffusion and solubility decreases with an increase in Cr content as per the experimental observations. The diffusion and solubility values were found to be decreasing with an increase in the temperature for a particular composition.

### Simulation of Oxygen-18 water distillation cascade

Two models for producing oxygen-18 using nuclear-grade heavy water were developed, an equilibrium-based model and a rate-based model. By testing various operating parameters, optimal conditions were identified using validated process model. A scaled-up system capable of producing 300 kg of oxygen-18 enriched water per year, based on optimization insights from in-house rate-based water distillation model, was also designed.

### Performance of $\text{CaSO}_4:\text{Dy}$ /PTFE TLD Badges on ISO Phantoms for Photon and Beta Dosimetry: FLUKA and GEANT4 Analysis

The angular response of  $\text{CaSO}_4:\text{Dy}$  PTFE disc-based thermoluminescent dosimeter (TLD) badges was evaluated using FLUKA and GEANT4 Monte Carlo simulations. The badges were placed on ISO slab, cylindrical, and pillar phantoms to simulate photon exposures (12.3 keV to 1.25 MeV) and beta sources ( $^{90}\text{Sr}/^{90}\text{Y}$ ,  $^{106}\text{Rh}/^{106}\text{Ru}$ ) at angles from  $0^\circ$  to  $60^\circ$ . Thermoluminescent responses were analyzed as  $\text{Hp}(10)$ ,  $\text{Hp}(3)$ , and  $\text{Hp}(0.07)$  versus photon energy for each phantom type. Additionally, relative responses of open TLD discs under various filter regions at normal incidence on the pillar phantom were calculated in terms of  $\text{Hp}(3)$ . These results characterize the energy and angular dependence of  $\text{CaSO}_4:\text{Dy}$  PTFE TLDs for photon and beta radiation dosimetry.



## Cancer Studies

### Fork processing sensitizes Ovarian Cancer to PARP inhibitors

Targeting replication fork processing sensitizes PARP inhibitor induced ovarian cancer cell death. Combining dihydroxystilbene (DHS) with the PARP inhibitor talazoparib synergistically kills ovarian cancer cells. DHS causes replication stress by slowing and disrupting replication forks, leading to DNA gaps and PARylation. Talazoparib blocks PARylation, worsening these gaps, which are then converted into lethal double-strand breaks by MRE11 at stalled forks. This combined action of PARP inhibition and defective replication fork processing induces synergistic cell death in ovarian cancer cells. Replication fork stabilization has been identified as a potential mechanism of PARPi resistance in the absence of restored homologous recombination.

### PSMA-Targeted Chemotherapeutics: Synthesis and evaluation

Prostate-specific membrane antigen (PSMA) is highly expressed in prostate cancer (PCa) cells, making it a target for therapy. PSMA-targeted radioligand therapy ( $^{177}\text{Lu}$ -PSMA) is commonly used to treat prostate cancer. Following the concept of targeted cancer treatment, a PSMA-doxorubicin conjugate to specifically target prostate cancers had been synthesized. In vitro screening showed the conjugate induced greater cell death in PSMA-positive cell lines (LNCaP and C4-2) compared to PSMA-negative cell lines (PC3). This PSMA-targeted approach delivers chemotherapy directly to cancer cells, potentially minimizing damage to healthy tissues and improving outcomes.

### CHK1 Kinase regulation of Topoisomerase 1 in Cancer

Topoisomerase 1 (TOP1) is crucial for DNA replication and transcription, making it a cancer therapy target. TOP1 inhibitors stabilize TOP1-DNA complexes (TOP1ccs), but resistance mechanisms limit their effectiveness. Phosphorylation regulates cellular response to TOP1 inhibitors. To identify novel regulators of TOP1ccs, a kinase inhibitor library was screened. The screen identified known regulators like CDK1 and DNAPK, validating its robustness. Novel hits, CHK1 and ATR, were also identified as potential regulators of TOP1cc levels.

### WRN and RECQL1 Helicases in cellular response to Topoisomerase 1 inhibitors

RECQL helicases, like WRN and RECQL1, are crucial for maintaining genomic stability and replication fork integrity, especially when TOP1 is inhibited. To study the interaction between WRN and RECQL1, cells with individual and combined depletions (WRNKD, RECQL1KD, DKD) were created. Depleting WRN or RECQL1 alone increased sensitivity to the TOP1 inhibitor camptothecin (CPT). Surprisingly, DKD cells (both depleted) showed less sensitivity to CPT. DKD cells also accumulated less DNA damage and recovered faster after CPT treatment. This suggests WRN and RECQL1 interact in a complex way; their combined loss counteracts the negative effects seen when either is depleted individually.

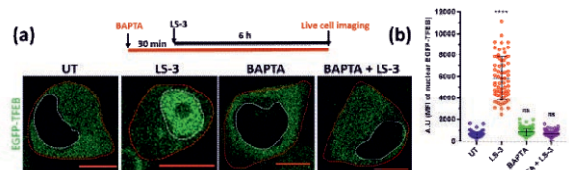
### Lysotilbene as potential anticancer agent for Pancreatic Ductal Adenocarcinoma

Evaluation of the potential of lysotilbene as anticancer agent to treat pancreatic ductal adenocarcinoma. Lysotilbene (LS-3) demonstrates cytotoxicity against pancreatic cancer cells, prompting investigation into its mechanisms. Studies revealed that LS-3 induces nuclear translocation of the transcription factor TFEB and causes lysosome damage in these cells. The TFEB shuttling process involves calcineurin-activated dephosphorylation of p-TFEB. Given that lysosome damage releases calcium, explorations on calcium's role in calcineurin activation were done. Results indicate that calcium-calcineurin-mediated dephosphorylation is essential for TFEB nuclear localization following LS-3 treatment in pancreatic cancer cells. These findings highlight a novel mechanism by which LS-3 may exert its anticancer effects in pancreatic cancer.

### Transcription Factor TFEB's role in Cancer replication

TFEB, a transcription factor, is crucial for DNA repair and genomic stability in pancreatic cancer. TFEB knockdown (KO) cells show increased DNA damage and stalled replication forks compared to wild-type cells. TFEB-KO cells downregulate key DNA repair proteins like RAD51 and SMARCA1, with evidence suggesting TFEB directly regulates their expression. Consequently, TFEB-KO cells exhibit impaired homologous recombination (HR) and increased sensitivity to PARP inhibitors. PARP inhibitors further increase genomic instability, especially in TFEB-KO

cells. This study highlights TFEB as a potential therapeutic target for pancreatic cancer due to its role in DNA repair.



Representing images of live cell confocal microscopy displaying the localization status of GFP-TFEB under the indicated treatment condition.

### Synthesis & Supply of PSMA-617 and [Cu(MIBI)<sub>4</sub>]BF<sub>4</sub>

Indigenously synthesized PSMA-617, a radiopharmaceutical ligand for prostate cancer therapy, was supplied to BRIT for preparing <sup>177</sup>Lu-PSMA kits (LUM-5). In 2024, seven batches were synthesized using locally developed protocols and purified to pharmaceutical grade (>99.9% purity). Approximately 159 mg was supplied, enabling treatment of around 500 patients across India. Also, indigenously synthesized [Cu(MIBI)<sub>4</sub>]BF<sub>4</sub>, a radiopharmaceutical ligand for myocardial perfusion imaging, was regularly supplied to BRIT for <sup>99m</sup>Tc-MIBI kit preparation (TCK-50). Approximately 5g was supplied this year, benefiting over 15,000 patients nationwide.

### Standardization of synthetic protocol of OTBN

The technology for synthesizing orthotolylbenzonitrile (OTBN), an intermediate for anti-hypertensive sartan drugs, was further refined. Technical support was provided to licensees through scientific inputs and quality assessment of product batches to promote local manufacturing and reduce import dependency.

### Synthesis & evaluation of Oxabicyclo dicarboxamide for <sup>90</sup>Sr-<sup>90</sup>Y separation

Oxabicyclo dicarboxamide (OBDA) was synthesized via multistep organic synthesis as a promising alternative to CMPO for <sup>90</sup>Sr-<sup>90</sup>Y separation. This addresses the quality challenges in the current two-stage Supported Liquid Membrane purification process that supplies carrier-free <sup>90</sup>Y to RMC for patient administration.

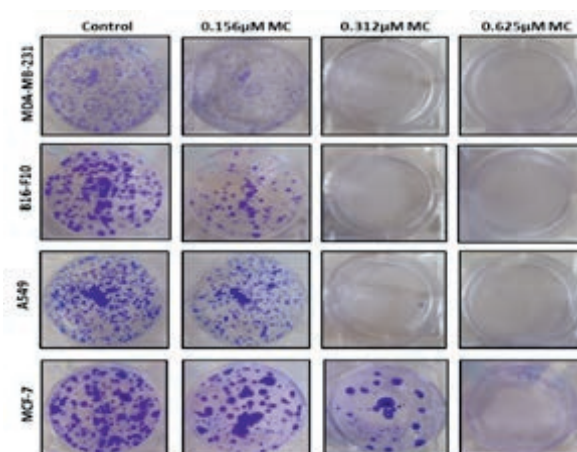
### Synthesis & evaluation of a drug loaded hydrogen bonded organic framework

A porous hydrogen bonded organic framework (HOF) composed of 4,4',4''-(1,3,5-Triazine-2,4,6-triyl)tribenzoic acid was synthesized and

characterized using various analytical techniques. The FDA-approved chemotherapeutic drug DOX was successfully incorporated, and its pH-dependent release kinetics were evaluated. In-vitro testing against MCF-7 cells demonstrated comparable anti-proliferative activity to free DOX under slightly acidic conditions, with confirmed cellular internalization.

### Mitochondria targeted Curcumin effectively kills Human Breast & Pancreatic Cancer cells

Mitocurcumin (MC) showed superior anti-cancer activity against pancreatic cancer cell lines (PANC-1 and Mia-Pa-Ca-2) with 30-fold lower IC<sub>50</sub> compared to curcumin. MC treatment eliminated clonogenic potential, reduced viability of PANC-1 spheroids, and demonstrated DNA groove binding as a potential mechanism of action. In vivo studies using SCID mice with pancreatic tumors confirmed significant reduction in tumor burden, highlighting the therapeutic potential of this mitochondria-targeted approach.



Anti-proliferative effect of mitocurcumin on different cancer cells.

### PSIP1 protein reduces R-loops at transcription sites to maintain genome integrity

PC4 SRSF Interacting Protein 1 (PSIP1) was identified as a key regulator of R-loop homeostasis. Proteomic analyses and proximity ligation assays confirmed PSIP1's association with R-loops. PSIP1 depletion led to elevated R-loop levels and increased DNA damage, particularly at gene bodies, which could be reversed by RNaseH overexpression or PSIP1 restoration. PSIP1 promotes homologous recombination to repair R-loop-induced DNA damage and prevents transcription-replication conflicts, thereby maintaining genome integrity.

## Radio-sensitizing effect of Clobetasol Propionate

Clobetasol propionate (CP) demonstrated potent radiosensitization in lung cancer cells by inhibiting the Nrf-2 pathway. Transcriptomic studies revealed modulation of ferroptosis, fatty acid metabolism, and glutathione metabolism pathways. Nrf-2 overexpression in A549 cells conferred resistance to CP-mediated ferroptosis and radiosensitization. A novel N-acetyl cysteine-CP adduct showed enhanced anti-cancer activity in A549 cells compared to CP alone, as confirmed by MTT and clonogenic assays.

## Investigating molecular mechanisms of radioresistance in Lung Cancer

A radioresistant lung cancer cell line was developed through stepwise selection with repeated doses of ionizing radiation (8 Gy per fraction, 40 Gy total). The radioresistant A549 subline exhibited reduced DNA damage, decreased lipid peroxidation, and lower ferroptosis upon radiation exposure compared to parental cells, suggesting a connection between ferroptosis and radiosensitivity. Ongoing investigations focus on characterizing molecular alterations in DNA repair pathways and epigenetic modifications associated with radioresistance.

## Role of PRDX6 in radiation response of A549 Lung Cancer cells

High Peroxiredoxin 6 (PRDX6) levels correlate with poor lung cancer survival. PRDX6 knockdown enhanced A549 cell radiosensitivity and significantly upregulated ferroptosis-related genes when combined with radiation. PRDX6 mitigates ionizing radiation-induced ferroptosis, indicating potential as a therapeutic target for radiosensitization through small molecule approaches.

### Radio-sensitizing effect of cold plasma activated medium

Plasma Activated Medium (PAM) demonstrated anti-cancer activity by inhibiting growth and confluence of 4T1 triple-negative breast cancer cells. Intraperitoneal PAM injection inhibited 4T1 tumor growth in BALB/c mice, with enhanced suppression when combined with radiation. PAM administered before whole-body irradiation (6Gy) effectively protected the spleen, evidenced by spleen size and weight measurements.

## Increased tumor progression and immune exhaustion in metabolically unhealthy obese Mice

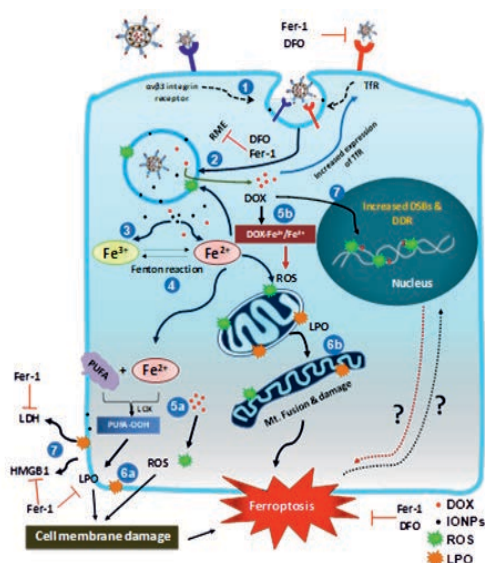
C57BL/6 mice on high-fat diet for >20 weeks developed metabolically unhealthy obese phenotypes with increased body weight, BMI, and cholesterol. Metabolomic analysis revealed decreased serotonin, which regulates appetite and body weight. This phenotype associated with increased tumor progression and immune exhaustion (measured by PD-1 expression) both in tumors and systemically in the spleen.

## Metabolomic, lipidomic, immune changes and tumor progression in MONW and MUO Mice

MONW-BALB/c mice showed decreased taurodeoxycholic acid, while MUO-C57BL/6 mice exhibited decreased serotonin. Similar lipidomic profiles appeared in both strains except for abundant triglycerides in C57BL/6 HFD mice. C57BL/6 mice progressed to MAFLD with alterations in portal/lobular inflammation, lipid accumulation, and hepatocyte ballooning, while MONW-BALB/c mice did not. Tumor progression increased only in C57BL/6 HFD mice, confirmed in two independent tumor models. Both strains showed sluggish T-cell responses on HFD, but immune exhaustion was tumor-localized in BALB/c mice while appearing both in tumors and systemically in C57BL/6 mice.

## Ferroptosis as a mechanism of anti-tumor efficacy of targeted nanoparticles in TNBC

Targeted nanoparticles (T-LMD, Indian Patent No. 441803) demonstrated significant killing of



Schematic illustration for mechanism of activation of ferroptosis by T-LMD.



chemo-resistant human TNBC cells (MDAMB-231, MDAMB-468) and activated ferroptosis markers. T-LMD significantly inhibited tumor growth in mice xenograft models. Mechanistic studies revealed ferroptosis hallmarks: mitochondrial fusion, extracellular LDH and HMGB-1 release, and increased lipid and cytosolic ROS. Pre-treatment with ferroptosis inhibitor rescued cells, restored mitochondrial morphology, prevented LDH/HMGB-1 leakage, and inhibited ROS generation.

### Identification of Blood Biomarkers & dysregulated systemic cancer hallmarks in NET patients

A NET diagnostic model achieved 98.4% specificity in asymptomatic controls and 91.2% in symptomatic controls across 2,955 samples from 26 studies. In a pilot study, NET prediction scores decreased after 2nd/3rd PRRT cycle. Analysis of 58 NET patients revealed dysregulated myeloid and lymphoid cell balance. Peripheral blood transcriptome analysis of 59 GEP-NET patients versus 38 healthy donors showed significant enrichment of cancer hallmarks related to immune responses and carcinogenesis, with fourteen cancer hallmarks shared between peripheral blood and tissue transcriptomes.

### Mechanistic insights into RNase H1 in alternative splicing & BRD4 in radioresistance

RNase H1's role in co-transcriptional alternative splicing through R-loop structures was demonstrated via co-localization and proximity ligation studies with spliceosome complex. R-loops may serve as scaffolds for splicing machinery binding. R-loop levels are directly controlled by FUS, suggesting that FUS mutations may cause disease and genomic instability through R-loop dysregulation. Phosphoproteomic studies showed BRD4 contributes to breast cancer radioresistance by regulating DNA damage response, cell cycle progression, DNA replication, and epithelial-to-mesenchymal transition.

### Oral nutraceutical AKTOCYTE for radiotherapy side-effect management

AKTOCYTE, a chlorophyllin-based oral tablet, was developed as an adjuvant to cancer radiotherapy. It demonstrated favorable pharmacokinetics and pharmacodynamics in healthy subjects. A Phase II clinical trial showed very good response in pelvic cancer patients,

specifically mitigating radiotherapy-induced bladder cystitis and salvaging bladders in severe cystitis patients who would otherwise require cystectomy.



Chlorophyllin-based oral tablet - AKTOCYTE.

### siRNA-mediated COX-2 Gene (PTGS2) knockdown for improving Anti-PD-1 immunotherapy response

Combined PTGS2-siRNA and anti-PD-1 immunotherapy significantly reduced tumor burden in 4T1 breast cancer mice compared to individual treatments. This combination therapy increased anti-tumor immune response, evidenced by higher CD8/Treg ratio in spleen cells and enhanced IFN- $\gamma$  secretion by cytotoxic T cells.

## Bio-Science

### QTL analysis for Electron Beam, Large Seed Mutant located on A05 Chromosome in Groundnut

An electron beam-induced mutant with 70% higher seed weight was developed in groundnut. Quantitative Trait Locus(QTL) analysis identified a major locus on chromosome A05 between AhMITE470 and SNP\_05\_103140987, spanning 4.53 Mbp. This region contains the BIG SEEDS 1 (TIFY) gene at 102.47 Mbp. RNA-seq and qRT-PCR analyses showed this gene was down-regulated in the mutant, suggesting a loss-of-function mutation is responsible for the increased seed size.

### Ammonium Transporter Genes in Millets

This study identified 53 ammonium transporter (AMT) genes across six millet species. Analysis revealed these genes belong to two subfamilies (AMT1 and AMT2/AMT3/AMT4), with segmental duplications playing a major role in their evolution. Phylogenetic classification using AMT1.1 genes confirmed speciation patterns consistent with matK gene sequences. Promoter analysis identified cis-elements related to light response, anaerobic induction, growth hormones,

stress response, and developmental signals. This research provides a foundation for utilizing AMTs to improve nitrogen use efficiency.

### **Characterization of MusaDREB1-like Protein of *Musa x paradisiaca* to understand its role in Abiotic Stress Tolerance in Banana**

Climate change has increased the need for stress-tolerant crops. This study investigated DREB transcription factors, crucial for stress tolerance but poorly understood in banana. Transgenic banana plants overexpressing MusaDREB1-like protein showed stunted growth but enhanced tolerance to cold and drought stresses. Biochemical and molecular analyses revealed that MusaDREB1-like protein regulates cold-regulated (*COR*) genes and the abscisic acid (ABA) hormone pathway to confer stress tolerance.

### **Metabolic Profiling of Camptothecin Biosynthesis Pathway in *Ophiorrhiza rugosa***

LCMS was employed to analyze three *O. rugosa* samples with different camptothecin (CPT) levels: callus, rooted callus, and hairy roots. Principal component analysis showed three distinct clusters with 88% variance. Functional pathway analysis revealed significant enrichment of metabolites in the indole alkaloid biosynthetic pathway (enrichment factor 6.24). Twenty-one intermediates in the CPT biosynthesis pathway were identified based on m/z values, with MS/MS fragmentation patterns matching standard metabolites. The relative distribution of these metabolites across different tissues was represented in a clustered heat map.

### **Stomata-photosynthesis Synergy mediates Combined Heat and Salt Stress Tolerance in sugarcane Mutant M4209**

This study evaluated a radiation-induced salt-tolerant sugarcane mutant (M4209) under heat (42/30°C), salt (200 mM NaCl), and combined stress conditions. While heat application improved growth in both mutant and control plants (Co 86032), the benefits were reduced in the control under combined stress due to higher Na<sup>+</sup> accumulation and lower triacylglycerol levels. The mutant's "Open Small Dense" stomatal phenotype, resulting from regulation of SoEPF9 and SoEPF2, enhanced gas exchange, transpirational cooling, and photosynthesis. This stomatal-photosynthetic synergy improved plant growth across all stress conditions.

### **Understanding efficiency of Biochar for reducing Arsenic levels in Rice**

This study explored using biochar to reduce arsenic toxicity in rice. Two types of biochar were prepared from kitchen and temple waste at an optimal pyrolysis temperature of 500°C. Rice plants (var. Satabdi) grown in arsenic-spiked soil (50 mg/kg) with biochar amendments showed improved growth compared to those without amendments. The optimal biochar concentration was 2.5% w/w, with temple waste biochar proving more effective than kitchen waste biochar. Antioxidant enzyme activity confirmed this finding. Both biochars increased rice yield and reduced arsenic levels in rice grains.

### **Understanding the crosstalk between hormone and arsenic stress induced signaling pathways in plants**

The transcriptome data was analyzed to understand how plant hormones influence arsenic stress responses in rice. The results showed the highest overlap (47%) between arsenic-responsive genes at 24 hours and abscisic acid (ABA) responsive genes. Other hormones showed lower overlaps: jasmonic acid (46%), cytokinin (18%), IAA (12%), brassinolide (9%), and gibberellic acid (5%). The proportion of ABA-arsenic shared genes increased over time with a positive correlation ( $R^2=0.72$ ). The top shared genes were associated with plant-water homeostasis, confirming ABA's dominant role in regulating arsenic-induced gene expression.

### ***Trichoderma virens* alleviates potassium Deficiency induced symptoms in Soybean**

This study assessed *T. virens* G2 strain's ability to improve potassium deficiency tolerance in soybean variety Maus47. *T. virens* showed inherent tolerance to potassium deficiency and effectively colonized soybean roots under deficient conditions. *T. virens*-colonized plants had 1.85-fold and 2.54-fold more lateral roots under potassium-sufficient and deficient conditions, respectively, compared to controls. Root biomass increased 2-fold, shoot biomass 1.81-fold, and shoot length 1.61-fold, coinciding with upregulated potassium transporters and increased potassium accumulation. The findings were validated in both soybean and in model plant *A. thaliana*, with lower ROS accumulation suggesting redox signaling involvement in the tolerance mechanism.



### Role of oxalate decarboxylase gene in oxalic acid detoxification and biocontrol of *Sclerotium rolfii* in *Trichoderma virens*

Two oxalate decarboxylase genes (*Tvoxdc1* and *Tvoxdc3*) were knocked out in *Trichoderma virens*. The *Tvoxdc3* mutant lost its ability to parasitize *Sclerotium rolfii*, while the wild type and *Tvoxdc1* mutant remained effective biocontrol agents. In sclerotia parasitism assays, the *Tvoxdc3* mutant showed a 50% reduction in killing ability. Growth of the *Tvoxdc3* mutant was significantly inhibited by oxalic acid, confirming its role in oxalic acid detoxification and biocontrol of *S. rolfii*.

### Elucidation of Antifungal Properties of Short antimicrobial peptides on Rice Blast Fungus

Histatin 5 (Hst5), an antimicrobial peptide, as an eco-friendly alternative to chemical fungicides for controlling rice blast disease caused by *Magnaportheorizae* was evaluated in a study. Hst5 induced morphological defects in the fungus, affecting chitin distribution, hyphal branching, and septa formation, ultimately causing cell lysis. It also inhibited conidial germination, appressorium formation, and blast lesion development on rice leaves. Hst5's interaction with fungal DNA suggests it may regulate gene expression. This is the first study exploring this human salivary peptide for plant disease control, highlighting its potential as a bio-fungicide.

### Standardization of Microtuber Induction in Potato (*Kufriajyoti*) under in vitro conditions

Nodal explants from in vitro potato shoots were cultured in MS medium with various



Potato Microtuber development.

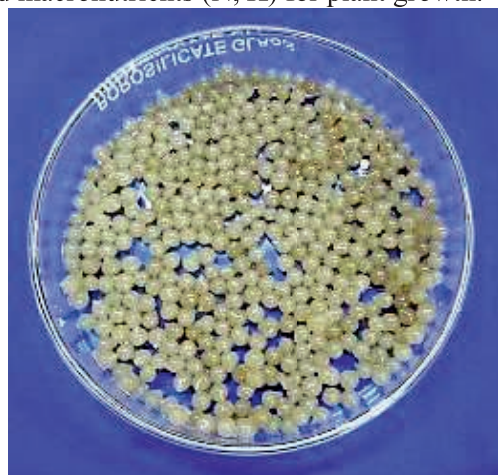


Generation of healthy plants in Potato (*Kufriajyoti*).

combinations of sucrose and plant hormones. Plain MS media with 8% sucrose proved most effective for microtuber induction. The resulting microtubers produced healthy plants, showing potential as a tool for induced mutagenesis.

### Development of bio-hybrid material as a slow-release fertilizer

A slow-release zinc fertilizer by loading zinc onto banana peel waste (which naturally contains potassium) under varying conditions of pH, temperature, and salinity was developed. Chitosan, which contains nitrogen and acts as a growth stimulant, was used to entrap the zinc-loaded banana peel in alginate-chitosan beads. The study demonstrated chemisorption of zinc onto banana peel. ICP-OES analysis showed slower zinc release from the bio-hybrid material compared to non-entrapped biomass. This formulation provides both micronutrients (Zn) and macronutrients (N, K) for plant growth.



Zinc pre-loaded banana peel entrapped in alginate-chitosan bead.



### Phage-based Bio-control and Engineered Antimicrobials against *Aeromonas dhakensis*

Fourteen unique bacteriophages were isolated against multidrug-resistant *Aeromonas dhakensis* strains from diverse locations. Four phages (E1, P5, P19, and G2) showed strong lytic activity. Genomic analysis confirmed they lack virulence, lysogeny, or antibiotic resistance genes, making them safe for biocontrol. The phages remained stable across temperatures (4–50°C) and pH levels (6–12). Biocontrol trials on fish fillets achieved 99% reduction of *A. dhakensis* within 2 hours. P19lysin, an endolysin from phage P19, lysed only *Bacillus subtilis*, while engineered artilysins with peptide fusions expanded activity to include *B. pumilus* and *B. licheniformis*. Artilysin A2 showed optimal activity at pH 5.5–7 but was sensitive to zinc and copper ions.

### Understanding programmed cell death in *Xanthomonas axonopodis* pv. *Glycines*

A potential quorum molecule was detected in Xag wild-type cells at 16 hours but was absent at 24 hours. The molecule had similar properties to a previously characterized death-inducing factor. Genome analysis revealed several genes related to programmed cell death and quorum sensing. Protein aggregation, a marker of reactive oxygen species damage, was significantly higher in cells undergoing programmed cell death.

### Starvation studies in *Salmonella* Typhimurium

DNA-binding proteins CbpA and CbpB in stress physiology were studied. Complementation of knockout strains restored growth in M9+ maltose medium. The knockouts showed decreased negative DNA supercoiling. Various stress conditions (anaerobic, alkaline pH, cold, and heat) reduced growth lag in knockout strains in M9+maltose medium. Transforming the *malQ* gene into  $\Delta$ *cbpB* mutant restored normal growth. Treatment with oxolinic acid upregulated maltose operon genes in the mutant, suggesting DNA supercoiling regulates the maltose operon.

### Physico-chemical analysis of IDPs (Intrinsically Disordered Proteins) from *Anabaena* PCC 7120 proteome

*Anabaena* PCC 7120 has a higher proportion of proteins with intrinsically disordered regions (over 11%) than *E. coli*. Of 6,174 protein-encoding genes, 688 encode at least one

intrinsically disordered region. These proteins exhibit diverse structures from tadpole/globular to coil or chimeric shapes. Charge-hydropathy analysis showed that most IDPs in *Anabaena* have low mean hydropathy and higher charged residue fractions compared to ordered proteins. In silico and transcriptome analysis identified at least five stress-induced IDPs that form interaction hubs with other proteins.

### RecFOR pathway proteins in radiation resistance of *Nostoc*

Overexpression of two RecQ helicases (Alr4842 and Alr0205) individually enhanced radiation tolerance in *Nostoc* 7120. GFP fusion studies showed RecQ1 and RecF co-localize with DNA. Protein interaction studies revealed strong interaction between RecF and RecO proteins, which is uncommon in most bacteria. The weakest interactions were between RecF-RecR and SSB3-RecO, while all three proteins interacted equally well with RecA. These findings suggest the presence of RecFOR, RecOR, and RecOF pathways for double-strand break repair in *Nostoc*.

### Functional characterization of DR1143 and DR0041 proteins of *D. radiodurans*

Two proteins that interact with RecA/SSB were characterized. The radiation-inducible DR1143 protein, expressed as a GFP fusion, localized as distinct foci in both *E. coli* and *Deinococcus*. This protein protected single-stranded DNA but not double-stranded DNA from nuclease degradation. DR0041 was characterized as a DNA compacting and protecting protein. To study structure-function relationships, DR0041 and its domains were purified for crystallization in collaboration with RRCAT, Indore.

### Oxidative stress response in *Chryseobacterium* sp. PMSPI on exposure to uranium

Uranium exposure induced oxidative stress in *Chryseobacterium* PMSZPI cells, as evidenced by increased free radical generation. At 300  $\mu$ M uranium, cells showed lipid peroxidation through elevated malondialdehyde content. Cell permeability increased based on zeta potential measurements, indicating membrane damage. qRT-PCR analysis revealed increased expression of oxidative stress response genes under uranium stress, with log<sub>2</sub> fold changes of 6.36 for thioredoxin, 3.76 for ferritin, and 3.33 for superoxide dismutase.

### Analysis of DNA metabolism genes in *Nostoc* PCC 7120

This study investigated nucleoside mono/diphosphate kinases (NMPKs and Ndk) in DNA repair in *Nostoc*. Overexpression of Ndk altered the phosphorylation status of several proteins, particularly those involved in photosynthesis. This resulted in changed heat dissipation mechanisms, decreased photosynthetic efficiency, and reduced abiotic stress tolerance. The cytidylate kinase (CMK) in *Nostoc* is uniquely fused with pantothenate kinase (PanC). Overexpression of the full-length PanC-CMK protein increased radioresistance, while overexpressing individual domains resulted in lower tolerance than the vector control.

### Characterization of plant bromodomain homologs and superoxide dismutase mutants

Full-length cDNAs of Arabidopsis bromodomain homologs (AtBRD8, AtBRD9, AtBRDPG2b) were isolated and cloned. Two AtBRD9 isoforms were expressed in *E. coli*, with AtBrd9.1 optimized for soluble expression. In rice, two isoforms of OsBRD4a were cloned for interaction analysis, revealing that OsBRD4a.2 exists as a monomer. Site-directed mutagenesis of rice cytosolic CuZn superoxide dismutase showed that the P108A mutation reduces thermostability but enhances enzyme activity at alkaline pH.

### Characterization of response regulator Rrel and phosphatase CikA from *Anabaena*

*Anabaena* Rrel is a two-component response regulator in the NarL family. Its expression increases under salinity stress, and knockdown mutants show reduced growth and photosynthesis, suggesting it regulates multiple physiological processes. The protein was overexpressed and purified for further analysis. CikA phosphatase, involved in dephosphorylating RpA (a master stress response regulator), was also purified. The 77 kDa CikA protein showed proteolytic cleavage into 22 and 55 kDa fragments.

### Whole genome sequencing, genetic manipulation, and analysis of gliding proteins of *Chryseobacterium* sp. PMSZPI

Whole genome sequencing of *Chryseobacterium* sp. PMSZPI yielded a single circular contig of 4.7 MB, and the DNA sequencing data was deposited in the NCBI SRA database under accession number PRJNA1175970. Because

genetic manipulation tools for introducing foreign DNA into *Chryseobacterium* are not well-known, a conjugation method was used for transformation using a stable plasmid shuttle vector of *Flavobacterium*, pCP29, containing an antibiotic cassette of cefoxitin (cfx). Stable recombinants that can survive in the presence of cefoxitin were obtained, which established the conjugation protocol for *Chryseobacterium* as a means of genetic manipulation. Gliding motility, a major characteristic of this organism, plays a role in response to uranium stress. GldN (35.6 kDa) and GldJ (59.2 kDa) are gliding proteins and components of the T9SS system found in the periplasmic space and inner-leaflet of the lipopolysaccharide layer (LPS), respectively. Genes encoding these proteins were amplified from *Chryseobacterium* sp. PMSZPI, then cloned, overexpressed, and purified from *E. coli* for further analysis.

### Characterisation of the role of Thioredoxin Reductase, Peroxiredoxin, and catalases of *Anabaena*

In *Anabaena*, 2-Cys-Peroxiredoxin, which helps maintain the cellular redox environment, relies on a newly identified TR (Alr2204) / Trx (Alr2205) couple located adjacent to each other in the genome of *Anabaena* PCC 7120. The TR and Trx couple were found to interact physically and their co-expression reduced the in vivo levels of 2-Cys-Prx in *Anabaena*. Another peroxiredoxin (Alr4641) of *Anabaena* 7120 contributes to tolerance to Se(VI) by overcoming the oxidative stress induced by the metal ion. When monitored over a range of temperatures at a high concentration of H<sub>2</sub>O<sub>2</sub> (50 mM), only a mixed *E. coli* KatB+KatA culture in a 1:3 ratio, but not *E. coli* KatA or *E. coli* KatB alone, could effectively decompose most of the H<sub>2</sub>O<sub>2</sub> present in the reaction up to 70°C. Co-expression of the two proteins resulted in better activity than by mixing the cultures expressing the individual proteins.

### Metal bioremediation and tolerance studies using *Nostoc* / *Anabaena* sp.

*Nostoc muscorum* biofilm, which was earlier shown to bind Cd, Ni, and Pb, was later shown to also bind Sr (II), decreasing Sr concentration in aqueous solutions from 2 ppm to <0.5 ppm in 24 h. Overexpression of a glycosyltransferase (All4493) in *Nostoc* 7120 resulted in enhanced synthesis (4-6-fold) of EPS and Released Polysaccharide (RPS), along with increased metal tolerance, and the RPS was shown to bind

Cd(II). Metals that bind to the cysteine groups of metallothioneins are also amenable to oxidation. Purified NmtA from *Anabaena* bound to Zn was shown to release the bound metal in the presence of oxidants like DTNB and SNAP. His-tagged NmtA was immobilized onto citrate functionalized Fe<sub>3</sub>O<sub>4</sub> magnetic nanoparticles (MNPs). These MNPs were shown to bind approximately 85% of U and Cd, and the metal-loaded NmtA MNPs could be easily separated by a magnet.

### Role of P<sub>IB</sub> type ATPase of *Chryseobacterium* sp. PMSPZI in metal tolerance and efflux

Characterisation of the P<sub>IB</sub> type ATPase of *Chryseobacterium* PMSPZI cells based on site directed mutagenesis revealed the importance of C318, C320, K620A and residues in efflux of heavy metals to cell exterior providing metal tolerance. The P<sub>IB</sub> type ATPase protein could also confer metal tolerance (Cd and Zn) in the heterologous host *E. coli* when overexpressed.

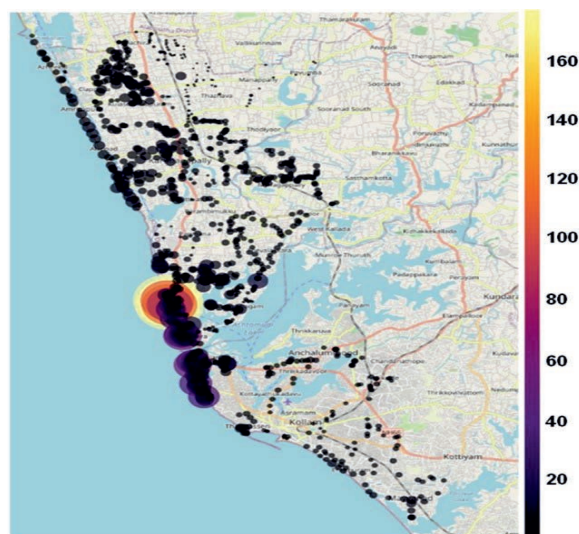
## Healthcare and Drug Discovery

### *In vitro* and *In vivo* investigation of Thorium-induced alterations in lung surfactant proteins

The study examined how thorium dioxide affects surfactant proteins in human lung cells. Thorium enhanced SP-D mRNA expression in A549 cells while reducing it in WI26 cells, with protein levels following similar patterns. Thorium exposure altered extracellular release of SP-D/A from A549 cells but not from WI26 cells. Oxidative stress and HSP90 signaling played differential roles in these alterations. These *in vitro* effects were consistent with findings in mice exposed to thorium aerosols, suggesting surfactant proteins may be involved in thorium-associated lung disorders.

### Molecular mechanism of radio-adaptive responses in Humans

Research in Kerala's high-level natural radiation areas revealed radiation levels ranging from 0.6 to 172mGy per year. Analysis of 12 years of lifespan data showed residents of these areas had better lifespans compared to others. Ongoing mechanistic studies are investigating the role of epigenetic factors, genes, proteins, immunity, and metabolites in these radio-adaptive responses.



External radiation dose rate in Kollam, Kerala. Size and color of the bubble show annual dose rate (mGy/year).

### Effect of chronic ionizing radiation on microbial diversity

Soil samples from areas with varying gamma radiation doses (1-150mGy per year) were analyzed, showing up to 1400-fold differences in thorium content. Despite these variations, overall soil microbial diversity remained stable. However, certain species in the rare microbiome showed significant abundance changes in high-radiation areas. The study identified over 250 microbial species present only in soil samples from very high background radiation areas.

### Fractionated irradiation equips cells for faster mis-repair

A549 lung cancer cells were subjected to ten fractions of 2 Gy radiation over 5-7 weeks to create radioresistant cells (10F-A549). The study found that radioresistance in these cells was transient and significant only at doses of 2 Gy or less. DNA repair genes were downregulated while mesenchymal markers were upregulated. Despite faster DNA repair, chromosomal studies revealed higher translocations in 10F-A549 cells, suggesting increased mis-repair in multi-fraction irradiated cells.

### Role of Bystander Effect in radio-resistance of A549 Lung Cancer cells

When medium from radioresistant 10F-A549 cells was transferred to unirradiated A549 cells, significant activation of DNA repair protein ATM was observed in both the bystander cells and in directly irradiated cells that received medium from these bystander cells. Proteome analysis revealed alterations in thousands of proteins, with upregulation of processes related to cell cycle, division, and chromosome



organization in bystander cells, suggesting soluble factors from irradiated cells mediate radiation-induced bystander effects.

### Serum sample analysis from Hemorrhagic Cystitis patients treated with Chlorophyllin

Serum proteomics analysis of hemorrhagic cystitis patients treated with chlorophyllin showed significant protein expression alterations. Enriched pathways included blood clotting, complement activation, wound healing, inflammation, and metabolic reprogramming. Key upregulated proteins in the blood clotting cascade included von Willebrand factor, coagulation factors, fibrinogen chains, and Protein S1, particularly in patients who responded positively to treatment.

### Effect of Clobetasol Propionate on T-cell proliferation

Clobetasol propionate (CP), which has radiosensitizing effects in lung cancer cells by inhibiting the Nrf2 pathway, was found to effectively suppress T-cell proliferation in wild-type mice. However, this effect was absent in Nrf2 knockout mice, highlighting the critical role of the Nrf2 pathway in regulating T-cell proliferation.

### Therapeutic radioprotection by oral suspension of Probiotics Spore

The study investigated the radioprotective potential of probiotic *Bacillus clausii* in mice exposed to localized radiation. Administration of the probiotic significantly restored gut length and integrity in mice exposed to 15 Gy gamma radiation in the abdominal region. Gut permeability assessment confirmed recovery of compromised intestinal barrier function following probiotic treatment.

### Lithium chloride restored the Spleen index in sub-lethally irradiated Mice

Oral administration of lithium chloride (50 mg/kg) at 4, 24, 48, and 72 hours post-exposure to lethal radiation significantly improved survival rates in mice by approximately 50% compared to controls. In sub-lethally irradiated mice, the same dosing regimen effectively restored the spleen index, suggesting potential for mitigating radiation-induced damage to hematopoietic tissues.

### Exploration of radioprotective mechanism of Bosutinib

Molecular docking analyses showed strong binding affinity of bosutinib to upstream kinases MKK4 and MKK7, with binding energies of -7.7 kcal/mol and -7.2 kcal/mol respectively. Molecular dynamics simulations confirmed stable complex formation, supporting bosutinib's potential role in modulating the JNK signaling pathway.

### Characterization of clinical variants of SARS-CoV-2 Papain-like protease

Analysis of 14 million SARS-CoV-2 sequences identified five globally circulating PLpro mutants. Biochemical characterization revealed the K232Q mutation increased enzymatic activity against various substrates with significantly enhanced deubiquitination activity, while A145D and V187A mutations reduced activity. P77L and P77S mutants showed activity similar to wild-type PLpro. Structural analysis indicated that shortening of the side-chain in K232Q leads to faster product release, increasing catalytic activity.



Increase in the interaction distance between Lys/Gln232 of PLpro (top) and Ala46 of Ub (below).

### Role of Ubl Domain in SARS-CoV-2 Papain-like protease

A truncated version of PLpro lacking the Ubl domain retained proteolytic activity against key substrates but showed decreased catalytic efficiency and increased instability compared to wild-type. Structural analysis revealed important interactions between the Ubl domain and catalytic core, suggesting the Ubl domain plays a critical role in stabilizing protein structure and guiding substrate orientation. The results highlight the Ubl domain's essential contribution to PLpro's functional and structural integrity.

### Crystal structure of single domain antibodies developed against Thyroglobulin

Two nanobodies, KT75 and KT76, with high affinities for thyroglobulin were identified. Their crystal structures were determined at high resolutions of 1.3 Å and 1.6 Å respectively. Both nanobodies demonstrated exceptional binding affinities in the pico-molar range to human thyroglobulin, as measured using ITC and SPR-based methods.



Crystal structure of KT75 (1.3 Å, Left panel) and KT-76 sdAbs (1.6 Å, Right panel). The variable regions (CDRs) are highlighted with different colours.

### Enzymatic bio-degradation of plastics

A double mutant (W159H/S238F) and inactive mutant (H237Q) of IsPETase were created to degrade poly-ethylene terephthalate. The double mutant showed four times greater catalytic efficiency than the wild-type enzyme, with SEM micrographs confirming more efficient degradation of plastic surfaces. X-ray diffraction data revealed the inactive H237Q mutant's structure at 1.5 Å resolution, showing that the Gln residue is not hydrogen-bonded to catalytic serine.

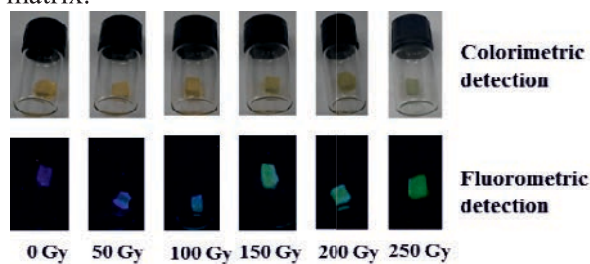
### Effect of aqueous extract of Rampatri Fruit Rind on Metabolic Syndrome Model

Therapeutic treatment with rampatri extract (REW) significantly reduced blood sugar and systolic blood pressure in a diet-induced

metabolic syndrome model. REW corrected dyslipidemia by reducing total cholesterol and LDH levels, improved hepatic and renal functions, enhanced cardiac pumping efficiency, and reduced organ damage and fibrosis. The extract was non-toxic up to 2g/kg body weight and effectively mitigated hypertension, dyslipidemia, and hyperglycemia.

### Development of in-house solid-state dosimeter for gamma radiation

A novel BODIPY-Malachite green conjugate dye was developed for gamma radiation detection. The dye shows visual color change from yellow to greenish upon gamma exposure, with non-fluorescent dye exhibiting fluorogenic response at 524 nm that increases 15-fold after 20 Gy exposure. The system demonstrates linear relationship up to 11 Gy with a very low detection limit of 0.006 Gy. The dye was also successfully loaded in semi-solid polymer gel matrix.



Colorimetric & fluorometric detection of gamma dose in semi solid matrix.

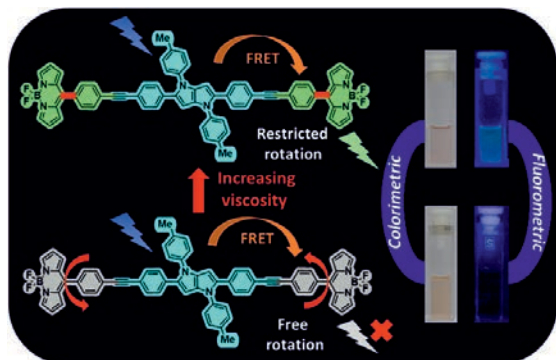
### Design & synthesis of functional Organo Boron complexes for Targeted Cellular Imaging

One-step methods for functionalizing BODIPY dyes at the meso/C-8 center for sensing/imaging applications were developed. Cross-coupling at the meso-methyl position was achieved via C(sp<sup>3</sup>)-N(sp<sup>3</sup>) bond formation using PIDA oxidant, allowing attachment of various biologically important secondary amines and chelators. The dyes show green and red fluorescence under acid vapor, making them effective pH sensors for both in vitro and in vivo conditions.

### Synthesis of Tetraaryl pyrrolo[3,2-b]pyrrole-BODIPY Dyad for FRET-based viscosity sensing

Two dyad molecules combining tetraaryl pyrrolo[3,2-b]pyrrole (TAPP) and BODIPY dyes were synthesized as molecular rotors for viscosity sensing. They showed very high energy transfer efficiency (>99%) from TAPP to BODIPY moiety upon excitation. In

increasing solvent viscosities, emission from BODIPY moieties increased due to restricted rotation, with fluorescence intensity correlating linearly with viscosity according to the Förster-Hoffmann equation.



Viscosity sensing mechanism in TAPP-BODIPY dyad system.

### Synthesis of Hydroxy/Amino Azobenzene derivatives and evaluation of their Anti-Cancer activity

A series of hydroxy/amino azobenzene derivatives were synthesized to overcome stability issues in hydroxy stilbenes by replacing carbon-carbon double bonds with azo groups. Bio-activity studies revealed compounds 1, 2, 6, and 7 had promising anti-cancer activity against SKOV3 ovarian adenocarcinoma cell lines, with  $IC_{50}$  values of approximately 12.5, 19.8, 7.5, and 19.7  $\mu$ M, respectively.

### BODIPY-Helicene based heavy-atom-free Photocatalyst

Two BODIPY-helicene dyes were synthesized by fusing BODIPY core with modified [5]helicene structures, creating twisted molecules with increased twisting angles. These dyes showed broad absorption across the UV-visible spectrum with high triplet conversions and long triplet lifetimes compared to planar BODIPY. One dye efficiently catalyzed oxidative coupling of amines and aerobic oxidation of sulfides, with the catalyst being recoverable and reusable for several cycles.

### Development of CPL active-BODIPY emitter using supramolecular chiral induction strategy

A supramolecular assembly of chiral peptide and achiral BODIPY was developed to generate circularly polarized luminescence (CPL) with  $glu$  values reaching up to  $\sim 1.2 \times 10^{-2}$ . The CPL generation relies on halogen bonding to transfer chirality from the peptide template to BODIPY fluorophores. The co-assembly demonstrates

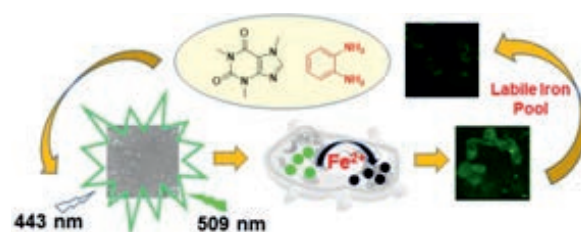
temperature-dependent On/Off CPL switching, opening new perspectives on halogen bonding in regulating supramolecular chirality.

### Design and development of Tetraarylpyrrolo[3,2-b]pyrrole-BODIPY Dyads as EET-based system

Two dyads combining TAPP and BODIPY were synthesized: one with BODIPYs directly connected to TAPP and another with connections through phenylethynyl linkers. Both showed nearly complete energy transfer from TAPP to BODIPY units. Ultrafast spectroscopy revealed energy transfer dynamics of 125 fs in one dyad (one of the fastest reported) and 480 fs in the other, following the Förster mechanism.

### N-rich Carbon Nanosphere as Fluorescent Nanoprobe for Intracellular Iron

Nitrogen-rich carbon nanospheres (G-CNS) were synthesized from caffeine and o-phenylenediamine. These highly fluorescent nanospheres ( $\lambda_{em}$  at 509 nm) showed selective fluorescence turn-off response toward  $Fe^{2+}/Fe^{3+}$ , making them effective for detecting intracellular labile iron pools in live cells. The fluorescence quenching mechanism involves an excited state charge transfer process with non-radiative decay.



Synthesis and application of carbon nanospheres.

### Single stage synthesis of $\gamma$ -Graphyne

$\gamma$ -Graphyne, a 2D layered carbon allotrope containing both  $sp^2$  and  $sp$  hybridized carbon atoms, was synthesized via palladium-catalyzed chemical route. Its structural and morphological properties were characterized using Raman spectroscopy, XRD, SEM, and AFM. The material's band gap was approximately 1.5 eV and showed excellent sensitivity toward uranyl oxide, suggesting potential applications in catalysis, sensing, energy storage, and microwave absorption.

### Transition-metal-free decarbonylation-oxidation of 3-arylbenzofuran-2(3H)-ones

A transition metal-free procedure was developed to produce substituted 2-hydroxybenzophenones with good to excellent yields using



hydroperoxide generated in-situ from tetrahydrofuran autooxidation. The UV-protection abilities of the synthesized benzophenones were evaluated mathematically, showing that 5'-substituted-2-hydroxybenzophenones with electron-donating groups at the 4'-position are promising candidates for further in vitro and in vivo evaluation.

#### **Strippable Gel based on Deep Eutectic Solvent for radioactive decontamination**

A strippable gel coating (RADGEL) composed of deep eutectic solvent and polyvinyl alcohol was developed for radioactive decontamination. Testing on various simulated surfaces achieved up to 99.9% decontamination efficiency for both alpha and gamma radionuclides. Parameters including complexing agent amount, polymer film thickness, radioactivity characteristics, and surface properties were optimized. FTIR and SEM analyses suggested RADGEL's capability for both physical and chemical interactions with contaminants.

#### **Organocatalytic Deuteration using D<sub>2</sub>O as Deuterium source**

A metal-free organocatalyzed method was developed for  $\alpha$ -deuteration of ketones using D<sub>2</sub>O under mild conditions. The versatile protocol achieved good to excellent deuterium incorporation (90-97%) in various cyclic and linear ketones in a single run. Pharmaceutical molecules including 2-acetylphenothiazine, nabumetone, pentoxifylline, and estrone-3-methyl ether were successfully deuterated, with practicality demonstrated in gram-scale synthesis.

#### **Organocatalyzed Asymmetric Synthesis of Coumarin-pyrazole Hybrids**

Chiral thiourea catalyzed 1,6-conjugate addition of pyrazolones to 3-cyano-4-styrylcoumarins was developed to create optically pure coumarin-pyrazole hybrid molecules. The protocol delivered 18 hybrid compounds with moderate to excellent yields (up to 98%) and good enantioselectivities (up to 99:1 er), demonstrating value in preparative scale applications.

#### **Development of Human ACE2 Mimic Miniprotein Binders for SARS-CoV-2 variants**

Human angiotensin-converting enzyme 2 (ACE2) is the natural binding partner for the

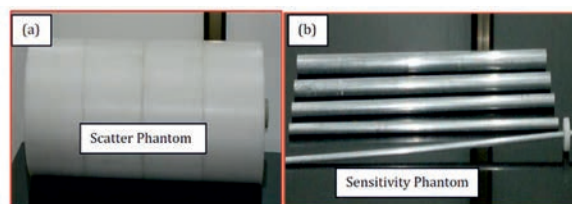
SARS-CoV-2 spike protein and plays a crucial role in viral entry into human cells. Based on the ACE2 interaction interface, we designed and synthesized three mini-protein binders that demonstrate submicromolar to nanomolar affinities for variants of concern in SARS-CoV-2. These binders have numerous potential applications in diagnosis.

#### **Biocompatible Protein-based formulations and their therapeutic & cosmetic applications**

Novel protein-based materials were developed for both therapeutic and cosmetic applications. A serum albumin-based chemotherapeutic agent conjugated bovine serum albumin (BSA) with 3,3'-diselenodipropionic acid (DSePA), resulting in a stable compound with approximately five DSePA molecules per BSA molecule that selectively induced apoptosis in lung adenocarcinoma cells (A549). Similarly, a Pickering emulsion for cosmetic use combined protein coacervates, coconut oil, and curcumin, stabilized by  $\beta$ -carboxymethyl chitosan and gelatin, achieving an SPF of 8.5 and effectively delivering curcumin to fibroblast cells. Both formulations demonstrate the versatility of protein-based materials across healthcare and cosmetic industries.

#### **Performance evaluation of Sensitivity and Scatter Phantoms in Nuclear Medicine**

The performance of a PET/CT system was evaluated using in-house developed sensitivity and scatter phantoms, following the NEMA NU2-2007 guidelines. Key parameters assessed included system sensitivity, scatter fraction, count-rate performance, count loss accuracy, and random corrections. The measured values closely matched the vendor-specified limits, confirming that these phantoms are suitable for routine quality assurance procedures in nuclear medicine. This validation supports the reliability of the in-house phantoms for ongoing system performance monitoring.

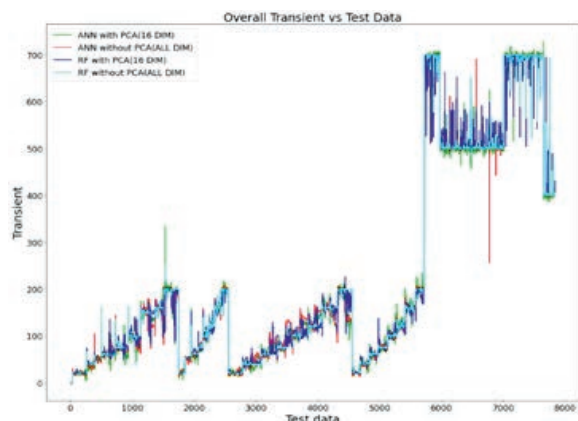


From left to right: Scatter Phantom and Sensitivity Phantom.

## Machine Learning and AI

### ML Models for Identifying Accident Scenarios in Nuclear Power Plants

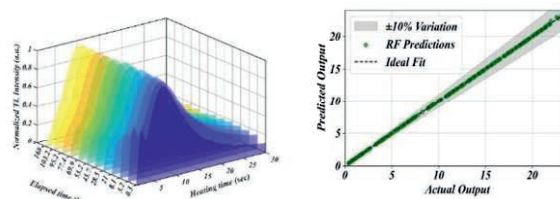
To enable identification of accident scenarios — such as Loss of Coolant Accident (LOCA) and Main Steam Line Break (MSLB) — in a Pressurized Heavy Water Reactor (PHWR), Artificial Intelligence (AI) techniques have been applied to analyze real-time sensor data. Specifically, AI models based on Artificial Neural Networks (ANN) and Random Forest (RF) have been developed to detect 32 distinct LOCA and 18 MSLB scenarios in a 220 MWe PHWR. Among these, the Random Forest model demonstrated strong performance.



Comparison of performance of ANN and RF based AI models in MSLB scenarios.

### AI analysis of TL glow curves for assisting in assessment of excessive exposure cases

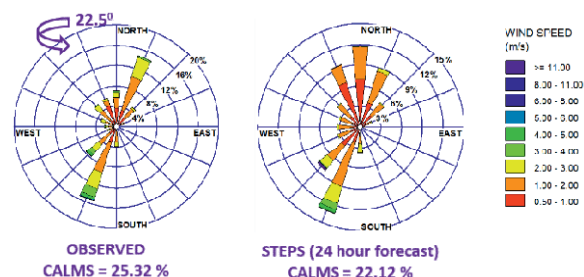
AI analysis of thermoluminescent (TL) glow curves can estimate elapsed time between radiation exposure and TLD badge readout, aiding dose correction. This study analyzed  $\text{CaSO}_4:\text{Dy}$ -based TLD glow curves using Artificial Neural Networks (ANN) and Random Forest (RF) models. Glow curves were deconvoluted with a 10-trap first-order kinetics model over 0.34 to 168 hours. The ANN model underestimated elapsed time as it increased, while the RF model with 100 trees closely matched actual times. Machine Learning models outperformed traditional analytical method, which struggle with deconvolution uncertainties and weakening low-temperature peaks. The RF model effectively used the full glow curve pattern without data normalization, proving more reliable for elapsed time estimation.



Trend in the shape of glow curve with time along with plot predicted vs. actual elapsed time after exposure by RF model using glow curve data.

### ML-based short-term forecasting of Meteorological variables

Accurate short-term forecasts of meteorological variables such as wind speed, wind direction, and solar radiation are crucial for local-scale atmospheric dispersion simulations during accidental releases. While Numerical Weather Prediction (NWP) models are commonly used, a machine learning-based system called the Short Term Prediction System (STEPS) has been developed. STEPS employs an Auto Regressive Integrated Moving Average (ARIMA) approach to predict wind speed, wind direction, air temperature, relative humidity, solar, and net radiation. It uses the past seven days of measured data to forecast these variables for the next three days. The model's performance is comparable to observed wind speed and direction data.

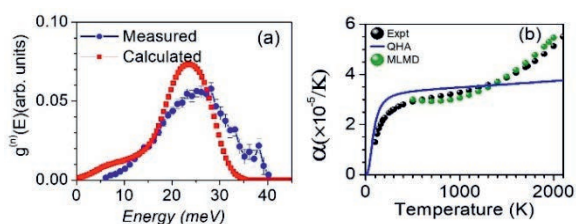


Annual Wind Rose from observed data and STEPS model.

### Anharmonic Phonons and Anomalous Thermal Expansion in Vanadium

Vanadium, a key transition metal in the alloy and steel industries, exhibits anomalous thermal expansion at high temperatures. Recent studies using neutron inelastic scattering at Dhruva and machine-learned force-field-based molecular dynamics (MLMD) simulations have clarified the role of phonon anharmonicity in this behavior. Comparisons between the quasiharmonic approximation (QHA), temperature-dependent effective potential (TDEP), and MLMD methods reveal that QHA significantly overestimates thermal expansion at

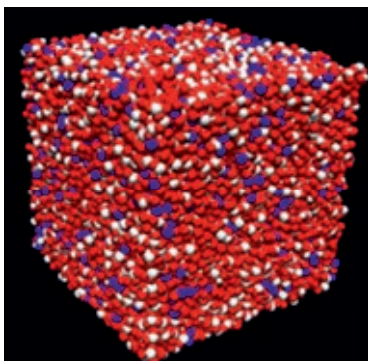
low temperatures and fails to capture the strong anharmonic effects evident at high temperatures. While TDEP improves agreement with experiments at lower temperatures, only MLMD—accounting for all orders of anharmonicity—accurately reproduces the anomalous thermal expansion observed in vanadium from 500 to 2000 K. This highlights the limitations of QHA in strongly anharmonic systems and underscores the necessity of advanced simulation techniques for predicting high-temperature properties in vanadium.



(a) The measured phonon density of states at DHRUVA were used to bench mark the simulation. (b) The calculated thermal expansion coefficient of vanadium and compared with measurements.

### Machine Learning based atomistic simulations of multi-component glass

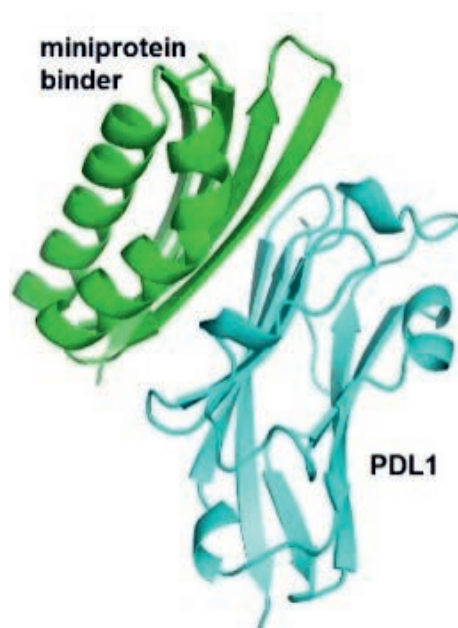
MD as well as AIMD simulations were completed for binary lithium silicate glass with composition 10%, 20%, and 30%  $\text{Li}_2\text{O}$ . The generated trajectories were analyzed for density and RDFs. A Machine Learning (ML) model is being developed for refinement of B-K-S interaction parameters of lithium silicate glass. AIMD studies were completed for calcium silicate glass. The generated data will be used to develop a ML model for forcefield refinement of calcium silicate glass. ML models were developed to predict the density, glass transition temperature and Young's modulus of sodium borosilicate glass using Linear Regression and Random Forest algorithms. The performance of these algorithms was used for the prediction of data with default and featured engineered models.



A snapshot of MD simulated lithium silicate glass.

### Design of protein binders against cancer target PDL1

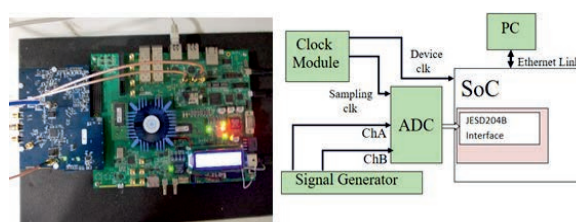
Mini-protein binders can be affordable substitute for monoclonal antibody for cancer diagnostic and therapy. Miniprotein binder which bind and inhibit the activity of the cancer protein PDL1 were designed using machine learning tool and recombinantly produced in biochemical facility of BL21 beamline. Their bindings are being evaluated using different biophysical and biochemical methods.



Model of designed miniprotein binding to PDL1.

### Control and DAQ system for Quantum Computing setup - Measurement of Qubit state

A prototype 1 GSps two-channel DAQ system was developed for qubit state measurement in quantum computing and it uses a 14-bit dual ADC evaluation board interfaced with an SoC enabling programmable trigger-delayed (System on Chip) via JESD204B. The custom VHDL code on the SoC acquires ADC data, processing. User-configurable parameters include data profile width, processing/averaging delay, and averaging duration, ensuring adaptable qubit readout for quantum experiments.



Prototype 1 GSps two-channel DAQ system.



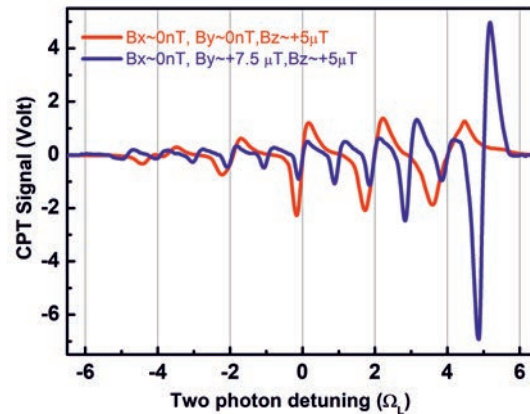
### Designing a Tunable Coupler: Simulations with Two Qubits

Electromagnetic and quantum simulations were conducted to design key components of a quantum processor comprising two qubits coupled via a tunable coupler. These simulations enabled the extraction of critical design parameters to realize the desired system Hamiltonian. The tunable coupler's frequency range was identified to effectively suppress static parasitic ZZ coupling between the qubits. Additionally, the controlled swapping of quantum states between the qubits through the tunable coupler was successfully demonstrated, highlighting its potential for precise qubit interaction management.

### Enhanced optical pumping of atomic population for Quantum Sensing

Enhancement of two-photon coherent population trapping (CPT) resonance in atoms has been demonstrated in quantum interference experiments, which is useful for atomic magnetometry. The experiments utilized a bichromatic circularly polarized light field in

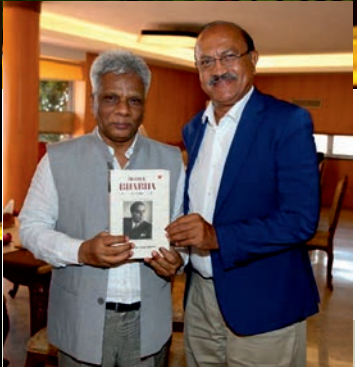
combination with mutually orthogonal magnetic fields applied to rubidium atoms in natural isotopic composition. An enhancement of atomic population in specific atomic states that contribute to the quantum interference signal was achieved. The experimental observations are consistent with theoretical calculations based on density matrix formalism and are of significant interest in various areas of quantum technology.



Two-photon resonances with longitudinal magnetic field  $B_z$  (red curve) and with longitudinal & transverse magnetic field  $B_z$  &  $B_y$  (blue curve). A phenomenal increase in the CPT signal is seen at  $5 \Omega_L$  (Larmour frequency) resonance.



# HUMAN RESOURCES, SCIENTIFIC INFORMATION AND TECHNOLOGY MANAGEMENT



BARC appoints scientific and technical manpower for its pan-India facilities through a carefully crafted testing process wherein selected candidates, mostly fresh graduate engineers, and masters from university systems are subjected to a rigorous program of training at its well equipped Training School facility in Mumbai. BARC houses a large treasure of scientific literature which is stored in physical as well as in digital form to meet the requirements of the centre. Understanding the growing desire among users to increasingly access information virtually, it is continuously implementing new state-of-the-art technologies to ensure seamless access to first-hand high quality scientific data. To boost entrepreneurial zeal among the young generation, BARC has expanded its technology incubation infrastructure at its Mumbai campus and is also offering a wide gamut of technologies for mass production.





Distinguished scientist and Member, Niti Aayog, Dr. V.K. Saraswat hands over passing certificate to a successful graduate of the 67<sup>th</sup> Batch (OCES-2023 program) of BARC Training School during the Graduation Function in September 2024 in Central Complex Auditorium, BARC Trombay.

# Human Resources, Scientific Information and Technology Management

## Human Resources

### BARC Training School

Dr. HomiJ. Bhabha strongly professed that in order to achieve self-reliance in the nuclear energy sector, it is imperative for the country to build a sustained pool of highly skilled human resources from the ranks of talented workforcereadily available within the country. In line with this philosophy, Dr. Bhabha had conceptualized the creation of Training School system in DAE, and the first training school was established in 1957 in Bombay (now Mumbai), as a centre of excellence for training of professionals through in-house efforts. Over the years, around 11,000 well-rounded individuals

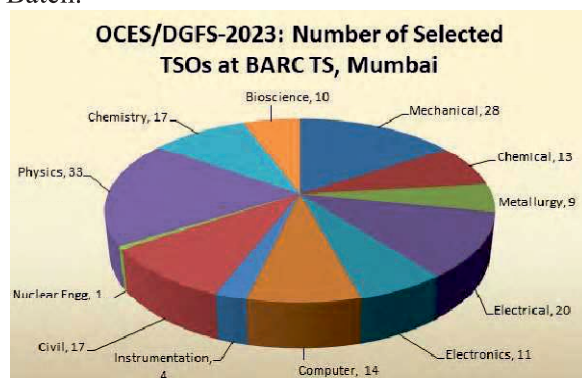
graduated from the ramparts of training schools with flying colors.

### Recruitment

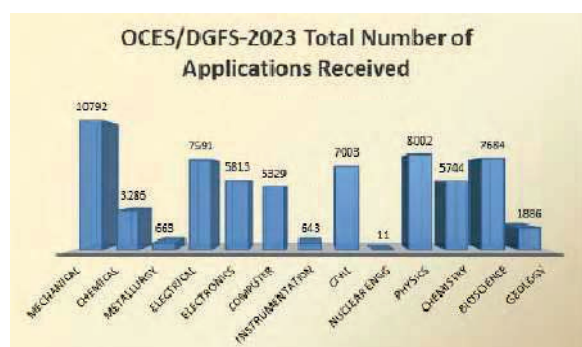
The Human Resources Development Division (HRDD) of BARC provides highly skilled human resources to DAE through two flagship programs, OCES (Orientation Course for Engineering graduates and Science Postgraduates) and DGFS (DAE Graduate Fellowship Scheme). Thelinkage of BARC Training School programs with Homi Bhabha National Institute (HBNI) ensures continuous availability of professionally qualified, well trained and motivated scientific and technical manpower for induction into various DAE units.



A total of 177 graduating TSOs of 67th batch of BARC Training School (73 Engineering + 58 Sciences, including 12 Radiological Safety & Environmental Science (RSES) among others) after successful completion of training, were placed in various divisions of BARC. There were 10 Trainee Defence Officers, who also passed out with this batch and were assigned to different Divisions/Units for undertaking project for M. Tech. In addition, 2 NTPC officers completed their training in the OCES-2023 Batch.



Discipline-wise break-up of TSOs selected for BARC Training School, Mumbai for OCES/DGFS-2023 programme.



Total applications received for various disciplines for OCES/DGFS-2023.

The one-year academic training programme at BARC Training School provides for course work in nuclear, core & elective courses as well as experimental and project work. This leads to broad based knowledge acquisition, in addition to gaining hands-on experience in project implementation. The selection of courses is meticulously formulated to ensure that the classical knowledge on the basics of nuclear science and technology is blended with the latest technological advances, leading to the holistic development. It also provides a sound platform for further career journeys.

The outreach for OCES/DGFS-2023 Training School programme was conducted in 61 colleges spread across several states of the country.

### BARC Doctoral Programme

The PhD programme at BARC combines rigorous classroom coursework with a substantial research component. Admission to the programme is based on candidates' performance in interviews. Students admitted to the PhD programme are registered under the Homi Bhabha National Institute (HBNI). For BARC-JRF 2023, a total of 105 Junior Research Fellowship positions were offered, distributed equally across Physical Sciences, Chemical Sciences, and Life Sciences (35 positions each). Of these, 83 research scholars joined the BARC-JRF 2023 programme. The inauguration ceremony for the 2023 cohort was organized by the Doctoral Programme & Internship Section of HRDD on May 6, 2024.

### Scientific Information Resources

#### Trombay Colloquium

BARC has orchestrated Trombay Colloquium, a distinguished intellectual forum that invited eminent leaders from diverse scientific domains to share groundbreaking insights/thoughts and transformative technological innovations. Last year, the speakers were: (a) Prof. Ashoke Sen, Honorary Fellow at NISER Bhubaneswar, (b) Prof. Balram Bhargava, Chief of Cardiothoracic Centre, AIIMS New Delhi, (c) Shri Raj Chengappa, Group Editorial Director at India Today Group, (d) Dr. Soumya Swaminathan, Former Chief Scientist at World Health Organization and (e) Shri A.S. Kiran Kumar, Member of the Space Commission, Government of India. Each speaker brought unique perspectives, exploring cutting-edge developments in their respective fields of expertise, thereby enriching the scientific discourse and fostering interdisciplinary knowledge exchange. Such Colloquia serve as a crucial platform for enabling scientists/engineers to share the emerging trends and their potential technological implications.



Prof. Ashoke Sen, Honorary Fellow at NISER Bhubaneswar.



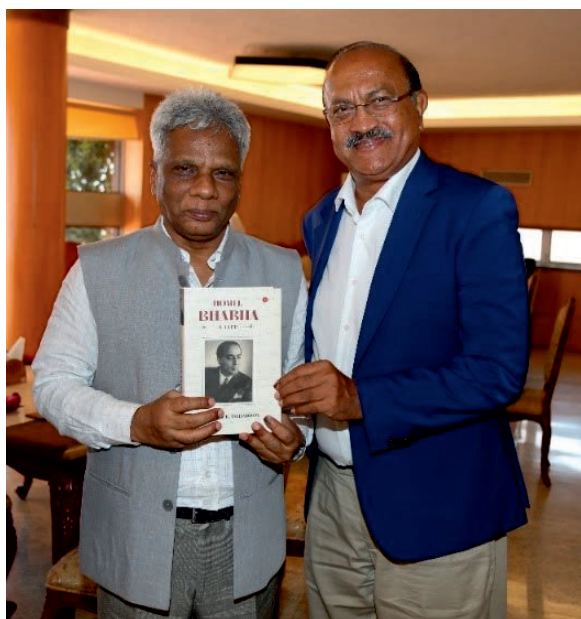
Prof. Balram Bhargava, Chief of Cardiothoracic Centre, AIIMS New Delhi with Shri Vivek Bhasin, Director, BARC.



Shri A.S. Kiran Kumar (right), Member of the Space Commission, Government of India with Dr. R.Chidambaram (1936-2025), Former Principal Scientific Advisor to the Govt. of India.



Top: Dr. Soumya Swaminathan (front row), Former Chief Scientist at World Health Organization.



Shri Raj Chengappa (on the right), Group Editorial Director at India Today Group with Dr. Ajit Kumar Mohanty, Chairman, AEC & Secretary, DAE.

Professor Ashoke Sen delivered a talk on “The Future of our Universe”, Prof. Balram Bhargava on “Indigenous Indian Vaccine: The Story of Human Compassion & Cooperation”, Raj Chengappa on “Media and Science”, Dr. Soumya Swaminathan on “My Journey as a Physician, Scientist and Researcher” and Kiran Kumar on “Indian Lunar Mission”.

### Chintan Baithak

Chintan Baithak, a unique platform for fostering collaboration in science and technology, is designed to create a stimulating environment that encourages open discussion among BARC community. This initiative aims to ensure concrete outcomes from various ongoing R&D activities. During this review, two rounds of discussions were conducted, focusing on critical topics such as ‘Proton Accelerators’ and ‘Aligning APAR work plan with Amritkaal Targets’. These discussions are pivotal in advancing BARC’s mission to enhance its capabilities and align them with national objectives.

### Publishing of Books

SIRD published books on interesting topics during last year. These include (a) *IMPACT* 2019-2024 (Editors: Dr. S. Adhikari & Manoj Singh): An illustrated publication and the inaugural edition in a new series documenting scientific, technical, academic and institutional activities of BARC from 2019 to 2024 was published in the name of *IMPACT* (IMPortant Activities Carried out at the Trombay Campus of BARC). This volume offers a comprehensive pictorial overview of the vibrant R&D culture at Trombay campus. It showcases important visits from distinguished personalities, including Nobel laureates, esteemed academicians &



influential leaders (both nationally & internationally). The inaugural edition of 'IMPACT', unveiled during the annual DAE Day (August 2, 2024) event in Mumbai.

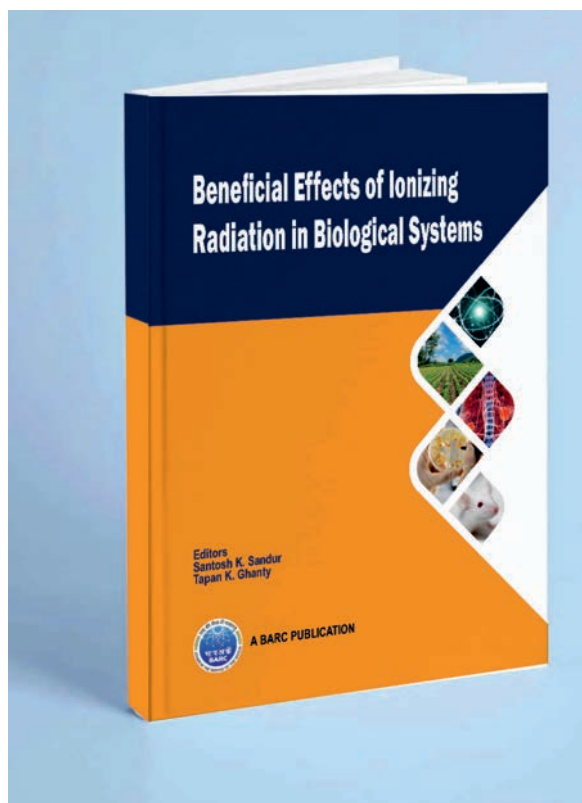
*Beneficial Effects of Ionizing Radiation in Biological Systems* (Editors: Dr. Santosh Kumar Sandur & Dr. Tapan Kumar Ghanty): This book chronicles the application of radiation for the benefit and socio-economic development of mankind. It gives an updated & succinct account of the outstanding contributions of scientists of DAE towards application of radiation in various

fields of biological sciences such as healthcare, agriculture, food preservation & defence against nuclear warfare.

*The Miniature Marvels: 70 Bonsai Specimens of BARC Trombay* (Editors: H.A. Barbhuiya & C.K. Salunkhe): This book is all about the captivating world of bonsai, focusing on the amazing collection nurtured at BARC Trombay since 1962. It is a compendium of 70 bonsai specimens, each a testament to the skill and dedication of their caretakers.



*IMPACT 2019-2024* presents a visual journey, featuring visits from Nobel laureates, top academicians, and global leaders to BARC.



*Beneficial Effects of Ionizing Radiation in Biological Systems* chronicles the application of radiation for the benefit and socio-economic development of mankind.



*The Miniature Marvels: 70 Bonsai Specimens of BARC Trombay* is a compendium of 70 bonsai specimens, each a testament to the skill and dedication of their caretakers in BARC.

### Special Exhibition of Scientific Books

Exhibition of new books from book vendors on various subjects - Physics, Chemistry, Nuclear Engineering, Food Technology, Computer Science, Library Science, Agriculture, Environmental Science, Bioscience, etc. was held from February 26 - March 01, 2024. The exhibition received overwhelming response from BARC staff. More than 600 books were selected by them during the special drive.





Front covers of newsletter issues published during the year.

### Newsletters, Web Digests and Information Bulletins

During the year, the bi-monthly Newsletters have comprehensively covered cutting-edge research & innovations, highlights of BARC's multidisciplinary activities focusing:

- Theoretical & Computational Chemistry,
- Advancements in Health, Food, Water, Agriculture and their role in ensuring national security,
- Technology development efforts in state-of-the-art Radio Frequency Systems
- Ultrafast spectroscopy research with femtosecond laser applications and
- Research and Technology Innovations in BioScience Landscape.

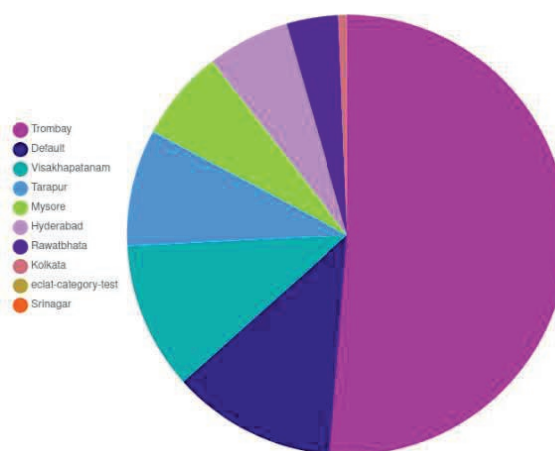
The weekly Web Digests and the Scientific Information Resource Bulletins were published regularly during the year. News coverages of developments in nuclear energy domain in popular media networks and other related sources are collated and published regularly in the weekly Nuclear News Web Digest.

### One DAE One Subscription (ODOS)

A dedicated section of ODOS journals that includes Springer Nature Pvt. Ltd. which provides access to the collection of 1353 journals including archives from 1997; and 2,686 Journals from Wiley (John Wiley & Sons, Inc.) is created under 'Lakshya online Gateway' along with procedures to apply for Article Processing Charges (APC) waiver. It is working

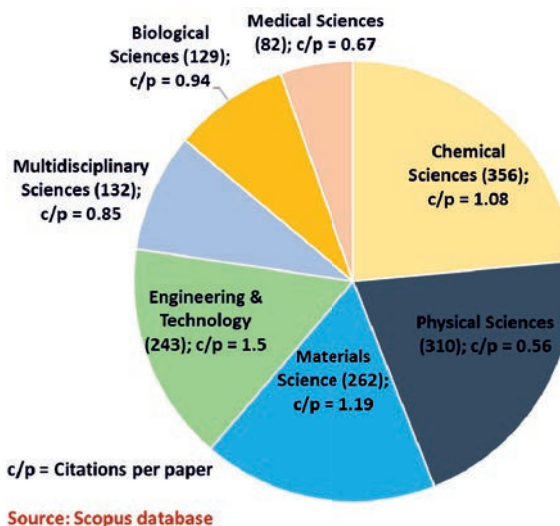
proactively for the implementation of One Nation One Subscription (ONOS) initiative floated by the Government of India for enhancing the accessibility of wide spectrum of journals. Author workshop was also arranged for the patrons from the editors of Wiley and Springer nature group on, "Open Access Publishing highlighting ODOS Agreement". Nearly 200 Authors attended the workshop. Feedback from the patrons was also collected for further initiatives.

Categorywise Total PDF Downloads



### Journal Publications

Institutional publication output is often used as a measure of the research productivity and impact made by the institution, as well as the intellectual contributions of its researchers. Group-wise percentage of journal articles published by BARC scientific community in the calendar year 2024 is depicted here. There were 1481\* publications in 2024.



Journal articles published by BARC scientists across various disciplines during the calendar year 2024 is presented below.

S. No	Journal	No. of articles	Impact Factor
1	Mapan - Journal of Metrology Society of India	31	1
2	Journal of Radioanalytical and Nuclear Chemistry	30	1.96
3	International Journal of Hydrogen Energy	23	8.1
4	Applied Radiation and Isotopes	22	1.874
5	Journal of Alloys and Compounds	19	5.8
6	Ceramics International	18	5.2
7	Journal of Molecular Liquids	18	6.3
8	Physica Scripta	18	2.1
9	Physical Chemistry Chemical Physics	18	2.9
10	Inorganic Chemistry	17	4.3
11	Journal of Physical Chemistry C	15	3.3
12	ChemistrySelect	14	1.9
13	Clinical Nuclear Medicine	14	4.6
14	Journal of Applied Physics	14	2.7
15	Physical Review C	14	3.2
16	Industrial and Engineering Chemistry Research	13	4
17	Journal of Materials Engineering and Performance	13	2.2
18	Physical Review B	13	3.2
19	Radiation Physics and Chemistry	13	2.8
20	Radiation Protection Dosimetry	13	0.8
21	Journal of Energy Storage	12	8.9
22	Langmuir	12	3.7
23	Radiochimica Acta	12	1.4
24	International Journal of Biological Macromolecules	11	8.2
25	Small	11	13
26	ACS Applied Energy Materials	10	5.4
27	ACS Applied Nano Materials	10	5.3
28	Journal of Materials Science: Materials in Electronics	10	2.8
29	Journal of Nuclear Materials	10	4.3
30	New Journal of Chemistry	10	2.7
31	Nuclear Instruments and Methods in Physics Research, Section A: Accelerators, Spectrometers, Detectors and Associated Equipment	10	1.5
32	Other journals	1046	

## Official Language (Rajbhasha Hindi) Implementation in BARC

### Training Programs

BARC has been proactively conducting regular training and interactive sessions to expand the Official Language implementation among its workforce. Quarterly Hindi workshops trained 118 officials in Official Language Policy, noting and drafting, incentive schemes, and practical applications through hands-on sessions. Under the Hindi Teaching Scheme of the Ministry of Home Affairs, 80 officials received training in Prabodh, Praveen, Pragya, and Paarangat programs, with an action plan prepared to train remaining employees within the prescribed timeframe. Special Hindi typing programs were conducted to familiarize workforce with the Hindi keyboard on computers. Additionally, intensive refresher training in Hindi stenography was provided to 49 stenographers during March 18-22, 2023, utilizing the services of senior Hindi Section officials from Heavy Water Plant, Manuguru.



Training in Hindi stenography, organized during March 18-22, 2024 in BARC.

### Incentives and Awards

Officials who completed Hindi language training programs received various incentives, including cash awards for passing exams with prescribed marks, and lumpsum awards. The Atomic Energy Official Language Implementation Scheme (ATOLIS) was effectively implemented to encourage maximum work in Hindi, with cash prizes awarded quarterly. A total of 81 officials received cash prizes under this incentive scheme during the year.

### Visit of Parliamentary Committee

The Committee of Parliament on Official Language conducted an inspection of BARC's

Official Language implementation on January 19, 2024. Assurances given to the committee were fulfilled within the stipulated timeframe, with compliance reports submitted to the Secretariat through the Department. The Committee members visited key facilities including Dhruva research reactor, Food Technology Division, Waste Management Division, and Indigenous Gantry Cargo Scanner, interacting with senior scientists to understand ongoing scientific R&D activities and societal contributions. BARC successfully coordinated the inspection of 34 offices during the committee's Mumbai visit from January 17-19, 2024.



At a meeting of the Committee of Parliament on Official Language Implementation, held in Mumbai on January, 19, 2024. BARC Director, Shri Vivek Bhasin, and other senior officials of BARC and DAE were present at the meeting.

### Events and Celebrations

World Hindi Day was celebrated on January 10, 2024, featuring a noted kathak dancer, actress and TEDX speaker's presentation on "Kathak Katha," which combined narration and action. BARC hosted preparation meetings for the 'Nuclear Definitional Glossary' at BARC Training School Hostel in Anushakti Nagar, Mumbai on June 27-28 and November 5-7, 2024, with significant contributions from scientific and Official Language staff. Hindi Month was celebrated jointly by OLIC and Kendriya Sachivaalaya Hindi Parishad from September 14 to October 13, 2024, featuring 10 competitions with 689 participants. The celebrations awarded 117 prizes and certificates, along with two 'Vishisht Pratibhagita Purasakar' and one 'Hindi Sitara' awards. A special Hindi book exhibition was organized that received excellent feedback from employees. 340 new Hindi books were added to the BARC central library collection during the year.





Meeting for preparation of 'Nuclear Definitional Glossary' at TSH, Mumbai on 27-28 June, 2024, attended by Scientific & OL Cadre officials from BARC and other DAE institutes.



BARC Director, Shri Vivek Bhasin, visited the specially curated gallery of Hindi books, organized in the Central Library by SIRD.



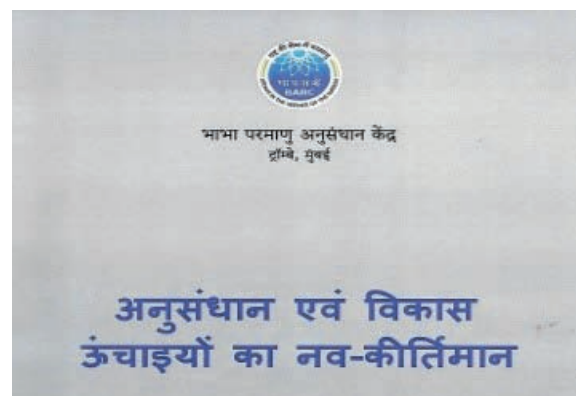
BARC Director, Shri Vivek Bhasin (center), launched the official website of BARC in Hindi on the occasion of World Hindi Day 2025.

Three officials represented BARC at the Fourth All India Official Language Conference held at 'Bharat Mandapam' in New Delhi on September 14-15, 2024. BARC celebrated World Hindi Day on January 10, 2025, demonstrating its commitment to promoting Rajbhasha. The event aligned with Prime Minister of India's message themed "Hindi: A Global Voice of Unity and Cultural Pride." Director, Shri Vivek Bhasin,

dedicated BARC's new Hindi website to the nation, showcasing linguistic inclusivity with comprehensive information across 49,000 files, developed through in-house efforts by SIRD.

### Publications in Official Language

BARC started publishing Hindi summaries of technical articles about its research activities in its popular newsletter. It also published several important Hindi works: NUCDECA (presentation of Department of Atomic Energy achievements), VISHISHT SANKALAN (a collection of BARC Newsletter articles), and "Research & Development - New Records of Touching Heights." BARC also made promotional materials in Hindi.



New publications in Hindi.

## Technology Management

### Technology Sharing

The Department of Atomic Energy (DAE) and its constituent units steadfastly engage with the industry ecosystem for sharing of new technologies emanating time-to-time from nuclear energy research and development activities. BARC/DAE inked 60 agreements with 53 firms during the calendar year 2024 for licensing of 43 state-of-art technologies. Industry partners, apart from securing non-exclusive technology licenses and detailed know-how, are also offered significant hand-holding by the respective DAE units for ensuring early market commercialization of these technologies.

### A glimpse of notable developments in technology transfer landscape during the year.

Technology Category	Technologies (no.)	Transfer Agreements (no.)	Firms (no.)
Advanced Instrumentation	5	5	5
Agriculture & Bioscience	9	19	14
Chemical	7	7	6
Engineering	10	11	7
Environment	4	7	11
Medical Equipment	1	1	1
Radiation	2	2	2
Water	5	7	7

During the period-under-review, 9 new technologies have been released into public domain for the benefit of the industry. These include;

1. 'ANUDOSE' –A low dose dosimeter for food irradiation applications.
2. 'AuRo Clean' – An autonomous robot for cleaning applications.
3. '10 MHz ICAPPS-10' – A cold atmospheric pressure plasma system.
4. Leakage Arresting Gripper for Piping.
5. Atmospheric pressure portable catalytic air plasma system for fast synthesis of aqueous Nitrate & Nitrite fertilizers.
6. A Kit for Detection of Intracellular Iron ( $\text{Fe}^{2+}$ ) in live cells.
7. Environmental Radiation Monitor (ERM).
8. A Kit for detection of Arsenic in Water.
9. Emergency in-situ advanced leakage arresting devices for piping technologies.



A portable air plasma system for fast synthesis of aqueous Nitrate & Nitrite fertilizers.

### Technology Incubation

DAE institutes actively promote entrepreneurship activities under the Government of India's flagship Atal Incubation

Mission. New Atal Incubation Centers (AICs) have been established in BARC, RRCAT, IGCAR and IPR and these are equipped with Technology Development-cum-Incubation infrastructure with the mandate of linking India's robust start-up ecosystem to nuclear energy sector.

At the newly established AIC-BARC, six technologies are undergoing incubation activities under in-house category and three technologies are progressing in a collaborative incubation mode whereas two companies have already graduated from the centre with flying colors. As part of its efforts for expanding incubation activities, AIC-BARC released eight additional technologies for incubation.



M/s. ACE-Ex India Ltd., handed over Incubation Graduation Certificate by Dr. S.M. Yusuf, Director, Physics Group, BARC and Dr. S. Adhikari, Director, KMG, BARC in presence of Shri Daniel P. Babu, Head, TT&CD, BARC. Senior officials of Physics Group and TT&CD were present during the event.



Start-up Entrepreneurship workshop (third in the series) organized by AIC-BARC on food processing technologies.

### Advanced Knowledge and Rural Technology Implementation initiative (AKRUTI)

AKRUTI program demonstrates the usefulness of BARC technologies for rural and urban sector leading to societal benefits. The program implementation was being carried out through AKRUTI-Kendra to create structured and scalable network of DAE-BARC based RUrban Technology and to provide easy access to modern technologies to all rural and urban sectors. During the period-under-review, eight agreements were inked with academic institutes for deployment of BARC technologies in rural and urban areas. Under sustainability plan of AKRUTI-Kendra, three licenses for eight



technologies were disbursed with a mop up of considerable revenue.



Public awareness campaign at an AKRUTI Kendra in Maharashtra.



BARC and Mahatma Gandhi University in Kottayam formalized an agreement for establishing an AKRUTI Kendra.



BARC and Uttar Banga Krishi Vishwavidyalaya in Cooch Behar signed an agreement for establishment of AKRUTI Kendra.



This page intentionally left blank



# SCITECH OUTREACH

Being a highly reputed multi-disciplinary R&D centre for advancement of nuclear energy activities in the country, BARC is committed towards educating citizens on the positive benefits of nuclear energy in the long term. Students of all levels, Private persons, Defence staff, VIPs and members of the Press are provided multiple opportunities to visit BARC to gain first-hand information on important activities of BARC.





The Chief of Defence Staff General Anil Chauhan is welcomed by Dr. Ajit Kumar Mohanty, Chairman, AEC & Secretary, DAE and Shri Vivek Bhasin, Director, BARC during the National Technology Day 2024 inaugural day program on May 11 in DAE Convention Centre, Anushakti Nagar, Mumbai.

## SciTech Outreach

### Engaging Youth in Science and Technology Through Outreach

A key pillar of BARC's life-long mission is to sensitize and engage citizens of all demographics, enthuse them about the exciting aspects of scientific research and technology development underpinning BARC's research and its positive impact on overall S & T landscape. As a part of its outreach program, BARC offers students from across the country with an opportunity to visit facilities in Trombay campus to gain first-hand knowledge about the range of multidisciplinary activities in BARC. Such events are also focused towards inspiring students to pursue careers in science and engineering.

As part of its institutional outreach program, BARC has hosted students and faculty members from colleges in and around Mumbai, as well as from other regions of Maharashtra and neighbouring states during the year. The list of

participating institutions includes: SVNIT, Surat - Carmel College of Arts, Science, and Commerce, Goa - Vivekananda Pharmacy College, Mumbai - Wilson College, Mumbai - LTM Medical College, Mumbai - Shah and Anchor Kutchhi College of Engineering, Mumbai - Podar International School, Mumbai - Fabtech Engineering College, Solapur - R.J. Somaiya College of Science, Mumbai among others. This initiative reflects BARC's commitment to fostering academic collaboration and promoting scientific awareness among educational institutions. From August 5 to 10, 2024, BARC conducted an outreach program in Raipur, engaging approximately 1,200 students and faculty from five colleges - Guru Ghasidas University, Dr. C.V. Raman University, Government G.N.A.P.G. College and Pandit Ravishankar Shukla University. The initiative aimed to enhance understanding of nuclear technology and dispel myths about nuclear energy.





Glimpses of outreach program conducted by BARC in Raipur.

### Prominent Personalities at BARC

BARC organizes various programs annually to commemorate significant events. In 2024, for the Graduation Function of 67<sup>th</sup> Batch of BARC Training School (OCES/DGFS-2023) programme pass outs—Dr. V.K. Saraswat, a distinguished scientist and Member, Niti Aayog, Government of India— was invited as the chief guest. During the event, Dr. Saraswat shared insightful perspectives aimed at inspiring the scientific community at BARC to excel in research and technological innovation.



Dr. V.K. Saraswat, a distinguished scientist and Member, Niti Aayog, Government of India speaks during the Graduation Function of 67<sup>th</sup> Batch (OCES/DGFS - 2023 programme) of BARC Training School pass-outs.

### Science and Technology Events in BARC

Events of national importance in science and technology, such as National Science Day and National Technology Day, are celebrated at the

Bhabha Atomic Research Centre with great enthusiasm. Eminent personalities from the fields of science and technology are invited to deliver engaging lectures on contemporary themes, benefiting both the BARC scientific community and visiting students. These events provide an excellent platform for school and college students to interact with renowned scientists and connect with BARC's vibrant scientific community.

The National Science Day (NSD) 2024 was celebrated with the theme *Atoms for Society: Securing Water, Food, and Health*, highlighting BARC's remarkable achievements in science and technology that significantly impact daily lives. Professor K. Vijayraghavan, Homi Bhabha Chair Professor and former Principal Scientific Adviser to the Government of India, graced the occasion as the Chief Guest. He delivered an insightful inaugural address focusing on fascinating scientific aspects of biological systems.



National Science Day-2024 Inaugural Day program in BARC.

Similarly, for National Technology Day (NTD) 2024, commemorating India's advancements in nuclear science and technology, General Anil Chauhan was invited as the Chief Guest. His address emphasized India's historical and contemporary scientific accomplishments aligned with the event's theme. Both NSD and NTD served as platforms to showcase BARC's contributions to national development while inspiring the scientific community and students alike.



The Chief of Defence Staff, General Anil Chauhan, welcomed by Dr. Ajit Kumar Mohanty, Chairman, AEC & Secretary, DAE and Shri Vivek Bhasin, Director, BARC during the National Technology Day inaugural day program on May 11, 2024.

## Parmanu Jyoti Program

Parmanu Jyoti is a novel school-outreach initiative, aligned with the Scientific Social Responsibility (SSR), where the young and experienced scientific officers of DAE designated as 'Parmanu Mitras' reach out to school students in remote areas. The campaign-IV of the programme was conducted from 18<sup>th</sup> to 22<sup>nd</sup> November 2024. 'Parmanu Mitras' (Scientific Officers from BARC and VECC) visited 48 Jawahar Navodaya Vidyalaya schools in 4 states in North India and conducted various activities towards imparting knowledge in the field of nuclear energy and basic sciences. A similar programme was conducted for the first time in 10 AEC schools, 7 in Mumbai and 3 in Jaduguda. The ParmanuMitras have reached out to over 18,000 students with the aim to inspire and educate the student community about the contributions and achievements of atomic energy towards nation building.

## Glimpses of Parmanu Jyoti-2024



Dr. Ajit Kumar Mohanty, Chairman AEC and Secretary, DAE addressing the stakeholders of Parmanu Jyoti program remotely from his office in Mumbai.

*...this programme is aptly named Parmanu Jyoti as it aims to spread the light of knowledge about atomic energy in India.*

**-Dr. Ajit Kumar Mohanty**  
Chairman, AEC & Secretary, DAE



## परमाणु ज्योति

**75000+** STUDENTS

**200+** SCHOOLS

**100+** SCIENTISTS

**34** STATES & Uts

**4** CAMPAIGNS

**1** MISSION



#BackToSchool



JNV DAMOH, MADHYA PRADESH



JNV BHOPAL, MADHYA PRADESH





Students of JNV Jhabua (Madhya Pradesh) express jubilation during an event organized as part of Parmanu Jyoti Campaign-IV in 2024.



Students of JNV participate in a cultural activity organized as part of Parmanu Jyoti Campaign-IV.





# SAFE AND SECURED WORKPLACE

BARC has been working proactively for the development of advanced technologies and systems in order to address the potential dangers to its physical and virtual infrastructure through deterrence, avoidance, prevention, detection and reaction to events promptly. In addition, fire safety is given utmost importance within the BARC campus, and the scientific community is provided with comprehensive training sessions to equip them with the knowledge and skills necessary for the prevention and mitigation of fire-related incidents in high duty engineering plants and workplaces.







BARC Security personnel perform march past during the Republic Day 2024 function in BARC Trombay.

## Safe and Secured Workplace

### Proactive Safety at Workplace

The BARC Safety Council (BSC) and its associated committees have conducted comprehensive safety reviews of all BARC facilities. These include research reactors, reprocessing plants, spent fuel storage facilities, fuel fabrication units, waste management facilities, particle accelerators, radiological laboratories, conventional facilities, and related projects.

### Safety Reviews & Committee Activities

Second-tier committees under the BSC framework, such as the Operating Plants Safety Review Committee (OPSRC), Conventional and Fire Safety Review Committee (CFSRC), Committee to Review Applications for Authorization of Safe Transfer/Disposal of Radioactive Waste (CRAASDRW), Physical Protection Systems Review Committee (PPSRC), and Design Safety Review

Committees (DSRC), held multiple meetings to assess safety proposals and statuses.

The BSC has published a new safety guide titled “Regulatory Consenting Process for Radiation Facilities” and has drafted two additional documents on “Event Reporting” and “Regulatory Inspection,” which are currently under review. It also organized three training courses on “Safety and Regulatory Measures for BARC Facilities” at Trombay, Tarapur, and Kalpakkam, along with a specialized course on material handling equipment for crane and forklift operators at NRB Tarapur. Additionally, a theme meeting on “Regulatory Measures for Radiation Facilities” was held for personnel from Ministry of Defense and Department of Space facilities.

This structured approach underscores BSC’s commitment to maintaining high standards of safety across all BARC operations.





Director, BARC delivered the inaugural address at the theme meeting titled “Regulatory Measures for Radiation Facilities,” which took place on December 14, 2024.



Inaugural function of 48<sup>th</sup> BSC training course on “Safety and Regulatory Measures in BARC Facilities” conducted at Kalpakkam during August 28-31, 2024.

### CCTV Surveillance System for Central Library

During the year, a Close-Circuit Television (CCTV) surveillance system has been commissioned in BARC Central Library to ensure proper surveillance of entire library floors & facilities. The suite of equipment that was

installed to support CCTV system functioning includes more than 50 IP based cameras of different coverage ranges, dedicated monitoring screens with supportive hardware like network, workstations, and servers of latest technology. This CCTV surveillance has enhanced the library security and monitoring the footfall in the library.



The footage relayed on CCTV display monitors through the cameras installed at multiple locations in Central Library.



An expansive view showcasing the periodicals and the thoughtfully arranged seating in Central Library.





The security contingent camped at BARC Trombay perform the ceremonial march-past as a part of Independence Day 2024 function held in Trombay.



The ceremonial march-past by security contingent at BARC Trombay during the Republic Day 2024 function organized in Trombay.

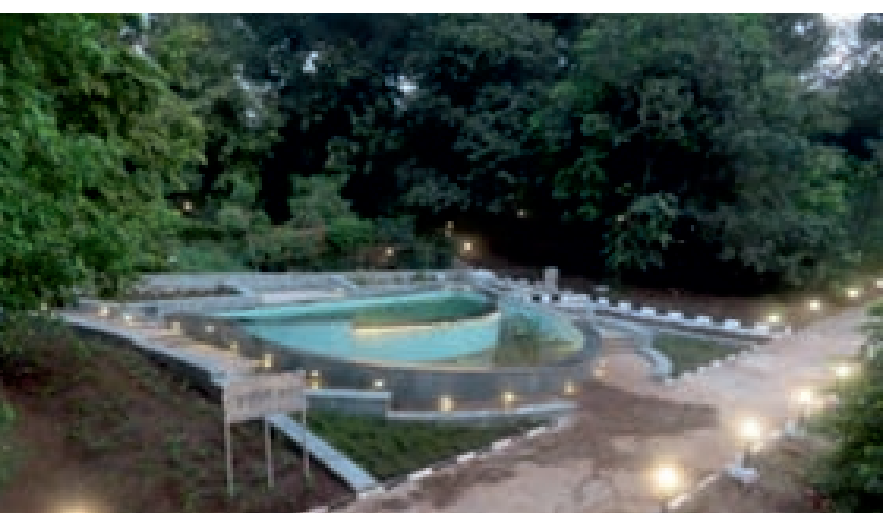




## INFRASTRUCTURE DEVELOPMENT



BARC has implemented numerous infrastructure projects to enhance its facilities and sustainability. This integrated infrastructure enables BARC to drive innovations in major spheres of nuclear energy, healthcare, and materials science while maintaining stringent safety standards.







Artistic entrance portal featuring BARC logo at the North Gate entry of BARC Trombay, Mumbai.

## Infrastructure Development

### Digital Studio establishment at HRDD Training School Complex

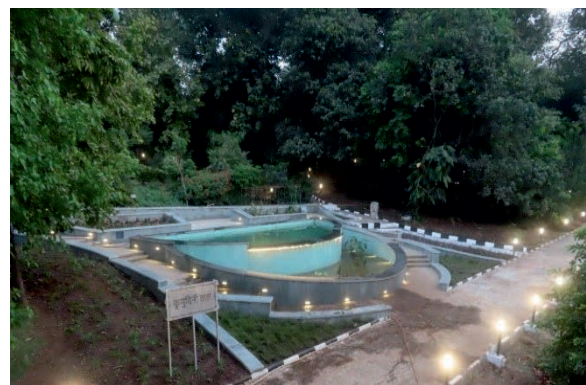
A state-of-the-art Digital Studio has been established with precision acoustic design and advanced audio-visual equipment. The facility enables broadcast-quality e-learning content in Nuclear Science & Engineering. The studio supports video recording, AV mixing, editing, video conferencing, web streaming, broadcasting, classroom recordings, remote teaching, and interview sessions.



Digital Studio Establishment at Training School.

### Bhabha Botanical Garden redevelopment with specialty features

The redeveloped Bhabha Botanical Garden serves as a living repository of plant species that preserves biodiversity while functioning as a center for botanical research and education. The meditation area incorporates 70-year-old twin wells planned for solar-powered irrigation, with trellised climbers creating a tranquil, shaded space for visitors.



Lily Pond at Bhabha Botanical Garden.



### Seawater intake system development at OSCOM, Odisha

This system was developed for a 5.0 MLD seawater desalination project to test indigenous technologies while meeting freshwater needs of OSCOM centre and its colony.

### Portable biogas plant commissioning at TSH Complex

A portable Nisargruna Plant with 50kg daily capacity has been commissioned at TSH Complex, designed specifically for small housing societies. The compact design requires minimal floor space and installation time, featuring a spiral pipe design for the main digester that eliminates the need for conventional pits. The plant produces enriched organic manure usable as fertilizer for gardens or marketable to nearby nurseries.



A portable Nisargruna Plant with 50kg daily capacity.

### Lecture Hall modernization at Training School Complex and Sports & Multiple Purpose Hall Renovation

Six lecture halls have been refurbished with state-of-the-art AV systems, and acoustic lining, and wooden-finish PVC flooring.



Fully refurbished Multipurpose Hall.

### High-Altitude Guest House construction in Ladakh

The guest house accommodates officials visiting the MACE facility at an elevation of 14,000 feet (4,300m). The solar-passive building incorporates REM earth walls, insulated flooring and ceilings, and geo-mesh with 3-inch soil cover over the slab to enhance thermal efficiency in extreme conditions. Water storage tanks

feature polycarbonate sheet enclosures creating a greenhouse effect to prevent freezing, while exposed connections and pipes are equipped with heat tapes. The completed facility includes comprehensive electrical systems with LED lighting, maintenance-free earthing, lightning protection, and networking infrastructure.

### Micro Hydro Power Generation

A 15kW capacity micro hydro power unit has been indigenously developed and commissioned at Plutonium Plant lake, BARC. The system is now actively generating electrical power utilizing harvested rainwater.



Micro Hydro Power Generation unit.

### Automated Polyhouses for Specialized Plant Cultivation

Three new fully automated polyhouses have been developed at BARC Trombay for cultivating exotic flowers and tropical orchids, while supporting plant propagation, conservation, and acclimatization of newly introduced species.



New polyhouses with temperature control systems established for better flower production and plant propagation.



Tropical orchids cultivated inside polyhouse.

*Glimpses of Flora in BARC Trombay*

